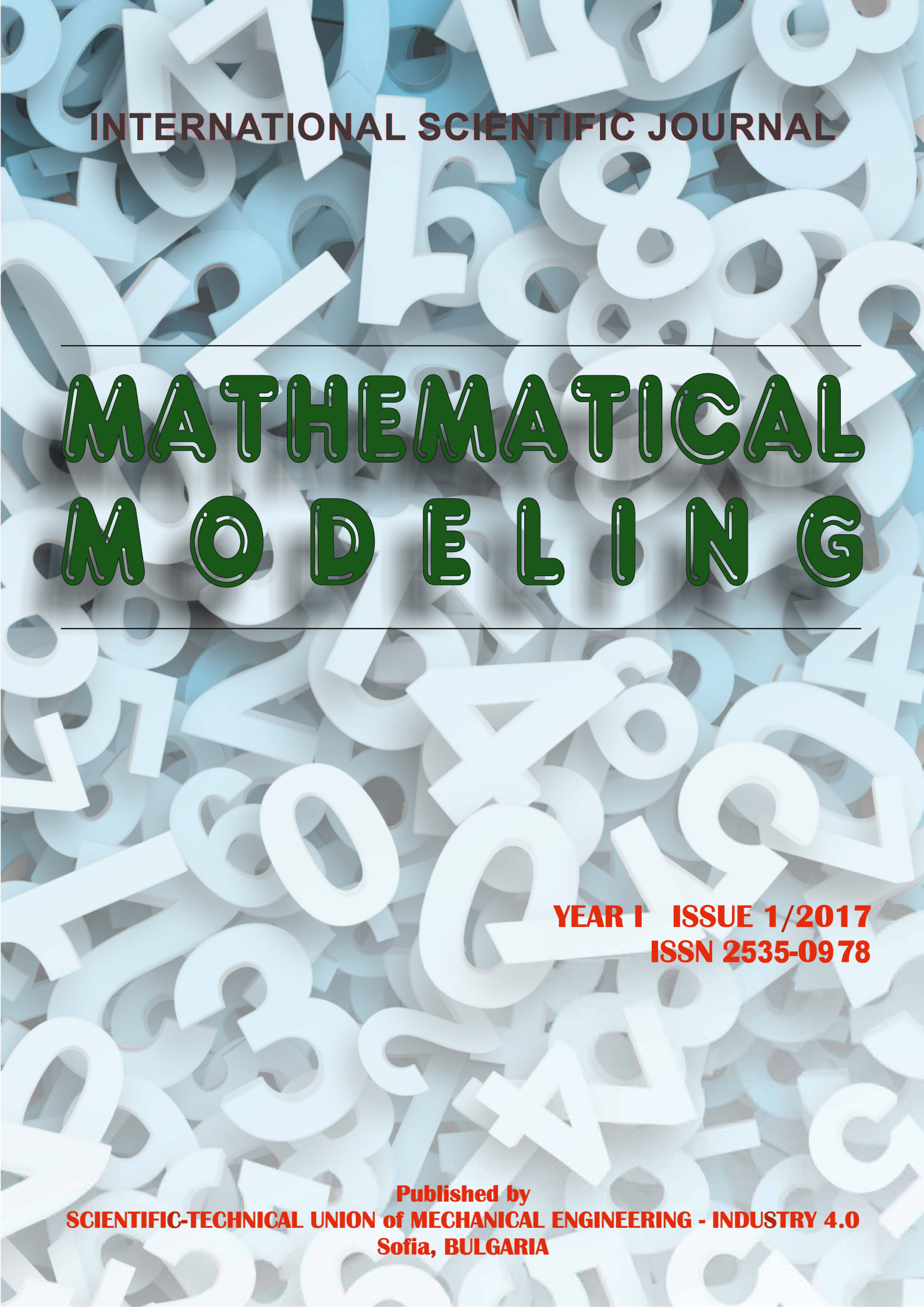

INTERNATIONAL SCIENTIFIC JOURNAL

MATHEMATICAL MODELING

YEAR I ISSUE 1/2017
ISSN 2535-0978

Published by
SCIENTIFIC-TECHNICAL UNION of MECHANICAL ENGINEERING - INDUSTRY 4.0
Sofia, BULGARIA

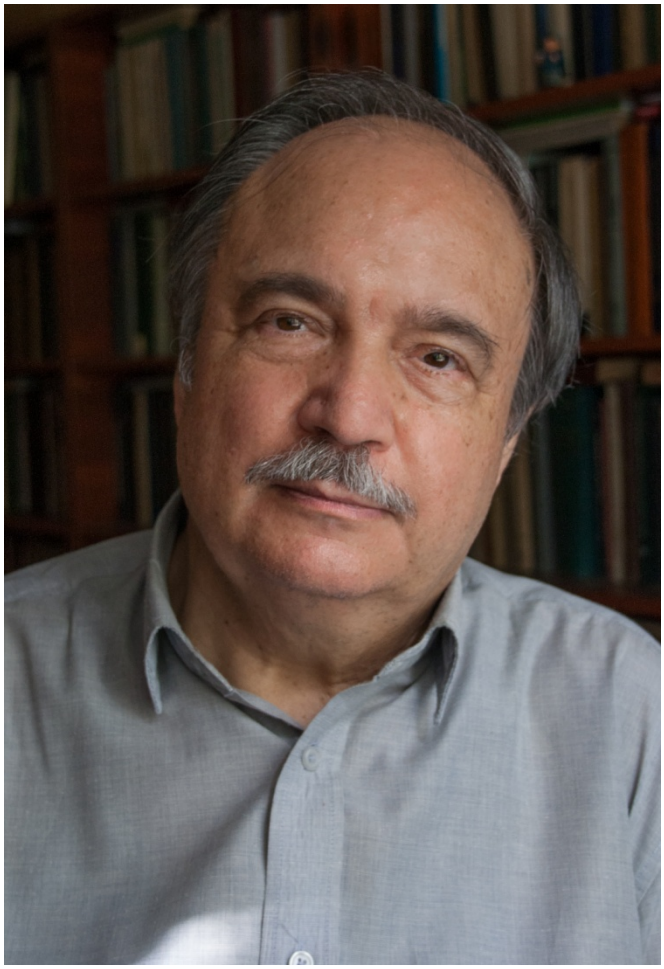

Уважаемые коллеги!

Задача нашего журнала – предоставить возможность широкой научной общественности познакомиться с новыми идеями и исследованиями теоретического и прикладного характера из разных областей научного творчества, но объединенных общим языком описания – языком математики. Использование этого языка позволяет лучше осознать единство и взаимозависимость различных, на первый взгляд, явлений и процессов. Мы надеемся, что наш журнал поможет молодым исследователям научиться грамотно излагать свои мысли, а также сможет подсказать им новые направления для творческого поиска. Мы надеемся также, что журнал сможет стать ареной содержательных профессиональных дискуссий, ибо, как хорошо известно, «в споре рождается истина». Со своей стороны, мы сделаем все от нас зависящее, чтобы создать для авторов комфортные и объективные условия общения с Редакционной коллегией. Успехов!

Dear colleagues!

Our journal is aimed to provide an opportunity for the wide-range scientific community to get acquainted with new ideas in theoretic and applied research, in various areas of scientific creativity, united by a common language - the language of mathematics. This language is able to clarify an understanding of the unity and interdependence of phenomena and processes, which initially are seemed to be different. We hope that our journal could be helpful for young researchers, who want to learn how to express correctly their thoughts, and also show them new directions of creativity. We hope that our journal will become an arena for meaningful professional discussions, cause, as it’s well known, "Discussio mater veritas est". For our part, we will do our utmost to create comfortable and objective conditions for communication of authors with the Editorial Board. Good luck!

Andrei Firsov



INTERNATIONAL SCIENTIFIC CONFERENCE



MATHEMATICAL MODELING

PROCESSES AND SYSTEMS

13-16. DECEMBER 2017, BOROVETS, BULGARIA

ORGANIZERS

SCIENTIFIC-TECHNICAL UNION of MECHANICAL ENGINEERING - INDUSTRY 4.0
BULGARIA
PETER THE GREAT ST.PETERSBURG POLYTECHNIC UNIVERSITY
RUSSIA

BULGARIA, Sofia 1000, 108 G.S.Rakovski Str., office 411
phone: + 359 2 987 7290
office@mathmodel.eu http://www.mathmodel.eu

INTERNATIONAL EDITORIAL BOARD

EDITOR I CHIEF	
Prof. ANDREY FIRSOV Peter the Great St.Petersburg Polytechnic University	RU

Members:		
Abilmazhin Adamov, Prof.	L.N.Gumilyov Eurasian National University	KZ
Alexander Guts, Prof.	Omsk State University	RU
Alexei Zhabko, Prof.	Saint Petersburg State University	RU
Andrey Markov, Prof.	Baltic State Technical University	RU
Andrii Matviichuk, Prof.	Kyiv National Economics University	UA
Andrzej Nowakowski, Prof.	University of Lodz	PL
Anton Makarov, Dr.	Saint Petersburg State University	RU
Armands Gricans, Assoc. Prof.	Daugavpils University	LV
Artūras Dubickas, Prof.	Vilnius University	LT
Avinir Makarov, Prof.	Saint Petersburg State University of Industrial Technologies and Design	RU
Christo Boyadjiev, Prof.	Institute of Chemical Engineering, BAS	BG
Daniela Marinova, Dssoc. Prof.	Technical University of Sofia	BG
Dimitrios Poulakis, Prof.	Aristotle University of Thessaloniki	GR
Evgeniy Smirnov, Assoc. Prof.	Volgograd State Technical University	RU
Giovanni Borgioli, Assoc. Prof.	University of Florence	IT
Haskiz Coskun, Prof.	Karadeniz Technical University of Trabzon	TR
Idilia Bachkova, Prof.	University of Chemical Technology and Metallurgy	BG
Igor Anufriev, Assoc. Prof.	Peter the Great St.Petersburg Polytechnic University	RU
Irena Stojkovska, Prof.	Ss. Cyril and Methodius University in Skopje	MK
Ivana Štajner-Papuga, Prof.	University of Novi Sad	RS
Kanagat Aldazharov, Assoc. Prof.	Kazakh Economics University	KZ
Karl Kunisch, Prof.	University of Graz	AT
Mahomed Agamirza ogly Dunyamalyev, Prof.	Azerbaijan Technical University	AZ
Marius Giuclea, Prof.	The Bucharest University of Economics Studies	RO
Mihail Okrepilov, Prof.	D.I. Mendeleyev Institute for Metrology (VNIIM)	RU
Milena Racheva, Assoc. Prof.	Technical University of Gabrovo	BG
Mohamed Kara, Dr.	Ferhat Abbas Sétif 1 University	DZ
Mohamed Taher El-mayah, Prof	MTI University	EG
Neli Dimitrova, Prof.	Institute of Mathematics and Informatics, BAS	BG
Nina Bijedic, Prof.	Dzemal Bijedic University of Mostar	BA
Oleg Obradović, Prof.	University of Montenegro	ME
Olga Pritomanova, Assoc. Prof.	Oles Honchar Dnipropetrovsk National University	UA
Özkan Öcalan, Prof.	Akdeniz University of Antalya	TR
Paşc Găvruţă, Prof.	Politehnic University of Timisoara	RO
Pavel Satrapa, Assoc. Prof.	Technical University of Liberec	CZ
Pavel Tvrdík, Prof.	Czech Technical University in Prague	CZ
Pavlina Yordanova, Assoc. Prof.	Shumen University	BG
Petr Trusov, Prof.	Perm State Technical University	RU
Rannveig Björnsdóttir, Prof.	University of Akureyri	IS
Roumen Anguelov, Prof.	University of Pretoria	ZA
Sándor Szabó, Dr. Prof.	University of Pécs	HU
Sashko Martinovski, Assoc. Prof.	St. Kliment Ohridski University of Bitola	MK
Sergey Bosnyakov, Prof.	Moscow Institute of Physics and Technology	RU
Sergey Kshevetskii, Prof.	Immanuel Kant Baltic Federal University	RU
Snejana Hristova, Prof.	University of Plovdiv	BG
Svetlana Lebed, Assoc. Prof.	Brest State Technical University	BY
Tomasz Szarek, Prof.	University of Gdansk	PL
Valeriy Serov, Prof.	University of Oulu	FI
Vasily Maximov, Prof.	Saint Petersburg State University of Industrial Technologies and Design	RU
Ventsi Rumchev, Prof.	Curtin University, Perth	AU
Veronika Stoffová, Prof.	University of Trnava	SK
Veselka Pavlova, Prof.	University of National and World Economy	BG
Viorica Sudacevschi, Assoc. Prof.	Technical University of Moldova	MD
Vladimir Janković, Prof.	University of Belgrade	RS
Vladislav Holodnov, Prof.	Saint Petersburg State Institute of Technology	RU
Vyacheslav Demidov, Prof.	Saint Petersburg State University of Industrial Technologies and Design	RU
Yordan Yordanov, Assoc. Prof.	University of Sofia	BG
Yuriy Kuznetsov, Prof.	Nizhny Novgorod State University	RU
Zdenka Kolar - Begović, Prof.	University of Osijek	HR

INTERNATIONAL SCIENTIFIC JOURNAL

MATHEMATICAL MODELING

PUBLISHER:

SCIENTIFIC TECHNICAL UNION OF MECHANICAL ENGINEERING "INDUSTRY 4.0"

108, Rakovski Str., 1000 Sofia, Bulgaria
tel. (+359 2) 987 72 90,
tel./fax (+359 2) 986 22 40**,**
office@stumejournals.com
www.stumejournals.com

ISSN: PRINT 2535-0978

YEAR I, ISSUE 1 / 2017

EDITOR IN CHIEF:

Prof. D.Sc. ANDREY FIRSOV
Peter the Great St.Petersburg Polytechnic University, Russia

CONTENTS

THEORETICAL FOUNDATIONS AND SPECIFICITY OF MATHEMATICAL MODELLING

THE MATHEMATICAL MODEL AS A BASIS FOR THE NATURAL CLASSIFICATION OF SYSTEMS AND PROCESSES
Prof., Dr. Tech. Sci. Firsov A.N. 4

FUNDAMENTALS OF THE MODELING AND SIMULATION IN THE CHEMICAL INDUSTRY
Prof. Christo Boyadjiev 7

APPLICATION OF THE THEORY OF MECHANISMS TO SOLVE PROBLEMS FROM GEOMETRY
M.Sc. Ćulafić S. 10

LAPLACIAN PRESERVING TRANSFORMATION OF SURFACES AND APPLICATION TO BOUNDARY VALUE PROBLEMS FOR LAPLACE'S AND POISSON'S EQUATIONS
Ph.D. Gospodinov I., M.Sc. Krumov K., M.Sc. Filipov S. 14

MATHEMATICAL MODELLING OF TECHNOLOGICAL PROCESSES AND SYSTEMS

MATHEMATICAL MODELING OF NON-STATIONARY FLOWS OF LIQUID HOMOGENEOUS VISCOUS MIXTURES BY PIPELINES
Prof., Dr. Tech. Sci. Firsov A., Asst., MSc Sorokina N. 18

TRANSFER PROCESSES IN INDUSTRIAL COLUMN APPARATUSES
Chr. Boyadjiev, M. Doichinova, B. Boyadjiev, P. Popova-Krumova 23

MODEL ADHESION WEAR OF FRICTION SURFACE
Candidate of Science, associate Professor. Shalygin M.G. 28

DEVELOPMENT OF AUTOMATED QUALITY CONTROL SYSTEMS AND METHOD FOR ABSOLUTE PRESSURE SENSORS
Dr. Tech. Sci. A.V. Markov 31

MATHEMATICAL MODELLING OF THE OSCILLATING BODY SUBMERGED IN THE LIQUID AT THE PRESENCE OF THE INITIAL AND CONSTANTLY ACTING DISTURBANCES
Dr. Vasily V. Maximov. Elena A. Krylatykh. 33

PARAMETRIC ANALYSIS OF SURFACES OF ACOUSTO-ELECTRONIC RESONATORS USING NI LABVIEW AND SCANNING PROBE MICROSCOPY
Ph.D. V.V. Spiridonov 37

AUTOMATION OF THE QUALIMETRIC METHOD OF SELECTING LAYOUT SOLUTION OF THE PUMPING EQUIPMENT FOR NPPS
postgraduate student, chair I., G.S. Vinogradova 41

PRODUCTION OF BORON CARBIDE BASED SANDBLASTING NOZZLE by USING LOW PRESSURE POWDER INJECTION MOLDING METHOD and MODELING of PRODUCTION PARAMETERS via ARTIFICIAL NEURAL NETWORK
S. Hartomacıoğlu. PhD., H.O.Gülsoy. PhD., A. Onat. PhD. 44

MODELING OF THE EFFECTS OF THREEFOLD TYPE RHVT AND SIX CASCADE TYPE RHVT ON THE PERFORMANCE OF COUNTER FLOW RHVTS BY FUZZY LOGIC APPROACH
Assist. Prof. Dr. Yusuf Yılmaz, Res. Asst. Sadık Ata, Assist. Prof. Dr. Kevser Dincer,Assist. Prof. Dr. Gürol Önal 48

COMPUTER AIDED ANALYSIS OF KINEMATICS AND KINETOSTATICS OF SIX-BAR LINKAGE MECHANISM THROUGH THE CONTOUR METHOD
Prof.Asoc.Dr. Likaj R., Prof.Asoc.Azem Kycyku, MSc. Qelaj M., Prof.Ass.Dr. Bajrami X. 51

VEHICULAR TRAFFIC FLOW MODELLING BY MEANS OF CAR-FOLLOWING APPROACH
Ph.D. student Kurtc V., Ph. D. Anufriev I. 57

MATHEMATICAL MODELLING OF SOCIO-ECONOMIC PROCESSES AND SYSTEMS

PERSPECTIVES AND CHALLENGES FOR RUSSIAN SYSTEM OF ENGINEERING EDUCATION
Ph.D., Aleksankov.A. 61

RISK-ORIENTED APPROACH IN QUALITY MANAGEMENT
PhD. Mager V., PhD. Stepanova M., Dr.Tech.Sc. Chernenkaya L., M.Sc. Chernenkii A. 67

MODEL OF QUICK RESPONSE PRODUCTION PLANNING SYSTEM
postgraduate student Skornyakova E.A. 70

THE MATHEMATICAL MODEL AS A BASIS FOR THE NATURAL CLASSIFICATION OF SYSTEMS AND PROCESSES

МАТЕМАТИЧЕСКАЯ МОДЕЛЬ КАК ОСНОВА ЕСТЕСТВЕННОЙ КЛАССИФИКАЦИИ СИСТЕМ И ПРОЦЕССОВ

Prof., Dr. Tech. Sci. Firsov A.N.
Peter the Great St. Petersburg Polytechnic University – St. Petersburg, Russia
E-mail: anfirs@yandex.ru

Abstract: *this paper attempts to provide a transparent and, if possible, a formal hierarchy of the main types of mathematical models used in the description of dynamic processes inside, at first glance, different systems. It is emphasized that the mathematical modeling is a natural and universal environment for effective analysis of system processes of different nature. From our point of view, the term "system analysis" means the methodology for classification of real systems (physical, biological, economic, social, etc.), which is based on the classification of mathematical models that are used to describe these systems.*
KEYWORDS*: SYSTEMS, SYSTEM ANALYSIS, MATHEMATICAL MODELS, MATHEMATICAL MODELING, CLASSIFICATION*

1. Introduction

We define a system as a collection (set) of objects[1] of a particular nature, interacting with each other and the external environment. Since every interaction presupposes the possibility of state changes as the objects themselves that make up the system, and the system as a whole, the first task of the researcher is to establish the patterns of these changes in order to predict the latter. The second task is the task of forming effects on the system as a whole (through changes in environmental conditions) or of its component objects to implement the required changes to the characteristics of the system and/or its objects. In other words, we have to talk about the study and management of the processes occurring in the system.

For definiteness, formulations, point to a sense that we put here in the term "characteristics". Under the characteristics of the system, we understand the qualitative or functional description important for the purposes of the study of the properties of the system as a whole and its constituent objects. A set of important characteristics are not cast in stone, and can vary in research depending on the results obtained, change the purposes of the study, further information (experiments, calculations, discoveries, etc.). Here are a few examples. In classical mechanics the important characteristics of the free material point are its coordinates (more precisely, the radius vector) and momentum. For holonomic system of material points – a set of generalized coordinates and velocities (momenta) of the system and the Lagrangian function[2], the latter, as you know, is a function of generalized coordinates and generalized speeds of the system and, possibly, time. In quantum mechanics, the important characteristics for the particles are, for example, the wave function, the energy (operator) and spin (number). In gas dynamics, the important characteristics are functions of the spatial coordinates and time (density, velocity, pressure, temperature, etc.). In classical molecular-kinetic theory of gases basic properties of a system of molecules are the distribution function and the law of interaction of molecules between themselves, representing the operator**.**

2. On the modeling of systems

In practice, the learning processes in any real system, is reduced to their modeling i.e. to approximate description by creating their simplified models. Traditionally, models of systems and processes are dividing into two main classes: physical and mathematical models, although this division is largely arbitrary, since, as we shall see below, the physical model without its mathematical counterpart loses much of its effectiveness and practical significance. These models should go "hand in hand" in serious research.

Under a *physical model*, we usually mean a product, device or imaginary system, which simplified the likeness of the object or system, and allows you to recreate the monitoring process or phenomenon with the required degree of accuracy. At the same time, elements of the system are associated with the physical equivalents, reproducing the structure, basic properties and relations of the studied object or process. Typically, the physical model of the object or system should have the same qualitative nature as the simulated object (system). The basis of constructing an adequate physical model are placed, as a rule, the idea of the theory of similarity and dimension.

Under a *mathematical model*, we usually mean an approximate description of a class of phenomena of the external world, expressed by mathematical symbols. Most often, the mathematical model is a set of equations and/or inequalities (algebraic, differential, integral, operator, functional). Arsenal research methods of mathematical models is extremely wide - from the logic of algebra to functional analysis[3]. In this case, since the mathematical model of the object is "mathematical world", it should be investigated on the received in this "world" level of rigor. Finally, it is important to understand that a mathematical model cannot "be proved". It is always a hypothesis, whose validity is checked only by its practical application**.**

3. Stages and features of mathematical modeling

The process of mathematical modeling, i.e. studying phenomena of any nature with the help of a mathematical model, can be divided into four stages [1].

The first phase - the formulation of laws connecting the main objects of the model. This stage requires a broad knowledge of the facts relating to the phenomenon, and deep penetration into their relationship. This stage is completed in mathematical terms formulated qualitative ideas about the links between model objects.

The second stage - the study of mathematical problems, which leads to a mathematical model. The main issue here is the solution of the direct problem, i.e., obtaining as a result of the analysis of model output (theoretical consequences) for further comparison with the results of observations of the phenomena studied. At this stage, the mathematical apparatus acquires the main role that is necessary for the analysis of mathematical models and computer engineering - a powerful tool for obtaining quantitative output data as a result of solving complex mathematical problems.

The third stage - clarification as to whether the adopted (hypothetical) model is the criterion of practice, i.e., asking the

[1] The objects that make up the system, often referred to as its elements.

[2] On the other hand, the total energy of the system.

[3] Including, of course, numerical methods. However, the method of their application and interpretation of the results must be mathematically strictly justified.

question of whether the results are consistent with the observations of the theoretical consequences of the model within the observational accuracy. If deviations are outside the limits of accuracy of the observations, the model cannot be accepted. It often happens in the construction of the model that some of its characteristics remain uncertain. Tasks, which define the characteristics of the model (parametric and functional) so that the output information was comparable within the accuracy of the observations with observations of the phenomena studied, called inverse problems. If such compatibility cannot be achieved for any choice of the characteristics, the model is not suitable for the study of the phenomena under consideration. The use of practical criterion to appraise a mathematical model allows to conclude that the validity of the assumptions underlying the study of the subject (hypothetical) model.

The fourth stage - the subsequent analysis of the model due to the accumulation of data on the phenomenon, and the model of modernization. In the development of science and technology, phenomenological data are more and more refined, and there comes a point of time when the conclusions derived on the basis of an adopted mathematical model do not correspond to our knowledge of the phenomenon. Thus, there is a need to build a new, more sophisticated mathematical model.

A good illustration of the above can be an example of the development of the theory of gravitation. The classical theory of gravitation Newton's mathematical point of view was based on Euclidean space-time model that eventually led to the description of the dynamics of the system of material bodies based on the Lagrange equations. Experience has shown that the Newton-Lagrange theory adequately describes the mechanical processes that we face on Earth and in space within the solar system. A brilliant example of this - the discovery of the planet Neptune, which was made in 1846 by German astronomer Johann Galle based on calculations, made by Urbain Le Verrier (France) and John Adams (England), is based on Newton's theory of gravitation. However, the development of cosmological studies in the early twentieth century led to the discovery of phenomena that could not be explained in the framework of the classical theory of gravitation. The search for answers to your questions led Einstein (in 1916) to construct a new mathematical model of space-time, which was the basis for the hypothesis of space-time as a Riemann space, in which the curvature tensor depends on the distribution and magnitude of the masses of space objects. In this space, in particular, light (more precisely, the photons) extends not straight (as is the Euclidean model), and on geodesic lines corresponding Riemann space. Einstein's theory was confirmed experimentally in 1919, when there was a ray of light deviation from the star as it passes close to the sun that qualitatively and quantitatively consistent with the predictions of the theory. On the other hand, in the absence of the objects near the large (on space standards) gravitating mass, corrections (with respect to the classical theory of gravitation), given by Einstein's theory, are, from a practical point of view, negligible. This allows you to successfully continue to use the relevant conditions of Newton's theory of gravitation.

A.N. Tikhonov in the article in «Mathematical encyclopedia» cited above gives another example illustrating the steps of mathematical modeling.

Concluding the topic of physical and mathematical models point to stand somewhat apart the analog model. This type of model clearly demonstrates the organic link between methods of physical and mathematical modeling. The essence of the analog simulation is as follows. Consider two systems of different physical nature (e.g., mechanical and electrical). Processes in these systems proceed according to qualitatively different physical laws. If, however, the mathematical models of both systems have the same form, i.e., from a mathematical point of view, these systems are the same, based on the study of the behavior of a system can be inferred about the behavior of another system[4].

As an example, consider the following mechanical and electrical systems [2]. Let the mechanical system with one degree of freedom is a mass m, moving under the action of which the exciting force *p*, elastic restoring force (e.g., spring), characterized by stiffness *c*, and the damping force of viscous friction with coefficient *r*. Let *h* - coordinate of the mass m, which determines its deviation from its equilibrium position. The equation of motion of a mechanical system has the form

$$m\ddot{h} + r\dot{h} + ch = p. \quad (1)$$

Suppose further that the electrical system is an electrical circuit consisting of series-connected source voltage (*e*), the inductance of *L*, resistance *R*, and the inverted container *S* (*S = 1 / C*). Let q - the electric charge transferred by a current *i* through the conductor cross-section:

$$q = q_0 + \int_0^t i dt.$$

The second Kirchhoff's law leads to the following equation:

$$L\ddot{q} + R\dot{q} + Sq = e. \quad (2)$$

If the values of *p* and *e* are changed as a function of one and the same law, the equations (1) and (2) are substantially identical and, therefore, to study the behavior of the mechanical system can be replaced by studying the electrical behavior of the system and vice versa. Thus, these two systems in terms of their mathematical models are similar to each other, although they are different systems of physical nature.

The above examples touch simulation "material and physical" systems, but all of the above applies equally to problems of mathematical modeling of systems of different nature - social, economic, etc. Let us give an example. According to T. Parsons (see [3], ch. 9), four numerical functions, depending on the time *t*, can be assigned to the socio-economic system, which sufficiently adequately describe the state of this system: *G*(*t*), characterizing the political system in society; *E*(*t*), characterizing the economic system; *K*(*t*), which characterizes the social community; and *D*(*t*), which characterizes the system of maintaining institutional ethnic images. Parsons showed that these functions must satisfy some autonomous system of differential equations of the form:

$$\frac{dG}{dt} = F_1(G,E,K,D); \quad \frac{dE}{dt} = F_2(G,E,K,D);$$

$$\frac{dK}{dt} = F_3(G,E,K,D); \quad \frac{dD}{dt} = F_4(G,E,K,D),$$

where the functions F_j are given sufficiently smooth functions of their arguments. Thus, for this system, for example, the Lyapunov theorem on stability in the first approximation is valid. This, in turn, allows us to formulate certain conditions for the parameters included in the expressions for F_j, which guarantee a stable dynamics of the social community.

In other words, the behavior of systems "made of different test" can be investigated effectively by using models built in one of them - mathematical. It is only necessary to select the appropriate mathematical apparatus. For example, for the construction and study of adequate mathematical models of social and economic processes have to resort to such seemingly quite abstract, analytical areas of mathematics as catastrophe theory and algebraic topology (see., e.g., [3, 4]).

4. System analysis and adequacy of mathematical models

The foregoing gives grounds to propose to classify the system (regardless of their actual nature) according to the classes of mathematical models used to describe these systems.

[4] It is necessary to distinguish between analogue and similar models studied in the theory of similarity and dimension. In the latter case, we are dealing with models of the same nature, while the analogue model is a model of a different nature.

Thus, it seems reasonable to take as a basis the following definitions.

System is a collection of objects highlighted by a researcher, which are interacting with each other and the environment.

Systems analysis is a methodology for classification of real (physical, technical, biological, economic, social, etc.) systems, based on the classification of mathematical models used for formalized description of these systems.

That is, we unite into the same class those real systems, formalized description of which requires the use of the same class of mathematical models (e.g., ordinary differential equations, partial differential equations, operator equations in function spaces, probability theory, mathematical logic, graph theory, etc.).

Speaking about the importance of mathematical modeling in the analysis of processes in different systems, it is necessary to say a few words about the features of this simulation. If we want to use mathematical methods for solving problems related to any technical, economic, biological or any other system, we must, as mentioned above, to start with the construction of a mathematical model of the relevant system. Build a model - which means indicate what mathematical objects under study is characterized by the system and how these mathematical concepts reflect the laws that describe the functioning of the system.

Since the mathematical model cannot display the studied reality in all its concreteness and fullness, when its construction is necessary to choose such factors and the relationships that are most important in this problem. In many cases, the right to choose the model - means to solve the problem by more than half. The main difficulty in this case lies in the fact that the construction of the model requires special connection (for the study of the qualitative features of the simulated process) and mathematical knowledge.

When constructing a mathematical model can meet and insurmountable (at the moment) the difficulty, for example,

– Insufficient knowledge of laws that describe the system (for example, biology, economics, sociology);

– We do not know some significant characteristics of the system (for example, the density distribution of matter in the interior of the Earth, the pressure in the blood vessels of a living organism).

In such cases, the construction of the model is necessary to make additional assumptions that have the character of hypotheses. Consequently, the conclusions drawn from the study of this model are conditional. But even if the laws are known and measured characteristics of the system, the model can get so complicated that it would be available for the study of well-known (for now) with mathematical methods.

Therefore, we often have to make some simplifications in the simulation of the real process, idealized model.

Thus, the construction of a mathematical model must meet two important criteria:

1) the model must be adequate, i.e. to the extent necessary correspond to reality.

2) The model must be simple enough to allow finding an effective solution within a reasonable time and with reasonable accuracy.

It is easy to note that these criteria are contradictory. On the one hand, to build adequate models requires consideration of more complete and varied number of factors, which inevitably complicates the model. This complexity leads to that the posed problem cannot be solved at all or for practical time. On the other hand, over-simple model, which does not take into account a number of important factors, is clearly inadequate, and therefore does not meet its intended purpose. Art researcher is to find a harmonious matching of these two mutually exclusive requirements. We should seek to ensure that the model is consistent with reality, other things being equal. However, the degree of compliance must be determined by the terms of the problem, i.e., the model should provide enough (within the required accuracy) true reflection of reality.

In connection with the above, you can specify the steps of the solution of applied problem using mathematical methods:

1. Correct application wording task is to extract the essential properties and relationships of the studied object or process.

2. Construction of mathematical model - display of quantitative (functional) relationships allocated for the first stage of the properties with the help of mathematical concepts and relationships. As noted above, this is the most difficult part of the study. Firstly, for the same phenomena of a variety of mathematical models can be built. Secondly, it is necessary to satisfy the requirements of the constructed model adequacy and simplicity.

3. Logical-mathematical analysis of the model: model checking for consistency, and the solution of a mathematical problem. Sometimes the implementation of this phase requires the development of new methods or even creating a new mathematical discipline. The solution of the mathematical problem cannot always be found for a particular formula, even if it exists. Therefore may require numerical solution methods, - i.e., methods which give no exact and approximate (with reasonable accuracy) response. This phase includes the theoretical study of mathematical problem and its practical solution (including baseline data collection, programming).

4. Interpretation of results from a known empirical data (the results of observations or experiments specially designed), i.e. translating mathematical answer to the specific language of science.

5. Concluding remarks

In conclusion, I would like to note the following. Due to the increasing amount of scientific information and the deepening of the process of differentiation of sciences one researcher has become almost impossible to work in several branches of knowledge. Therefore, in order to construct adequate models and effectively solve mathematical problems arising in connection with this (especially when it comes to major scientific problems), requires the cooperation of scientists from different specialties and, of course, the attraction of modern computer technology. Hence it follows that even a good specialist in a certain field of knowledge can now be unarmed against the problems arising in the investigation if he is not a kind of "synthesizer of knowledge": he must well imagine what and where is located in science. Only such a person can intelligently choose the appropriate research team and direct it to work in the right direction. Training and education of such specialists is not an easy, but extremely important problem, facing the system of higher education.

Literature

1. A. N. Tikhonov. Mathematical model. - In the book “Mathematical encyclopedia” in 5 volumes, vol. 3. - M.: Publishing house "Soviet Encyclopedia", 1982 (in Russian).

2. A.Yu. L’vovich. Electromechanical systems: Textbook. - L.: Publishing House of Leningrad Univ., 1989 (in Russian).

3. A.K. Guts, et al. Mathematical Models of Social Systems: Textbook – Omsk: Omsk State University, 2000 (in Russian).

4. Problems of optimization and economic applications: reports of the V All-Russian Conference (Omsk, 2 - 6 July 2012). - Omsk: Omsk State University, 2012 (in Russian).

5. I.I. Blekhman, A.D. Myshkis, Ya.G. Panovko. Applied Mathematics. The subject, logics, features of approaches. - Kiev, "Naukova Dumka", 1976 (in Russian).

6. I.I. Blekhman, A.D. Myshkis, Ya.G. Panovko. Mechanics and applied mathematics: logic and application features. - M.: “Nauka”, 1990 (in Russian).

FUNDAMENTALS OF THE MODELING AND SIMULATION IN THE CHEMICAL INDUSTRY

Prof. Christo Boyadjiev
Institute of Chemical Engineering, Bulgarian Academy of Sciences,

chr.boyadjiev@gmail.com

Abstract: *Direct Metal Laser Sintering[1] (DMLS) is a revolutionary technology that allows a production of fully functional metal parts directly from a 3D CAD data, eliminating the investment to production tools and technologies which brings considerable cost and time savings. Metal parts made by DMLS technology are fully comparable with casted or machined parts. A range of application of DMLS technologies is very wide – from prototypes, through short-run production to final products. Advantages of DMLS technology are arising along with complexity of parts – more complex geometry of parts (in terms of shape and occurrence of the detail) make DMLS technology even more economically effective.*

Keywords: MODELING, SIMULATION, THEORETICAL APPROXIMATION, THERMODYNAMIC LEVEL, HYDRODYNAMIC LEVEL, MECHANISM IDENTIFICATION, PARAMETERS IDENTIFICATION, STATISTICAL ANALYSIS.

1. Introduction

The modeling and simulation are a basic approach to quantifying processes and phenomena. They have become realistic as a result of the development of computing and applied mathematics. In the industry, the modeling and simulation offer a quantitative description of the kinetics of processes and systems for the purposes of their optimal design or control. In the industrial systems, the process models of the individual devices are known in advance, and system models offer quantitative descriptions of the systems (process systems engineering).

In the industry, quantification of systems can also be used for various other tasks. For example, in periodically operating systems, the optimal schedules of the apparatuses (machines) for conducting different processes (operations) of different duration and different sequence to obtain different substances (machined details) can be determined. In these cases, the mass service theory offers models that allow for optimal solutions.

The fundamentals of the modeling and simulation, as a part of human knowledge and science, are related to the combination of intuition and logic, that are in different scales in individual sciences [1, 2]. In mathematics, logic dominates intuition, where intuition is the axiom (unconditional truth that is not proof able), and logic is the theorem (the logical consequences of the axiom). In the natural sciences (physics, chemistry, biology), the logic/intuition ratio is maintained, but axioms are usually conditional (principles, postulates, laws). This ratio goes back to the humanities and reaches the extreme in religion.

The modeling and simulation offer quantitative (mathematical) descriptions that have different degrees of detail. The lowest level is the thermodynamic (non-equilibrium thermodynamics) that examines the volume of the phase (gas, liquid, solid). The next level is the hydrodynamic, which examines the elementary phase volumes (mechanics of continua), which are much smaller than the phase volumes, but much larger than the intermolecular volumes, i.e. the molecules are indistinguishable. The highest level is the molecular (the kinetic theory of the ideal gas).

The modeling and simulation of industrial processes has a wide application, so the processes in the chemical industry and related biotechnologies and heating technologies, will be discussed. The major part of these processes is the transfer of mass and heat as a result of phase or phase boundary reactions. By reaction, we will understand the creation or disappearance of a particular substance (or amount of heat) as a result of a chemical reaction in the phase or on the phase boundary, interphase mass transfer, adsorption on the phase boundary or a liquid-vapor-liquid phase transition. These reactions result in varying concentrations and temperatures in the phases, i. e. to a deviation from the thermodynamic equilibrium and as a result of the mass transfer and heat transfer to restore the thermodynamic equilibrium. The models of mass transfer and heat transfer are analogous and, therefore, the models of mass transfer in industrial processes will be presented.

2. Thermodynamic approximation

The reactions deviate the industrial systems from the thermodynamic equilibrium and the industrial processes for its recovery begin. The determining of the rate of these processes is a major problem in the industry, as it is the basis for their optimal design and control. This gives reason to use the thermodynamic laws of irreversible processes such as mathematical structures in the construction of the process models, described by extensive and intense variables (in the case of merging of two identical systems, the extensive variables double their values, while the intensive variables retain their values).

The kinetics of the irreversible processes use the mathematical structures resulting from Onsanger's "linearity principle" [3]. According to him, the mean values of the derivatives at the time of the extensive variables depend linearly on the mean deviations of the conjugated intensive variables from their equilibrium states (values). This principle is valid in the vicinity of the equilibrium, and proportionality coefficients are kinetic (rate) constants.

According to the principle of linearity, the mass derivative at time $J_0 = \frac{dm}{dt}$ [kg-mol.s^{-1}] depends linearly on the deviation from the thermodynamic equilibrium Δc [kg-mol.m^{-3}] of the concentration in two phase volumes or in one phase and the phase boundary, i.e.

$$J_0 = k_0 \Delta c, \tag{1}$$

where k_0 [m^3.s^{-1}] is a proportionality coefficient.

Consider a system that contains two identical volumes in one phase $v_1 = v_2 = v$ [m^3]. The system contains a substance whose masses m_i [kg-mol] and concentrations $c_i = \frac{m_i}{v_i}$ [kg-mol.m-3] are different in two volumes, $i = 1, 2, .$ The system is not in thermodynamic equilibrium. Let us assume for certainty $c_1 - c_2 > 0,\ i = 1, 2$. As a result, the mass of the substance starts to be transferred from volume v_1 to volume v_2 for to achieve the equilibrium. According to the principle of linearity, the mass transfer rate between the two volumes J_0 [kg-moll.s^{-1}] can be represented as:

$$J_0 = \frac{dm_1}{dt} = -\frac{dm_2}{dt} = k_0 \left(c_1 - c_2 \right), \tag{2}$$

where k_0 [kg-mol^{-1}.m^3.s^{-1}] is a proportionality coefficient. If we replace masses with concentrations $m_i = v_i c_i, i = 1,2$, the mass transfer rate in one phase J [kg-mol.m^{-3}.s^{-1}] between two points with different concentrations is:

$$J = \frac{dc_1}{dt} = -\frac{dc_2}{dt} = k\left(c_1 - c_2\right), \tag{3}$$

where k [s^{-1}] is a rate coefficient. This equation is capable of presenting the rate of interphase mass transfer in the case of adsorption or catalytic process, where c_1 is the concentration of the substance in the gas phase, while c_2 is the concentration of the substance in the gaseous portion of the solid (capillaries of the adsorbent or catalyst) phase.

In the cases, where the volumes $v_1 = v_2 = v$ are in different phases (for example, 1 is a gas phase and 2 is a liquid phase), the thermodynamic equilibrium law has the form $c_1 - \chi c_2 = 0$, i.e. this is the law of Henry and χ is the number of Henry. If $c_1 - \chi c_2 > 0$ the mass transfer is from phase 1 to phase 2 and the mass transfer rate between phases is:

$$J = k\left(c_1 - \chi c_2\right), \tag{4}$$

where k [s-1] is the rate coefficient of the interfacial mass transfer.

On the surface between two phases, the thermodynamic equilibrium is immediately established, practically, i.e. $c_1^* - \chi c_2^* = 0$, where $c_i^*, i = 1,2$, are the equilibrium concentrations on the phase boundary. Thus, the mass transfer rate can be expressed by mass transfer rate in two phases:

$$J = k_1\left(c_1 - c_1^*\right) = k_2\left(c_2^* - c_2\right), \tag{5}$$

where $k_i, i = 1,2$ [s^{-1}] are mass transfer rate coefficients.

The Onsanger principle of linearity represents the thermodynamic approximation of the mathematical description of the kinetics of irreversible processes, but it does not show the way to reach equilibrium, i.e. the mechanism of the process and as a result the rate coefficient, is not known. Obviously, this "thermodynamic level" does not allow a real quantitative description of the kinetics of irreversible processes in industry and the next level of detail of the description, the so-called "hydrodynamic level", should be used.

3. Hydrodynamic approximation

The processes in the chemical industry and related biotechnologies and heating technologies are realized in one-, two- and three-phase systems (gas-liquid-solid). They are a result from the reactions, i.e. processes of disappearance or creation of any substance. The reactions are associated with a particular phase and can be homogeneous (occurring in volume of the phase) or heterogeneous (occurring at the interface with another phase). Homogeneous reactions are usually chemical, while heterogeneous reactions may be chemical, catalytic and adsorption. Heterogeneous reaction is the interphase mass transfer too, where on the interphase boundary the substance disappears (created) in one phase and creates (disappears) in the other phase.

The volume reactions lead to different concentrations of the reagents in the phase volumes and as a result two mass transfer processes are realized – convective transfer (caused by the movement of the phases) and diffusion transfer (caused by the concentration gradients in the phases). The mass transfer models are a mass balance in the phases, where components are convective transfer, diffusion transfer and volume reactions (volume mass sources or sings). The surface reactions participate as mass sources or sings in the boundary conditions of the model equations. The models of this complex process are possible to be created on the basis of the mass transfer theory as a main approach to quantitative description of the industrial processes.

The mass transfer theory combines the chemistry, physics and mathematics and builds its logical structures on three main "axioms":

1. The postulate of Stokes for the linear relationship between the stress and deformation rate, which is the basis of the Newtonian fluid dynamics models;

2. The first law of Fick for the linear relationship between the mass flow and the concentration gradient, which is the basis of the linear theory of the mass transfer;

3. The first law of Fourier for the linear relationship between the heat flux and the temperature gradient, which is the basis of the linear theories of the heat transfer.

These are the laws of the impulse, mass and energy transfer.

In Boltzmann's kinetic theory of the ideal gas, these axioms are replaced by the "elastic shock" axiom (in a shock between two molecules the direction and the velocity of the movement change, but the sum of their kinetic energies is retained, i.e. there is no loss of kinetic energy) and the rate coefficients are theoretically determined by the average velocity and the average free run of the molecules.

The contemporary mass transfer theory is based of diffusion boundary layer theory (Landau, Levich [4]). This approach substitutes (physically justified) elliptic partial differential equations with parabolic partial differential equations, which facilitates their mathematical solution and offers a mathematical description of physical processes with free (not predetermined) ends.

The diffusion boundary layer theory is developed in the cases of drops and bubbles (Levich, Krylov [5]), film flows (Levich, Krylov, Boyadjiev, Beshkov[6, 7]), non-linear mass transfer and hydrodynamic stability (Krylov, Boyadjiev, Babak [8, 9]).

The diffusion boundary theory is not applicable to the modeling of chemical, absorption, adsorption and catalytic processes in column apparatuses, which necessitated the creation of new type of convection-diffusion and average-concentration models (Chr. Boyadjiev, M. Doichinova, B. Boyadjiev, P. Popova-Krumova [10]). where the unknown interphase surface requires substitution of the surface reactions with equivalent volume reactions and the unknown velocity distribution with the average velocity and experimentally determined parameters.

The theory of mass transfer allows the construction of the process model if its physical mechanism is known. The model thus obtained allows for the identification of this mechanism, i.e. the determining of the significant physical effects and rejection of the insignificant, using the generalized analysis method [11].

4. Physical mechanism identification

The qualitative analysis of the models permits to be made the physical mechanism identification, using generalized variables [11], whereas characteristic (inherent) scales are used the maximal or average values of the variables. The introduction of the generalized variables leads to ddimensionless model. As a result the unity is the order of magnitude of all functions and their derivatives in the model, i.e. the effects of the physical and chemical phenomena (the contribution of the terms in the model), are determined by the orders of magnitude of the dimensionless parameters in the model. If all model equations are divided by the dimensionless parameter, which has the maximal order of magnitude, all terms in the model equations will be classified in three parts:

1. The parameter is unity or its order of magnitude is unity, i.e. this mathematical operator represents a main physical effect;

2. The parameter's order of magnitude is 10^{-1}, i.e. this mathematical operator represents a small physical effect;

3. The parameter's order of magnitude is $\leq 10^{-2}$, i.e. this mathematical operator represents a very small (negligible) physical effect and has to be neglected, because it is not possible to be measured experimentally.

After the physical mechanism identification the model contains a minimum number of parameters which must be determined experimentally.

5. Parameters identification

In general case, the identification of the parameters in the model is made by the minimization of the least squares function by the inverse identification problem solution [11]. The least squares function represents the sum of the squares of the differences between the calculated and the experimental values of the functions in the model and its minimum must be obtained with respect to the parameters in the model. This inverse identification problem is very often incorrect and needs special methods for the solutions [11].

6. Statistical analysis of the model adequacy

The stochastic nature of the errors during the experimental data determination leads to subsequent errors of the mode parameters. The model is adequate if the variance of the statistical error of the model does not exceed the variance of the statistical error of the experimental data, i. e. the accuracy of the functions calculation by the model is not less than the accuracy of the function experimental measurement [11].

7. Processes simulation

The process simulation uses the most common numerical methods of applied mathematics to solve model equations. For this purpose, commercial software is usually used. In many cases, however, it is necessary to introduce this software into specialized algorithms [10, 11].

References

[1] Е. Л. Фейнберг, Две культуры. Интуиция и логика в искусстве и науке, ВЕК 2, Фрязино, 2004, 286 сс.

[2] Chr. Boyadjiev, Some Thoughts on Logic and Intuition in Science and Chemical Engineering, Open Access Library Journal, 1, №6, 1-5, 2014.

[3] Keizer J., Statistical Thermodynamics of Nonequilibrium Processes, Springer-Verlag, New York, 1987.

[4] L. D. Landau, E. M. Lifshitz, Fluid Mechanics, Pergamon, Oxford, 1989.

[5] V. G. Levich, Physicochemical Hydrodynamics, Prentice Hall, New York, 1962.

[6] Chr. Boyadjiev, V. Beschkov, Mass Transfer in Liquid Film Flows, Publ. House Bulg. Acad. Sci., Sofia, 1984.

[7] Хр. Бояджиев, , В. Бешков, Массоперенос в движущихся пленках жидкости. Москва, Изд. „Мир“, 1988.

[8] В. С. Крылов, Хр. Бояджиев, Нелинейный массоперенос. Новосибирск, Изд. Институт теплофизики СОРАН, 1996.

[9] Chr. B. Boyadjiev, V. N. Babak, Non-Linear Mass Transfer and Hydrodynamic Stability, New York, ELSEVIER, 2000.

[10] Chr. Boyadjiev, M. Doichinova, B. Boyadjiev, P. Popova-Krumova, Modeling of Column Apparatus Processes, Springer-Verlag, Berlin Heidelberg, 2016.

[11] Chr. Boyadjiev, Theoretical Chemical Engineering. Modeling and simulation, Springer-Verlag, Berlin Heidelberg, 2010.

APPLICATION OF THE THEORY OF MECHANISMS TO SOLVE PROBLEMS FROM GEOMETRY

M.Sc. Ćulafić S.[1]
Faculty of Mechanical Engineering – University of Montenegro, Montenegro [1]
stefanc@ac.me

Abstract: *This paper deals with the process by which pure geometric problems, such as determining the position of the triangle or line whose points should lie on circles or straight lines, or that edges of the triangle tangle circles or similar. By moving from the field of geometry to the field of the theory of mechanisms, it is possible to relatively simply describe problem with the system of nonlinear equations to reduce on the problem of finding zeros of the polynomials of a certain degree. Problem of solving a system of nonlinear equations reduces to the problem of linear algebra, which, from the aspect of numerical analysis, is a significant advantage. The paper deals with the solution of a concrete problem.*

Keywords: geometric problem, planar linkage mechanisms, mechanisms analysis

1. Introduction

The object of this paper is to solve some pure geometric problems by transforming the same into the problem of the analysis of the position of related kinematic structures, of which plain linkage mechanisms with rotational and sliding kinematic pairs are assembled. After the transformation has been made the problem of geometric analysis is solved by methods of the analysis of the position of the plain linkage mechanisms. The analysis of the position of the plain linkage mechanisms will be performed on the basis of the algebra of complex numbers. After obtaining the analysis solution of the position of the observed structure it is possible to present the solution of the initially observed geometric problem.

2. Setting and procedure for solving the problem

The following possible problems will be considered:

- Determining the position and number of possible positions that the ABC triangular plate occupies so that the ABC points are located on known circles C_A, C_B, C_C (see Fig 1.) or, instead of some circles, straight lines (see Fig 2.)

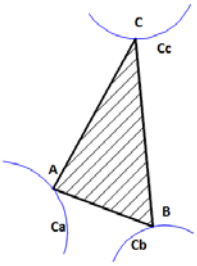

Fig 1.: Paths of points A,B,C are circles

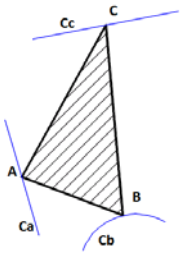

Fig 2.: Paths of points A and C are straight lines, and path of point B is circle

- Determining the position and number of possible positions that the triangular plate ABC occupies so that points A, B occupy on the known circles C_A and C_B, and that the third party of triangle tangles the third curve C_C (see Fig 3.) or that all three sides of the ABC triangle tangle the circles (see Fig 4.)

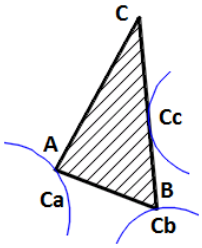

Fig 3.: Paths of points A and B are circles, and line BC tangles circle

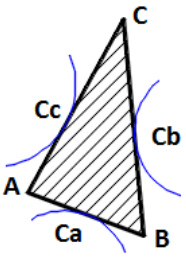

Fig 4. :Lines AB, BC and CA tangles the circles

- Determination of possible positions that line ABC takes along, so for example, points A, B, C of the line lie on circles (see Fig 5.) or, for example, the points A and B of the line lie on the straight lines, and line tangles known circle C_C (see Fig 6.).

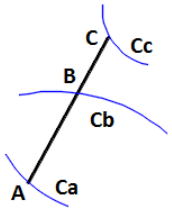

Fig 5.:Paths of points A, B and C are circles

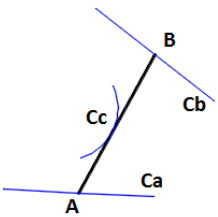

Fig 6. : Paths of points A and B are straight lines, and line AB tangles the circle

All of these problems will be solved forming of appropriate structures with rotational and sliding kinematical pairs. This will enable us to use methods of analysis of the mentioned structures, ie, the methods of analysis of plain linkage mechanisms to solve these problems.

Mechanisms that correspond to these problems look like on the Figure 7.

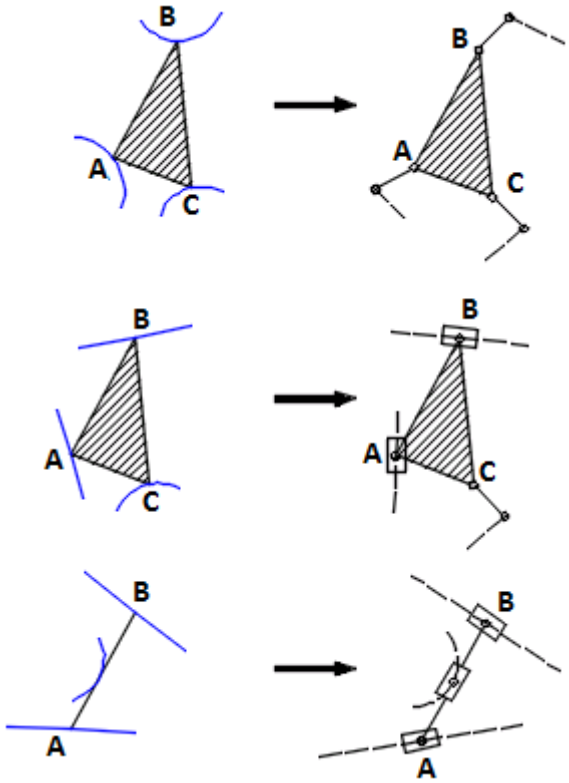

Fig 7. : Transformation of geometric problems into mechanisms

3. Solution of the problem

A concrete problem will be considered. Possible positions of the line AB (see Fig 8) should be found, so that points A and B are respectively located on straight lines C_A and C_B, and line AB passes through the point C (0,0) where $\overline{AB}$= 3.0, and point D has coordinates (-0.5 and 2)

The geometric problem shown in the Figure 8. is joined by the structure, i.e. a mechanism, with rotational and sliding kinematic pairs shown in the Figure 9. [1],[2],[3].

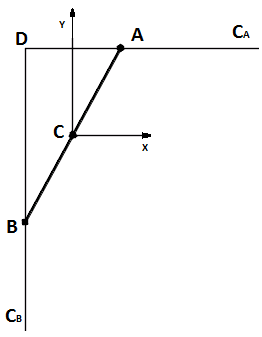

Fig 8.: Geometric problem

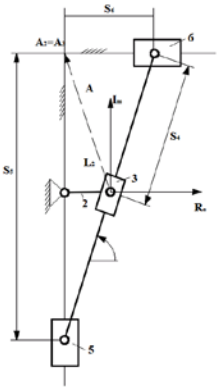

Fig 9.:Mechanism that corresponds to the problem from Fig 8.

$$L_1 e^{i(\varphi-\pi/2)} + S' e^{i(\theta)} + a_k e^{i(\varphi-\pi/2)} = \boldsymbol{A_k} + L_k e^{i\left(\alpha_{k-\pi/2}\right)} + S_k e^{i\alpha_k} = 0$$

$$\boldsymbol{t} = e^{i\varphi}$$

$$\boldsymbol{u} = S'$$

$$-L_1\, i\, \boldsymbol{t} + u\, t - a_k\, i\, \boldsymbol{t} = \boldsymbol{A_k} + S_k\, i\, e^{i\alpha_k} - i\, \boldsymbol{L_k} e^{i\boldsymbol{\alpha_k}} \quad / e^{-i\alpha_k}$$

$$\boldsymbol{t}\left[-(L_1 + a_k) i\, e^{i\alpha_k} + u e^{-i\alpha_k}\right] = \boldsymbol{A_k} e^{-i\alpha_k} + L_k\, i + S_k \ldots (*)$$

$$\boldsymbol{H} = -(L_1 + a_k) i\, e^{i\alpha_k}$$

$$F = Im\left(\boldsymbol{A_k} e^{-i\alpha_k}\right) - L_k$$

$$Im(*): Im(\boldsymbol{t}) Re(H + u\cos\alpha_k) + Re(\boldsymbol{t})(Im(H) - u\, sin\alpha_k) = F$$

$$i\,\frac{1-\boldsymbol{t^2}}{2\,\boldsymbol{t}} Re(\boldsymbol{H} + u\cos\alpha_k) + \frac{1+\boldsymbol{t^2}}{2\,\boldsymbol{t}}(Im(\boldsymbol{H}) - u\, sin\alpha_k) = F$$

$$\boldsymbol{t}^2 + \frac{-2\,\boldsymbol{F}}{Im(\boldsymbol{H}) - Re(\boldsymbol{H}) i - (\cos\alpha_k\ i + sin\alpha_k)\, u}\boldsymbol{t} + \frac{Re(\boldsymbol{H}) i + Im(\boldsymbol{H}) + (\cos\alpha_k\ i + sin\alpha_k) u}{Im(\boldsymbol{H}) - Re(\boldsymbol{H}) i - (\cos\alpha_k\ i + sin\alpha_k)\, u} = 0$$

gdje je: $\boldsymbol{2B} = \frac{-2\,\boldsymbol{F}}{Im(\boldsymbol{H}) - Re(\boldsymbol{H}) i - (\cos\alpha_2\, i + sin\alpha_2)\, u}$; $\boldsymbol{C} = \frac{Re(\boldsymbol{H}) i + Im(\boldsymbol{H}) + (\cos\alpha_k\, i + sin\alpha_k)\boldsymbol{u}}{Im(\boldsymbol{H}) - Re(\boldsymbol{H}) i - (\cos\alpha_k\, i + sin\alpha_k)\,\boldsymbol{u}}$

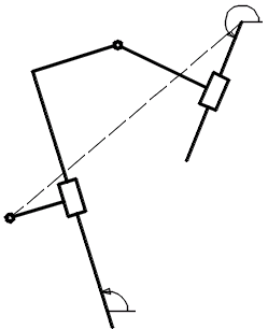

Fig. 10: Structure R-S-R-S

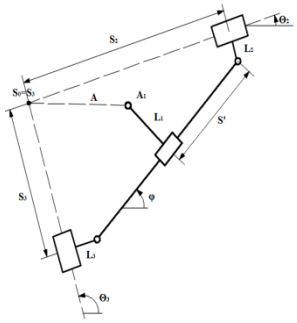

Fig. 11. :Structure R-S-R-S with symbols

In its structure Assur's structural group of III class (see Fig 9.) has three rotational and three sliding kinematic pairs of which two are external, and one is internal [1]. General shape of this structure is given on the Figure 11.

It can be concluded that observed structure consists of two chains of the same structure: R-S-R-S and R-S-R-S. For the chain R-S-R-S for k=2 it is: L_1=0; L_2=0; θ_2=0 so it has shape shown in Figure 12:

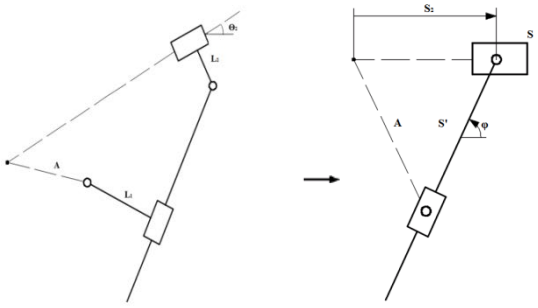

Fig 12.: First structure R-S-R-S

For the chain R-S-R-S for k=3 it is: L_1=0; L_3=0; θ_3=-$\pi/2$; a_3=3 so it has shape shown in Figure 13:

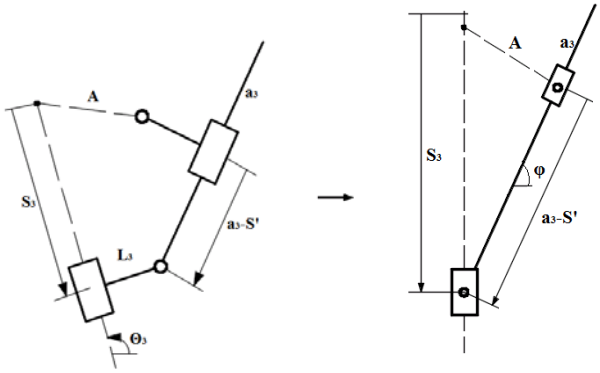

Fig 13.: Second structure R-S-R-S

For each of the chains (see Fig 12. and Fig 13.) equations of the following shape can be written:

$$\boldsymbol{t^2} + 2\boldsymbol{B_k}\,\boldsymbol{t} + \boldsymbol{C}_k = 0; k = 2{,}3$$

ie. equations can be written:

$$\boldsymbol{t^2} + 2\boldsymbol{B}_2\,\boldsymbol{t} + \boldsymbol{C}_2 = 0$$

$$\boldsymbol{t^2} + 2\boldsymbol{B}_3\,\boldsymbol{t} + \boldsymbol{C}_3 = 0$$

where: $\boldsymbol{t} = e^{i\varphi}$; $\boldsymbol{u} = S'$;

$\boldsymbol{A} = -0{,}5 \cdot i\ 1{,}2$; $\boldsymbol{H}_2 = -(L_1 + a_2)e^{i\alpha_2} = 0 + i0$; $F_2 = 1{,}2$; $2\boldsymbol{B}_2 = \frac{-2\cdot 1{,}2}{-u\cdot i}$;

$$\boldsymbol{c}_2 = \frac{u}{-u} = -1; \boldsymbol{H}_3 = 0 + i\ 0; F = -0{,}5; 2\boldsymbol{B}_3 = \frac{-2(-0{,}5)}{(3-u)i} = \frac{1}{(3-u)i}; \boldsymbol{c}_3 = \frac{u}{u} = 1$$

so previous system of the equations has shape as:

$$\boldsymbol{t^2} + \frac{2{,}4}{u\ i}\,\boldsymbol{t} - 1 = 0;$$

$$\boldsymbol{t^2} + \frac{1}{(3-u)\ i}\,\boldsymbol{t} + 1 = 0;$$

It is not hard to show that system of previously given two square equations, after elimination of **t**, can be written as polynomial of fourth degree with real variable **u** and real coefficients

$$\boldsymbol{u}^4 - 6{,}0\,\boldsymbol{u}^3 + 7{,}31\,\boldsymbol{u}^2 + 8{,}64\,\boldsymbol{u} - 12{,}96 = 0$$

4. Results and conclusion

With determining **u** geometry of the structure is defined, where all possible solutions of the equation are considered, which would not be as simple as if the given system of four equations as in the beginning of the example was to solve[3].

Four roots of the polynomial are:

$$u = (s)_1 = 1.252; t = e^{\theta_{41}} = 0{,}286 + 0{,}958i; \theta_{4_1} = 73.375$$

$$u = (s)_2 = 2.425; t = e^{\theta_{42}} = 0{,}869 + 0{,}495i; \theta_{4_2} = 29.664$$

$$u = (s)_3 = 3.532; t = e^{\theta_{43}} = -0{,}94 + 0{,}34i; \theta_{4_3} = -19.863$$

$$u = (s)_4 = -1.209; t = e^{\theta_{44}} = 0{,}119 - 0{,}993i; \theta_{4_4} = -83.177$$

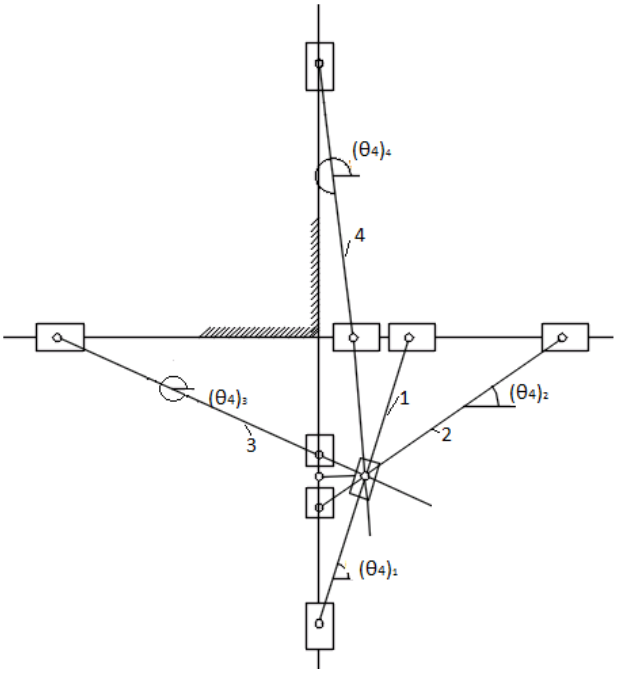

Fig. 14. :Solution of the mechanism positions

Solution of the problem of mechanism analysis is given on the Figure 14., and solution of the starting geometric problem is given on the Figure 15.

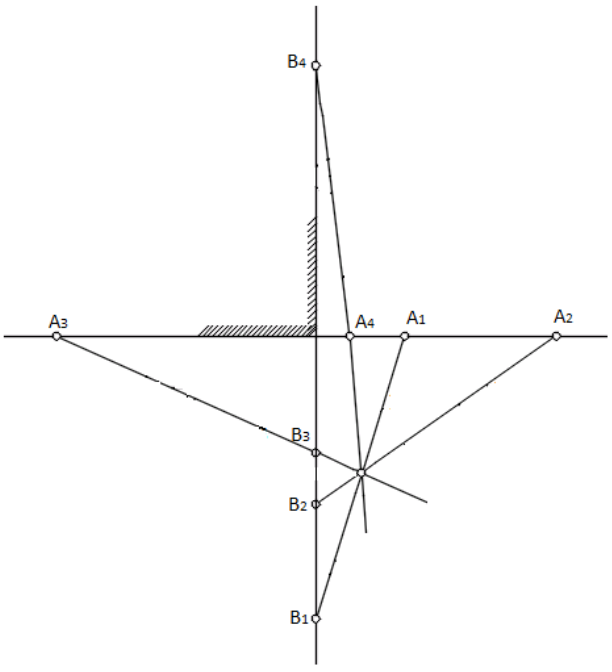

Fig. 15. :Solution of the starting geometric problem

First, a geometric problem is defined, that is: point A and point B, and line AB must lie on a horizontal and vertical straight line, and line AB should tangle the circle (whose radius is zero). Secondly, to the geometric problem corresponds the mechanism consisting of two R-S-R-S structures. Thirdly, the analysis of the observed structure, ie the mechanism, based on complex algebra was performed. The solutions obtained define the 4 positions of the mechanism. Fourth, by returning to the starting geometric problem, 4 positions of the line AB are defined such that point A is on the horizontal line, point B on a vertical line, and the AB line touches the circle with the center at the point C of the radius equal to zero, that is, line AB passes through point Č.

5. Literature

[1] S.ĆULAFIĆ: Numeričko modeliranje geometrije nepokretnih struktura; KODIP 2017, Budva, Montengro, 2017.

[2] B. POUL: Kinematics and dynamics of planar machinery; Prentice-Hall; Inc. Englewood Cliffs, N.J 07632, 1979

[3] G. ĆULAFIĆ: Analitička geometrijska analiza polužnih mehanizama više klase, XXI Jugoslovenski kongres teorijske i primijenjene mehanike, Niš, 1995

LAPLACIAN PRESERVING TRANSFORMATION OF SURFACES AND APPLICATION TO BOUNDARY VALUE PROBLEMS FOR LAPLACE'S AND POISSON'S EQUATIONS

Ph.D. Gospodinov I., M.Sc. Krumov K., M.Sc. Filipov S.
Department of Computer Science – University of Chemical Technology and Metallurgy, Bulgaria
idg2@cornell.edu

***Abstract**: This paper shows that the constrained similarity transformation of surfaces under boundary constraints is a Laplacian preserving transformation. First, a general proof is presented and then the result is verified for mesh-functions through particular examples. The fact that the constrained similarity transformation, subject to boundary constraints, is a Laplacian preserving transformation is used to construct a method for solving boundary value problems for the Laplace's and the Poisson's equations. Given any solution to these equations we apply the constrained similarity transformation to get the particular solution that satisfies the given boundary conditions.*

Keywords: CONSTRAINED SIMILARITY OF SURFACES, LAPLACIAN PRESERVING TRANSFORMATION, PARTIAL DIFFERENTIAL EQUATIONS, LAPLACE'S EQUATION, POISSON'S EQUATION, BOUNDARY VALUE PROBLEM

1. Introduction

Constrained similarity transformation for functions of one independent variable has been defined in [1] via minimizing the H^1 semi-norm [2] of the functional difference. An exact general solution for mesh-functions has been obtained. The results were used as basis to construct the *shooting-projection* method for solving two-point boundary value problems for second order ordinary differential and integro-differential equations [3], [4]. In [5] the results obtained in [1] have been extended to functions of two independent variables, i.e. to surfaces. An exact general solution for constrained similarity transformation of mesh-surfaces under linear constraints has been obtained. In the current paper these results will be used to construct a method for solving two-point boundary value problems for the Laplace's and the Poisson's equations. In what fallows we briefly summarise the main results for constrained similarity transformation of surfaces.

Let $z=z(x,y)$ and $z^*=z^*(x,y)$ be two real-valued functions of the real independent variables $(x,y)\in G$, where G is bounded domain in R^2. The functions z and z^* define two surfaces. Suppose the surface z is given together with a set of constrains that the surface does not meet. The surface z^* that satisfies the constraints and minimizes

$$\iint_G (\nabla z^* - \nabla z)^2 \, dxdy = \iint_G \left(\frac{\partial z^*}{\partial x} - \frac{\partial z}{\partial x} \right)^2 dxdy + \iint_G \left(\frac{\partial z^*}{\partial y} - \frac{\partial z}{\partial y} \right)^2 dxdy, \tag{1}$$

is called *similar* to the surface z under the imposed constraints [5]. In (1) $\nabla=(\partial/\partial x,\ \partial/\partial y)$ is the Nabla operator (gradient). The transformation of z into z^* is called *constrained similarity transformation of surfaces*.

Consider a rectangular domain $G=\{(x,y)|\ x\in[x_a,x_b], y\in[y_a,y_b]\}$. Suppose the intervals $x\in[x_a,x_b]$ and $y\in[y_a,y_b]$ could be partitioned by N_x and N_y mesh-points into N_x-1 and N_y-1 intervals of size h, respectively. The set of points $\{(x_k,y_l),\ x_k=x_a+(k-1)h,\ y_l=y_a+(l-1)h,\ k=1,2,\ldots,N_x,\ l=1,2,\ldots,N_y\}$ defines a *uniform mesh* on the rectangle. The constant h is the step-size of the mesh. Let the surface $z(x,y)$ be given as *mesh-surface*, i.e. $z=\{z_{k,l}=z(x_k,y_l),\ k=1,2,\ldots,N_x,\ l=1,2,\ldots,N_y\}$. In order to define constrained similarity between the given surface z and $z^*=\{z^*_{k,l}\ ,\ k=1,2,\ldots,N_x,\ l=1,2,\ldots,N_y\}$ expression (1) is discretized yielding the following *objective function*:

$$I = \sum_{k=1}^{N_x-1}\sum_{l=1}^{N_y} ((z^*_{k+1,l} - z^*_{k,l}) - (z_{k+1,l} - z_{k,l}))^2 + \sum_{k=1}^{N_x}\sum_{l=1}^{N_y-1} ((z^*_{k,l+1} - z^*_{k,l}) - (z_{k,l+1} - z_{k,l}))^2. \tag{2}$$

To use the formulas derived in [1] the following notation is used: $z_{k,l}=u_{k+(l-1).Nx}$, $z^*_{k,l}=u^*_{k+(l-1).Nx}$ for $k=1,2,\ldots,N_x$, $l=1,2,\ldots,N_y$ and the vectors $u=[z_{1,1},z_{2,1},..,z_{Nx,1},z_{1,2},z_{2,2},..,z_{Nx,2},..,z_{1,Ny},z_{2,Ny},..,z_{Nx,Ny}]^T$, $u^*=[z^*_{1,1},z^*_{2,1},..,z^*_{Nx,1},z^*_{1,2},z^*_{2,2},..,z^*_{Nx,2},..,z^*_{1,Ny},z^*_{2,Ny},..,z^*_{Nx,Ny}]^T$ are introduced. The minimum of I is sought subject to M linear constraints:

$$\sum_{i=1}^{N} A_{ji} u^*_i = c_j, \quad j=1,2,...,M < N. \tag{3}$$

where $N=N_xN_y$. The constraints (3) are written in a matrix form as $Au^*=c$, where

$$A = \begin{bmatrix} A_{11} & A_{12} & . & . & . & A_{1N} \\ A_{21} & A_{22} & . & . & . & A_{2N} \\ . & . & . & . & . & . \\ A_{M1} & A_{M2} & . & . & . & A_{MN} \end{bmatrix}, \quad c = \begin{bmatrix} c_1 \\ c_2 \\ . \\ c_M \end{bmatrix} \tag{4}$$

and u^* is the $N\times1$ column-vector of the unknowns. To find u^* that minimizes the objective function (2) and satisfies the constraints (3) the Lagrange's method of the undetermined coefficients [6] is employed obtaining (for derivations see [1] and [5]):

$$u^* = u - (\bar{L} + \bar{A})^{-1}\left(\frac{1}{2} A^T \lambda + \bar{A} u - \bar{c} \right), \tag{5}$$

$$\lambda = 2\left(A(\bar{L} + \bar{A})^{-1} A^T \right)^{-1} \left(Au - c - A(\bar{L} + \bar{A})^{-1}(\bar{A}u - \bar{c}) \right), \tag{6}$$

where $\bar{A}$ is the matrix A augmented with $N-M$ rows of zeros to an $N\times N$ matrix, the column-vector $\bar{c}$ is the column-vector c augmented with $N-M$ zeros to an $N\times1$ column-vector, λ is the $M\times1$ column-vector of the undetermined coefficients λ_j, $j=1,2,\ldots,M$, and $\bar{L}$ is the $N\times N$ ($N=N_xN_y$) matrix, given as block matrix by:

$$\bar{L} = \begin{bmatrix} \overbrace{\begin{matrix} L_1 & E & 0 & 0 & 0 & . & . & 0 \\ E & L_2 & E & 0 & 0 & . & . & 0 \\ 0 & E & L_2 & E & 0 & . & . & 0 \\ & & & . & . & & & \\ & & & & . & . & & \\ & & & & & . & . & \\ 0 & . & . & . & 0 & E & L_2 & E \\ 0 & . & . & . & 0 & 0 & E & L_1 \end{matrix}}^{N_y} \end{bmatrix}, \tag{7}$$

where

$$L_1 = \overbrace{\begin{bmatrix} -2 & 1 & 0 & 0 & 0 & . & . & 0 \\ 1 & -3 & 1 & 0 & 0 & . & . & 0 \\ 0 & 1 & -3 & 1 & 0 & . & . & 0 \\ & & & . & . & & & \\ & & & & . & . & & \\ & & & & & . & . & \\ 0 & . & . & . & 0 & 1 & -3 & 1 \\ 0 & . & . & . & 0 & 0 & 1 & -2 \end{bmatrix}}^{N_x},$$

$$L_2 = \begin{bmatrix} -3 & 1 & 0 & 0 & 0 & . & . & 0 \\ 1 & -4 & 1 & 0 & 0 & . & . & 0 \\ 0 & 1 & -4 & 1 & 0 & . & . & 0 \\ & & & . & . & & & \\ & & & & . & . & & \\ & & & & & . & . & \\ 0 & . & . & . & 0 & 1 & -4 & 1 \\ 0 & . & . & . & 0 & 0 & 1 & -3 \end{bmatrix},$$

the matrix E is the $N_x \times N_x$ unit matrix, and 0 is the $N_x \times N_x$ zero matrix.

The right-hand side of (6) contains only known quantities. Once the column-vector λ is calculated it is substituted into (5) and u^*_i, $i=1,2,\ldots,N$ are obtained. Then u^*_i are converted to $z^*_{k,l}$ and the sought function (surface) is found.

.

2. Laplacian preserving transformation of surfaces as constrained similarity under boundary constraints

In this paragraph we prove that the constrained similarity transformation of the surface $z(x,y)$, $(x,y)\in G$ into the surface $z^*(x,y)$, $(x,y)\in G$ under the boundary constraints $z^*(x,y)=z_0(x,y)$, $(x,y)\in\partial G$, where ∂G is the boundary of the domain G and $z_0(x,y)$ is a given continuous function on the boundary, is a *Laplacian preserving transformation*, i.e.

$$\Delta z^* = \Delta z, \quad (x,y)\in G, \tag{8}$$

where Δ is the Laplace operator (Laplacian):

$$\Delta = \nabla^2 = \frac{\partial^2}{\partial x^2} + \frac{\partial^2}{\partial y^2}. \tag{9}$$

Proof: If a function z^* with fixed values at the boundary ∂G should minimize the functional (1) then the following Euler-Lagrange equation for the integrand $(\nabla z^* - \nabla z)^2$ must hold [6], [7]:

$$\frac{\partial}{\partial x}\left(\frac{\partial(\nabla z^* - \nabla z)^2}{\partial(\partial z^*/\partial x)}\right) + \frac{\partial}{\partial y}\left(\frac{\partial(\nabla z^* - \nabla z)^2}{\partial(\partial z^*/\partial y)}\right) - \frac{\partial(\nabla z^* - \nabla z)^2}{\partial z^*} = 0, \tag{10}$$

Taking into account that

$$(\nabla z^* - \nabla z)^2 = \left(\frac{\partial z^*}{\partial x} - \frac{\partial z}{\partial x}\right)^2 + \left(\frac{\partial z^*}{\partial y} - \frac{\partial z}{\partial y}\right)^2 \tag{11}$$

and performing the differentiation in (10) with respect to $\partial z^*/\partial x$, $\partial z^*/\partial y$, and z^* yields:

$$2\frac{\partial}{\partial x}\left(\frac{\partial z^*}{\partial x} - \frac{\partial z}{\partial x}\right) + 2\frac{\partial}{\partial y}\left(\frac{\partial z^*}{\partial y} - \frac{\partial z}{\partial y}\right) = 0, \ (x,y)\in G, \tag{12}$$

which, after rearranging, is just equation (8).

3. Solving boundary value problems for Poisson's and Laplace's equations using constrained similarity transformation

Let a function $z(x,y)$, $(x,y)\in G$ satisfy the Poisson's equation:

$$\Delta z = -f(x,y), \ (x,y)\in G. \tag{13}$$

In the case when $f(x,y)\equiv 0$ the Poisson's equation is just the Laplace's equation so all the conclusions in this paragraph will hold for both equations. The problem of finding a solution $z^*(x,y)$, $(x,y)\in G$ that satisfies (13) and at the same time satisfies the boundary condition

$$z^*(x,y) = z_0(x,y), \ (x,y)\in\partial G, \tag{14}$$

where ∂G is the boundary of the domain G and $z_0(x,y)$ is a given continuous function on the boundary, constitutes a *boundary value problem* (BVP), more specifically *Dirichlet problem*, for the Poisson's equation [7], [8]. According to the result proven in the previous paragraph, if any function z that satisfies (13) is subjected to constrained similarity transformation under the boundary constraints (14), then the obtained function z^* will satisfy the boundary constraints (14) *and* the differential equation (8), hence also the Poisson's equation (13). Therefore, the obtained function z^* will be just the sought BVP solution.

In the case when G is a rectangular domain in R^2 and z is any solution to (13) given as mesh-function, then the BVP solution z^* can be obtained (as mesh-function) using formulas (5) and (6).

4. Results

In this paragraph two examples are presented. In Example 1 a particular Poisson's equation is considered and three different BVPs for this equation are solved using the constrained similarity transformation of surfaces. It is verified that the constrained similarity transformation is indeed Laplacian preserving transformation. In Example 2 the harmonic function, i.e. twice continuously differentiable function satisfying the Laplace's equation, is found for three particular boundary conditions. Again, the Laplacian is calculated to verify (8).

Example 1

Consider the function (surface) $z(x,y)=xy(y-x)$ defined on the rectangular domain $G=\{(x,y)|\ x\in[-2,2],\ y\in[-2,2]\}$. The function z satisfies the Poisson's equation:

$$\Delta z = -2(y-x), \ (x,y)\in G. \tag{15}$$

Find the function z^* that satisfies (15) and at the same time satisfies the boundary condition $z^*(x,y)= z_0(x,y)$, $(x,y)\in\partial G$, where ∂G is the boundary of the domain G. Solve the problem for the following three cases:

$$\text{(a) } z_0(x,y) = \frac{1}{4}(x-y) \quad \text{(b) } z_0(x,y) = \frac{1}{4}xy \quad \text{(c) } z_0(x,y) = \frac{1}{8}(x^2+y^2) \tag{16}$$

To solve the given BVPs first the intervals $x\in[-2,2]$ and $y\in[-2,2]$ are partitioned by $N_x=21$ and $N_y=21$ mesh-points into intervals of size $h=0.2$ and the surface z is calculated on the mesh: $z=\{z_{k,l}=x_k y_l(y_l-x_k)$, $x_k=-2+(k-1)h$, $y_l=-2+(l-1)h$, $k=1,2,\ldots,N_x$,

l=1,2,…,N_y}. Then the mesh-surface z is subjected consecutively to the constrained similarity transformation (5)-(6) for the three boundary constraints (16) (a)-(c). The obtained surfaces z^*={$z^*_{k,l}$, k=1,2,…,N_x, l=1,2,…,N_y} are shown in Fig. 1. They satisfy the Poisson's equation (15) and the respective boundary conditions (16) (a)-(c), hence they are the sought BVP solutions.

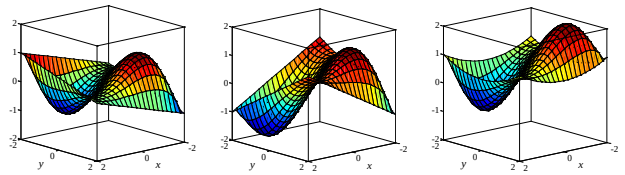

(a) ***(b)*** ***(c)***

Fig.1. *The surface z^* satisfying the Poisson's equation (15) for the respective boundary condition (15)* ***(a)***, ***(b)***, *and* ***(c)***.

To verify that the three surfaces shown in Fig. 1 satisfy the Poisson's equation (15) Δz and Δz^* for case (a), (b), and (c) are calculated for the inner points of the mesh using the central finite difference approximation:

$$\Delta z \approx \frac{z_{k+1,l} + z_{k-1,l} + z_{k,l+1} + z_{k,l-1} - 4z_{k,l}}{h^2}, \qquad (17)$$

where k=2,…,N_x–1, and l=2,…,N_y–1. All four results coincide yielding, within numerical precision, the plane 2(x–y) (see eqn. (15)).

Example 2

Consider the Laplace's equation:

$$\Delta z = 0, \quad (x, y) \in G. \qquad (18)$$

Any function $z(x,y)$ which has continuous second derivatives in the domain G and satisfies the Laplace's equation (18) is called *harmonic* in G [7], [8]. The plane $z(x,y)$=0, $(x,y)\in G$ is obviously harmonic. In this example we find the harmonic function $z^*(x,y)$ that satisfies the boundary condition $z^*(x,y)= z_0(x,y)$, $(x,y)\in\partial G$, where ∂G is the boundary of the domain G={(x,y)| $x\in$[–2,2], $y\in$[–2,2]}. The problem is solved for the following three cases:

$$\text{(a) } z_0(x,y) = \frac{1}{4}xy \qquad \text{(b) } z_0(x,y) = \frac{1}{4}(x^2+y^2) - 1$$

$$\text{(c) } z_0(x,y) = \frac{1}{2}\left(\cos\left(\frac{\pi}{2}y\right) - \sin\left(\frac{\pi}{2}x\right)\right) \qquad (19)$$

To solve the problem, as in Example 1, the intervals $x\in$[–2,2] and $y\in$[–2,2] are partitioned by N_x=21 and N_y=21 mesh-points into intervals of size h=0.2 and the plane $z(x,y)$=0, $(x,y)\in G$ is defined on the mesh: z={$z_{k,l}$=0, x_k=–2+(k–1)h, y_l=–2+(l–1)h, k=1,2,…,N_x, l=1,2,…,N_y}. Then the mesh-plane z is subjected to the constrained similarity transformation (5)-(6) for the three boundary constraints (19) (a)-(c). The obtained surfaces z^*={$z^*_{k,l}$, k=1,2,…,N_x, l=1,2,…,N_y} are shown in Fig. 2. They satisfy the Laplace's equation (18) and the respective boundary conditions (19) (a)-(c).

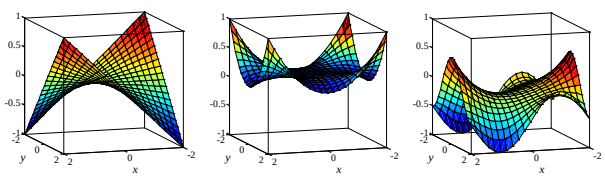

(a) ***(b)*** ***(c)***

Fig.2. *The three surfaces z^* satisfying the Laplace's equation (18) for the respective boundary condition (19)* ***(a)***, ***(b)***, *and* ***(c)***.

To verify numerically that the three functions z^* shown in Fig. 2 are harmonic, first the partial derivatives for the inner points are calculated using the central finite difference approximation:

$$\frac{\partial^2 z^*}{\partial x^2} \approx \frac{z^*_{k+1,l} - 2z^*_{k,l} + z^*_{k-1,l}}{h^2}, \quad \frac{\partial^2 z^*}{\partial y^2} \approx \frac{z^*_{k,l+1} - 2z^*_{k,l} + z^*_{k,l-1}}{h^2}, \qquad (20)$$

where k=2,…,N_x–1, and l=2,…,N_y–1. Then, using the calculated partial derivatives, the Laplacian $\Delta z^*=\partial^2 z^*/\partial x^2+\partial^2 z^*/\partial y^2$ for case (a), (b), and (c) is calculated for the inner points. The obtained results indicate that for all three cases the derivatives (20) are continuous and $|\Delta z^*(x,y)|<10^{-11}$ for all $(x,y)\in G$ (i.e. zero within the numerical precision). Therefore, the obtained functions z^* (Fig. 2) are indeed harmonic.

5. Conclusion

It was proven that the constrained similarity transformation of surfaces is a Laplacian preserving transformation. This fact was used to construct a method for solving boundary value problems for Poisson's and Laplace's equations on rectangular domain when any solution to the respective equation is present. Several examples were solved verifying that the Laplacian of the surface is indeed preserved when the surface is subjected to constrained similarity transformation under boundary constraints.

6. Appendix

In this appendix a MATLAB code for solving Example 1(a) is presented. The code could easily be adjusted to other cases. The variables `A_`, `c_`, and `L_` are used for $\bar{A}$, $\bar{c}$, and $\bar{L}$, while `zs`, `us`, `z0`, and `u0` are used for z^*, u^*, z_0, and u_0. The variable `lambda` is used for λ. To define the needed vectors and matrices first the corresponding vectors and matrices composed of zeros and having the required size are defined.

```
function main

    Nx=21; Ny=21; xa=-2; ya=-2; h=0.2;
    M=2*Nx+2*Ny-4; N=Nx*Ny;

    x=zeros(Nx,1); y=zeros(Ny,1);
    for k=1:Nx
        x(k)=xa+h*(k-1);
    end
    for l=1:Ny
        y(l)=ya+h*(l-1);
    end

    z=zeros(Nx,Ny); z0=zeros(Nx,Ny);
    u=zeros(N,1); u0=zeros(N,1);
    i=1;
    for l=1:Ny
        for k=1:Nx
            z(k,l)=x(k)*y(l)*(y(l)-x(k));
            u(i)=z(k,l);
            z0(k,l)=(1/4)*(x(k)-y(l));
            u0(i)=z0(k,l);
            i=i+1;
        end
    end

    A=zeros(M,N); c=zeros(M,1);
    j=1;
    for k=1:Nx
        i=k; A(j,i)=1; c(j)=u0(i); j=j+1;
    end
    for l=2:Ny-1
        i=Nx*(l-1)+1; A(j,i)=1; c(j)=u0(i); j=j+1;
        i=Nx*(l-1)+Nx; A(j,i)=1; c(j)=u0(i); j=j+1;
    end
    for k=1:Nx
        i=Nx*(Ny-1)+k; A(j,i)=1; c(j)=u0(i); j=j+1;
    end
```

```
    A_=zeros(N,N); c_=zeros(N,1);
    for j=1:M
        c_(j)=c(j);
        for i=1:N
            A_(j,i)=A(j,i);
        end
    end

    L_=zeros(N,N);
    L_(1,1)=-2; L_(Nx,Nx)=-2;
    L_(N-Nx+1,N-Nx+1)=-2; L_(N,N)=-2;
    for n=2:(Nx-1)
        L_(n,n)=-3; L_(N-Nx+n,N-Nx+n)=-3;
        L_(n+1,n)=1; L_(N-Nx+n+1,N-Nx+n)=1;
        L_(n-1,n)=1; L_(N-Nx+n-1,N-Nx+n)=1;
        L_(n+Nx,n)=1; L_(N-Nx+n-Nx,N-Nx+n)=1;
    end
    L_(2,1)=1; L_(Nx-1,Nx)=1;
    L_(1+Nx,1)=1; L_(Nx+Nx,Nx)=1;
    L_(N-Nx+2,N-Nx+1)=1; L_(N-Nx+1-Nx,N-Nx+1)=1;
    L_(N-1,N)=1; L_(N-Nx,N)=1;
    for n=Nx+1:N-Nx
        L_(n,n)=-4; L_(n+1,n)=1; L_(n-1,n)=1;
        L_(n+Nx,n)=1; L_(n-Nx,n)=1;
    end
    for n=1:Ny-2
        L_(Nx*n+1,Nx*n+1)=-3;
        L_(Nx*n+Nx,Nx*n+Nx)=-3;
        L_(Nx*n,Nx*n+1)=0;
        L_(Nx*n+Nx+1,Nx*n+Nx)=0;
    end

    H=inv(L_+A_); d=A_*u-c_;

    lambda=(A*H*A')\(A*u-c-A*H*d)*2;
    us=u-H*(A'*lambda/2+d);

    i=1;
    for l=1:Ny
        for k=1:Nx
            zs(k,l)=us(i);
            i=i+1;
        end
    end

    surface(x,y,zs');

end
```

7. References

[1] Filipov, S., Atanasov, A., Gospodinov, I., Constrained functional similarity by minimizing the H^1 seminorm and applications to engineering problems, Science, Engineering, & Education, 1, (1), pp. 61-67, Journal of Chemical Technology and Metallurgy, 2016.

[2] Adams, R., *Sobolev Spaces*, Academic Press, ISBN 978-0-12-044150-1, 1975.

[3] Filipov, S., Gospodinov, I., Faragó, I., Shooting-projection method for two-point boundary value problems, Applied Mathematics Letters, 72, pp. 10-15, Elsevier, 2017.

[4] Filipov, S., Gospodinov, I., Angelova, J., Solving Two-Point Boundary Value Problems for Integro-Differential Equations Using the Simple Shooting-Projection Method, Lecture Notes in Computer Science, 8962, Numerical Methods and Applications, pp. 169-177, Springer, 2015.

[5] Filipov, S., Nikolov, V., Gospodinov, I., Constrained similarity of surfaces by minimizing the L^2 norm of the gradient of the surface difference, Industry 4.0, Issue 2, pp. 78-80, Scientific Technical Union of Mechanical Engineering, 2016.

[6] Arfken, G., *Mathematical Methods for Physicists*, 3rd ed. Orlando, FL: Academic Press, 1985.

[7] Bronshtein, I. N. and Semendyayev, K. A., *Handbook of Mathematics*, 3rd ed. New York: Springer-Verlag, 1997.

[8] Sobolev S. L., *Partial Differential Equations of Mathematical Physics*, Dover Publications, 1989.

MATHEMATICAL MODELING OF NON-STATIONARY FLOWS OF LIQUID HOMOGENEOUS VISCOUS MIXTURES BY PIPELINES

МАТЕМАТИЧЕКОЕ МОДЕЛИРОВАНИЕ НЕСТАЦИОНАРНЫХ ТЕЧЕНИЙ ЖИДКИХ ОДНОРОДНЫХ СМЕСЕЙ ПО ТРУБОПРОВОДАМ

Prof., Dr. Tech. Sci. Firsov A.[1], Asst., MSc Sorokina N.[2]
Peter the Great St. Petersburg Polytechnic University – St. Petersburg, Russia
E-mail: anfirs@yandex.ru[1], snv_special@inbox.ru[2]

Abstract: *In the work a mathematical model for the non-stationary motion of liquid homogeneous viscous mixtures through pipelines is constructed. The corresponding integral equations expressing the laws of conservation of mass, momentum and energy are deriving, from which, in turn, we get the corresponding differential equations. The formulation of the initial and boundary conditions is given; the necessary additional relations that close the corresponding system of differential equations are indicated. A numerical algorithm for solving such a system is proposed. The corresponding numerical examples are given.*
Keywords: PIPELINES, HOMOGENEOUS VISCOUS MIXTURES, NONSTATIONARY MOTION, MATHEMATICAL MODELS, NUMERICAL ANALYSIS

1. Introduction

Trunk pipeline systems have become widespread in various areas of the economy, in particular in the oil and gas and oil refining industries.

Therefore, the task of improving the quality of control of such systems is an important task. One of the most effective ways to solve this problem is to improve the methods of mathematical modeling of the modes of pipeline systems and models for controlling stationary and transient modes of pipeline systems. Approach to the solution of these problems requires the development of mathematical models of pipe networks for numerical analysis of modes and mathematical modeling of control devices, providing the predetermined conditions of viscous liquids in pipe networks.

The difficulty of modeling for the analysis and synthesis of controls for such systems is determined by the complexity and variety of the dynamic description of the flow of viscous liquids in pipelines, as well as the need to take into account many additional factors. On the other hand, the mathematical modeling of pipeline networks is based on the problem of analyzing the solvability of the corresponding initial-boundary value problems for the differential equations of motion of a viscous liquid along a circular pipe, and also on the problem of choosing numerical algorithms for constructing the corresponding solutions. It is natural to base the mathematical modeling of the corresponding processes on the Navier-Stokes equations, but there is no exhaustive (from the mathematical point of view) analysis of the correctness of the initial-boundary value problems for these equations in publications available to authors. Moreover, for real processes, the Navier-Stokes equations are, as a rule, only "first approximation". Therefore, in practice, various simplified mathematical models are used by introducing additional hypotheses about the properties and nature of the motion of liquids in a particular problem. A fairly comprehensive review of simplified mathematical models describing the motion of viscous liquids through pipelines can be found, for example, in [1-4].

In this paper, we do not pretend to be exhaustive, but try to present a solution of the initial-boundary problem of the motion of a viscous liquid along a horizontal cylindrical tube without traditional simplifying hypotheses, relying on the full Navier-Stokes equation, and assuming only the cylindrical symmetry of the problem.

2. Basic equations and statement of the problem

In the basis of the investigation, we shall set the general equations of continuum mechanics in differential form (see, for example, [5]):

$$\frac{d\rho}{dt} + \rho\left(\vec{\nabla}\cdot\vec{\upsilon}\right) = q\,, \tag{1}$$

$$\rho\frac{d\vec{\upsilon}}{dt} = \rho\vec{F} + \frac{\partial\vec{\tau}_x}{\partial x} + \frac{\partial\vec{\tau}_y}{\partial y} + \frac{\partial\vec{\tau}_z}{\partial z}\,, \tag{2}$$

$$\rho\frac{d\vec{M}}{dt} = \rho\vec{\Pi} + \vec{i}\times\vec{\tau}_x + \vec{j}\times\vec{\tau}_y + \vec{k}\times\vec{\tau}_z + \frac{\partial\vec{\pi}_x}{\partial x} + \frac{\partial\vec{\pi}_y}{\partial y} + \frac{\partial\vec{\pi}_z}{\partial z}\,, \tag{3}$$

$$\rho\frac{dE}{dt} = \varepsilon + \vec{\tau}_x\cdot\frac{\partial\vec{\upsilon}}{\partial x} + \vec{\tau}_y\cdot\frac{\partial\vec{\upsilon}}{\partial y} + \vec{\tau}_z\cdot\frac{\partial\vec{\upsilon}}{\partial z} + \vec{\nabla}\cdot\vec{t}\,. \tag{4}$$

Here: $\vec{i},\vec{j},\vec{k}$ – are unit coordinate vectors of the corresponding Cartesian coordinate system; $\rho = \rho(x,y,z,t)$ – a liquid density at a point with Cartesian coordinates (x,y,z) at time t; $\vec{\upsilon} = \vec{\upsilon}(x,y,z,t) = \upsilon_x\vec{i} + \upsilon_y\vec{j} + \upsilon_z\vec{k}$ – the liquid velocity at a point (x,y,z) at time t; $\vec{t} = \vec{t}(x,y,z,t) = t_x\vec{i} + t_y\vec{j} + t_z\vec{k}$ – a heat flux vector; $\vec{F} = \vec{F}(x,y,z,t)$ – a (external) mass force per unit mass, acting in the fluid; $q = q(x,y,z,t)$ – a density of mass sources in the liquid per time unit; E – a mass density of the liquid internal energy; ε –a rate of volume absorption (excretion) of energy in the fluid; t_n – a rate of internal energy transmission in a continuous medium through a unit area with a normal $\vec{n}$, i.e. the $dQ_S = dt\iint_S t_n\,ds$ is the amount of energy (heat) have passed within time dt through the closed (virtual) surface S (with the external normal $\vec{n}$), bounding some liquid volume; $\vec{M} = \vec{M}(x,y,z,t)$ – an internal angular momentum of the fluid, which a unit of liquid mass possesses; $\vec{\Pi} = \vec{\Pi}(x,y,z,t)$ – an internal angular momentum per mass unit and time unit, which is generated in a volume unit of the liquid; $\vec{\pi}_n = \vec{\pi}_n(x,y,z,t)$ – an internal angular momentum per area unit with the normal $\vec{n}$, penetrating through a (virtual) surface in the liquid per time unit.

$$\vec{\vec{T}} = \begin{pmatrix} \tau_{xx} & \tau_{xy} & \tau_{xz} \\ \tau_{yx} & \tau_{yy} & \tau_{yz} \\ \tau_{zx} & \tau_{zy} & \tau_{zz} \end{pmatrix}$$ – stress tensor in the liquid;

$$\vec{\tau}_x = \tau_{xx}\vec{i} + \tau_{xy}\vec{j} + \tau_{xz}\vec{k},$$

$$\vec{\tau}_y = \tau_{yx}\vec{i} + \tau_{yy}\vec{j} + \tau_{yz}\vec{k}, \quad \tau_{\alpha\beta} \equiv \tau_{\alpha\beta}(x, y, z, t);$$

$$\vec{\tau}_z = \tau_{zx}\vec{i} + \tau_{zy}\vec{j} + \tau_{zz}\vec{k},$$

$$\frac{d}{dt} \equiv \frac{\partial}{\partial t} + \upsilon_x \frac{\partial}{\partial x} + \upsilon_y \frac{\partial}{\partial y} + \upsilon_z \frac{\partial}{\partial z} \equiv \frac{\partial}{\partial t} + \vec{\upsilon} \cdot \vec{\nabla};$$

$$\vec{\nabla} \equiv \vec{i}\,\frac{\partial}{\partial x} + \vec{j}\,\frac{\partial}{\partial y} + \vec{k}\,\frac{\partial}{\partial z}.$$

Equations (1)-(4) should be taken as a basis for mathematical modeling of a liquid continuous medium. However, this system is not complete.

Functions $\vec{F}, \vec{\Pi}, \varepsilon$, as a rule, are known, or relatively easy to establish empirically; equations (1)-(4) in total are 8. The number of required functions – 28. Hence it follows that in the solution of any problem connected with the motion of a liquid, in each particular case, it is necessary to complement the main system (1)-(4), based on some reasonable assumptions,. This also applies to the correct formulation of the corresponding initial and boundary conditions.

Thus, it makes no sense to talk about the problem of a correct solution of system (1)-(4) in itself (without additional conditions of a non-mechanical nature).

Additional relationships are needed that specify the physicochemical properties of the continuous medium under study. Such relationships are, as a rule, related to the assumptions about the structural and physicochemical features of the continuous medium under investigation, and are based, as indicated above, on empirical considerations and experimental studies.

For example, for an ideal liquid, the stress tensor contains only one unknown function (pressure), instead of nine, for a Newtonian fluid-the stress tensor is symmetric, and its components are expressed in terms of pressure and velocity; the Mendeleev-Clapeyron equation or the adiabatic equation is used for ideal gases. For a liquid that obeys the law of Fourier thermal conductivity, the heat flux vector (three components) is expressed in terms of temperature (one unknown function), and so on.

However, such additional relationships are not related to hydrodynamics as such, but to internal features of the structure of matter and, in addition, as a rule, while they are purely empirical or semi empirical in nature.

In connection with what has been said, we shall formulate the preliminary conditions that we in this paper will base on the exact formulation and solution of the problem.

1) The liquid is assumed to be viscous, isotropic, Newtonian and obeying the Fourier thermal conductivity law. In this case, as is known, the following relations hold:

$$\tau_{xx} = -p + \lambda(\vec{\nabla}\cdot\vec{\upsilon}) + 2\mu\frac{\partial \upsilon_x}{\partial x}, \tau_{xy} = \tau_{yx} = \mu\left(\frac{\partial \upsilon_x}{\partial y} + \frac{\partial \upsilon_y}{\partial x}\right),$$

$$\tau_{yy} = -p + \lambda(\vec{\nabla}\cdot\vec{\upsilon}) + 2\mu\frac{\partial \upsilon_y}{\partial y}, \tau_{yz} = \tau_{zy} = \mu\left(\frac{\partial \upsilon_y}{\partial z} + \frac{\partial \upsilon_z}{\partial y}\right), \quad (5)$$

$$\tau_{zz} = -p + \lambda(\vec{\nabla}\cdot\vec{\upsilon}) + 2\mu\frac{\partial \upsilon_z}{\partial z}, \tau_{zx} = \tau_{xz} = \mu\left(\frac{\partial \upsilon_z}{\partial x} + \frac{\partial \upsilon_x}{\partial z}\right),$$

$$t_x = k\frac{\partial T}{\partial x}, \quad t_y = k\frac{\partial T}{\partial y}, \quad t_z = k\frac{\partial T}{\partial z} \quad (6)$$

2) $f(p, \rho, T) = 0$ – is an equation of state of the liquid; in particular, for weakly compressible liquids $\rho = \rho_0\left(1 + \frac{p - p_0}{K}\right)$, where K is a bulk modulus of the liquid. In particular, experimental data and general physical considerations show, that any medium at a very high temperatures and pressure practically has the ideal liquid properties.

3) Finally, it is assumed, that the following relations are known:

$E = E(p, T), \quad \lambda = \lambda(p, T), \quad \mu = \mu(p, T), \quad k = k(p, T)$,

And in the first approximation one can take $\lambda = -\frac{2}{3}\mu$.

In the present paper we consider the case of a *homogeneous incompressible* $(\rho = const)$ *viscous liquid with a constant viscosity coefficient* μ, and $E = c_V T + const$ (here c_V – is the heat capacity for a constant volume). In this case, equations (1), (2) and (4) will be transformed into

$$\frac{\partial \upsilon_x}{\partial x} + \frac{\partial \upsilon_y}{\partial y} + \frac{\partial \upsilon_z}{\partial z} = 0, \quad (7)$$

$$\frac{\partial \upsilon_x}{\partial t} + \upsilon_x\frac{\partial \upsilon_x}{\partial x} + \upsilon_y\frac{\partial \upsilon_x}{\partial y} + \upsilon_z\frac{\partial \upsilon_x}{\partial z} = F_x - \frac{1}{\rho}\frac{\partial p}{\partial x} + \nu\Delta\upsilon_x,$$

$$\frac{\partial \upsilon_y}{\partial t} + \upsilon_x\frac{\partial \upsilon_y}{\partial x} + \upsilon_y\frac{\partial \upsilon_y}{\partial y} + \upsilon_z\frac{\partial \upsilon_y}{\partial z} = F_y - \frac{1}{\rho}\frac{\partial p}{\partial y} + \nu\Delta\upsilon_y, \quad (8)$$

$$\frac{\partial \upsilon_z}{\partial t} + \upsilon_x\frac{\partial \upsilon_z}{\partial x} + \upsilon_y\frac{\partial \upsilon_z}{\partial y} + \upsilon_z\frac{\partial \upsilon_z}{\partial z} = F_z - \frac{1}{\rho}\frac{\partial p}{\partial z} + \nu\Delta\upsilon_z,$$

$$\nu = \frac{\mu}{\rho}, \quad \Delta = \frac{\partial^2}{\partial x^2} + \frac{\partial^2}{\partial y^2} + \frac{\partial^2}{\partial z^2}$$

$$c_V\rho\left(\frac{\partial T}{\partial t} + \upsilon_x\frac{\partial T}{\partial x} + \upsilon_y\frac{\partial T}{\partial y} + \upsilon_z\frac{\partial T}{\partial z}\right) =$$

$$= \varepsilon + \Phi + \frac{\partial}{\partial x}\left(k\frac{\partial T}{\partial x}\right) + \frac{\partial}{\partial y}\left(k\frac{\partial T}{\partial y}\right) + \frac{\partial}{\partial z}\left(k\frac{\partial T}{\partial z}\right), \quad (9)$$

where

$$\Phi = \mu\left[2\left(\frac{\partial \upsilon_x}{\partial x}\right)^2 + 2\left(\frac{\partial \upsilon_y}{\partial y}\right)^2 + 2\left(\frac{\partial \upsilon_z}{\partial z}\right)^2 + \left(\frac{\partial \upsilon_x}{\partial y} + \frac{\partial \upsilon_y}{\partial x}\right)^2 + \left(\frac{\partial \upsilon_y}{\partial z} + \frac{\partial \upsilon_z}{\partial y}\right)^2 + \left(\frac{\partial \upsilon_x}{\partial z} + \frac{\partial \upsilon_z}{\partial x}\right)^2\right].$$

We call attention to the fact, that equations (7) and (8) form a closed system: the number of unknowns ($p, \upsilon_x, \upsilon_y, \upsilon_z$) and the number of equations coincide. Therefore, under our assumptions the system of equations (7) and (8) can be solved independently of the energy equation (9). Among other things we note that equations (8) – are the Navier-Stokes equations for the case under considerations.

Bearing in mind all that has been said above, we narrow down our problem in the following way. To investigate the motion of an isotropic viscous incompressible Newtonian fluid along a horizontal cylindrical tube of constant cross section and finite length, neglecting the action of mass forces.

In solving this problem we will base on equations (7), (8). For definiteness we take the axis of a straight-line horizontal cylindrical pipe of radius R and length l as z -axis. The liquid fills the entire pipe volume; on the left end of the pipe (at the origin of body axes) there is a pump, that sets the liquid pressure, in general, variable in time and equal in cross-section.

In this formulation it is natural to turn to cylindrical coordinate system. In these coordinates the basic equations (7) and (8) will be written as follows [6]:

$$\frac{\partial \upsilon_r}{\partial r} + \frac{1}{r}\frac{\partial \upsilon_\theta}{\partial \theta} + \frac{\partial \upsilon_z}{\partial z} + \frac{\upsilon_r}{r} = 0 \quad (11)$$

$$\frac{\partial \upsilon_r}{\partial t}+\upsilon_r\frac{\partial \upsilon_r}{\partial r}+\frac{\upsilon_\theta}{r}\frac{\partial \upsilon_r}{\partial \theta}+\upsilon_z\frac{\partial \upsilon_r}{\partial z}-\frac{\upsilon_\theta^2}{r}=$$
$$=F_r-\frac{1}{\rho}\frac{\partial p}{\partial r}+\nu\left(\frac{\partial^2\upsilon_r}{\partial r^2}+\frac{1}{r^2}\frac{\partial^2\upsilon_r}{\partial\theta^2}+\frac{\partial^2\upsilon_r}{\partial z^2}+\right.$$
$$\left.+\frac{1}{r}\frac{\partial \upsilon_r}{\partial r}-\frac{2}{r^2}\frac{\partial \upsilon_\theta}{\partial\theta}-\frac{\upsilon_r}{r^2}\right), \quad (12)$$

$$\frac{\partial \upsilon_\theta}{\partial t}+\upsilon_r\frac{\partial \upsilon_r}{\partial r}+\frac{\upsilon_\theta}{r}\frac{\partial \upsilon_\theta}{\partial \theta}+\upsilon_z\frac{\partial \upsilon_\theta}{\partial z}+\frac{\upsilon_r\upsilon_\theta}{r}=$$
$$=F_\theta-\frac{1}{\rho r}\frac{\partial p}{\partial\theta}+\nu\left(\begin{array}{l}\frac{\partial^2\upsilon_\theta}{\partial r^2}+\frac{1}{r^2}\frac{\partial^2\upsilon_\theta}{\partial\theta^2}+\frac{\partial^2\upsilon_\theta}{\partial z^2}+\\ +\frac{1}{r}\frac{\partial \upsilon_\theta}{\partial r}-\frac{2}{r^2}\frac{\partial \upsilon_r}{\partial\theta}-\frac{\upsilon_\theta}{r^2}\end{array}\right), \quad (13)$$

$$\frac{\partial \upsilon_z}{\partial t}+\upsilon_r\frac{\partial \upsilon_z}{\partial r}+\frac{\upsilon_\theta}{r}\frac{\partial \upsilon_z}{\partial \theta}+\upsilon_z\frac{\partial \upsilon_z}{\partial z}=$$
$$=F_z-\frac{1}{\rho}\frac{\partial p}{\partial z}+\nu\left(\begin{array}{l}\frac{\partial^2\upsilon_z}{\partial r^2}+\frac{1}{r^2}\frac{\partial^2\upsilon_z}{\partial\theta^2}+\\ +\frac{\partial^2\upsilon_z}{\partial z^2}+\frac{1}{r}\frac{\partial \upsilon_z}{\partial r}\end{array}\right), \quad (14)$$

Taking into account the assumptions made, regarding the axial symmetry of the flow, it is possible to assume $\vec{F}\equiv\vec{0}, \upsilon_\theta\equiv 0, \frac{\partial}{\partial\theta}\equiv 0$. Then equations (11)-(14) will take the form:

$$\frac{\partial \upsilon_r}{\partial r}+\frac{\partial \upsilon_z}{\partial z}+\frac{\upsilon_r}{r}=0 \quad (15)$$

$$\frac{\partial \upsilon_r}{\partial t}+\upsilon_r\frac{\partial \upsilon_r}{\partial r}+\upsilon_z\frac{\partial \upsilon_r}{\partial z}=$$
$$=\frac{1}{\rho}\frac{\partial p}{\partial r}+\nu\left(\frac{\partial^2\upsilon_r}{\partial r^2}+\frac{\partial^2\upsilon_r}{\partial z^2}+\frac{1}{r}\frac{\partial \upsilon_r}{\partial r}-\frac{\upsilon_r}{r^2}\right), \quad (16)$$

$$\frac{\partial \upsilon_z}{\partial t}+\upsilon_r\frac{\partial \upsilon_z}{\partial r}+\upsilon_z\frac{\partial \upsilon_z}{\partial z}=$$
$$=-\frac{1}{\rho}\frac{\partial p}{\partial z}+\nu\left(\frac{\partial^2\upsilon_z}{\partial r^2}+\frac{\partial^2\upsilon_z}{\partial z^2}+\frac{1}{r}\frac{\partial \upsilon_z}{\partial r}\right). \quad (17)$$

Remark 1. The assumption $\upsilon_\theta\equiv 0$, in general, is not critical: it is enough to assume that $\upsilon_\theta=\upsilon_\theta(t,r,z)$. In this case one mote equation will be added to equations (15)-(17):

$$\frac{\partial \upsilon_\theta}{\partial t}+\upsilon_r\frac{\partial \upsilon_r}{\partial r}+\upsilon_z\frac{\partial \upsilon_\theta}{\partial z}+\frac{\upsilon_r\upsilon_\theta}{r}=$$
$$=\nu\left(\frac{\partial^2\upsilon_\theta}{\partial r^2}+\frac{\partial^2\upsilon_\theta}{\partial z^2}+\frac{1}{r}\frac{\partial \upsilon_\theta}{\partial r}-\frac{\upsilon_\theta}{r^2}\right). \quad (18)$$

The system, however, remains closed: the number of unknown functions coincides with the number of equations.

Remark 2. When solving (in particular, numerically) partial differential equations (system of equations), it is important to investigate the correctness of the corresponding initial-boundary problems for the equations being solved. Such research is very nontrivial, especially for quasilinear partial differential equations of the second order, such as Navier-Stokes equations. For the equation system (11)-(14), fortunately, such investigation (with a positive result) was carried out by O.A. Ladyzhenskaya [7].

3. Numerical solution of the initial-boundary problem for the Navier-Stokes equation,

In this paragraph we will give an example of the calculation of the parameters of the flow of the viscous incompressible liquid through a straight pipe of the circular cross-section, described by equation system (15)-(17). We define initial and boundary conditions from some reasonable physical formulation of the problem.

1. At the pipe inlet and outlet the flow is supposed to be laminar, i.e.
$$\upsilon_r(r,0,t)=\upsilon_r(r,L,t)=0. \quad (19)$$
2. At the initial moment of time the flow is laminar and steady, i.e.
$$\upsilon_r(r,z,0)=0,\ \upsilon_z(r,z,0)=\varphi(r). \quad (20)$$
As an initial velocity distribution $\varphi(r)$ we take the Poiseuille distribution (see [5]).
3. Because of the viscous drag force at the wall of pipe the condition of flow adhesion is fulfilled
$$\upsilon_r(R,z,t)=0,\ \upsilon_z(R,z,t)=0. \quad (21)$$
4. We suppose the pressure to be set at the pipe inlet and outlet
$$p(r,0,t)=p_1,\ p(r,L,t)=p_2. \quad (22)$$
5. The condition of zero pressure gradient must be fulfilled at the wall of the pipe
$$\left.\left(\frac{\partial p}{\partial r}+\frac{\partial p}{\partial z}\right)\right|_{r=R}=0. \quad (23)$$

We shall seek the numerical solution of the problem (15)-(17), (19)-(23), prior reduced to the dimensionless form. We use the alternating direction method [8]. According to this method we will find the velocity projections from the following difference equations:

$$\frac{u_{i,j}^{k+0.5}-u_{i,j}^{k}}{0.5\cdot h_\tau}=\frac{u_{i+1,j}^{k+0.5}-2u_{i,j}^{k+0.5}+u_{i-1,j}^{k+0.5}}{h_\eta^2}+\frac{1}{\eta_i}\frac{u_{i+1,j}^{k+0.5}-u_{i-1,j}^{k+0.5}}{2h_\eta}-$$
$$-\frac{u_{i,j}^{k}}{\eta_i^2}+\frac{u_{i,j+1}^{k}-2u_{i,j}^{k}+u_{i,j-1}^{k}}{h_\xi^2}-\frac{u_{i,j}^{k}+\left|u_{i,j}^{k}\right|}{2}\frac{u_{i+1,j}^{k+0.5}-u_{i,j}^{k+0.5}}{h_\eta}-$$
$$-\frac{u_{i,j}^{k}-\left|u_{i,j}^{k}\right|}{2}\frac{u_{i,j}^{k+0.5}-u_{i-1,j}^{k+0.5}}{h_\eta}-\frac{w_{i,j}^{k}+\left|w_{i,j}^{k}\right|}{2}\frac{u_{i,j+1}^{k}-u_{i,j}^{k}}{h_\xi}-$$
$$-\frac{w_{i,j}^{k}-\left|w_{i,j}^{k}\right|}{2}\frac{u_{i,j}^{k}-u_{i,j-1}^{k}}{h_\xi}, \quad (24)$$

$$\frac{u_{i,j}^{k+1}-u_{i,j}^{k+0.5}}{0.5\cdot h_\tau}=\frac{u_{i+1,j}^{k+0.5}-2u_{i,j}^{k+0.5}+u_{i-1,j}^{k+0.5}}{h_\eta^2}+\frac{1}{\eta_i}\frac{u_{i+1,j}^{k+0.5}-u_{i-1,j}^{k+0.5}}{2h_\eta}-$$
$$-\frac{u_{i,j}^{k+0.5}}{\eta_i^2}+\frac{u_{i,j+1}^{k+1}-2u_{i,j}^{k+1}+u_{i,j-1}^{k+1}}{h_\xi^2}-\frac{u_{i,j}^{k+0.5}+\left|u_{i,j}^{k+0.5}\right|}{2}\frac{u_{i+1,j}^{k+0.5}-u_{i,j}^{k+0.5}}{h_\eta}-$$
$$-\frac{u_{i,j}^{k+0.5}-\left|u_{i,j}^{k+0.5}\right|}{2}\frac{u_{i,j}^{k+0.5}-u_{i-1,j}^{k+0.5}}{h_\eta}-\frac{w_{i,j}^{k+0.5}+\left|w_{i,j}^{k+0.5}\right|}{2}\frac{u_{i,j+1}^{k+1}-u_{i,j}^{k+1}}{h_\xi}-$$
$$-\frac{w_{i,j}^{k+0.5}-\left|w_{i,j}^{k+0.5}\right|}{2}\frac{u_{i,j}^{k+1}-u_{i,j-1}^{k+1}}{h_\xi}-\frac{\gamma_{i+1,j+1}^{k+1}+\gamma_{i+1,j-1}^{k+1}-\gamma_{i-1,j+1}^{k+1}-\gamma_{i-1,j-1}^{k+1}}{2h_\eta+2h_\xi}, \quad (25)$$

$$\frac{w_{i,j}^{k+0.5}-w_{i,j}^{k}}{0.5\cdot h_\tau}=\frac{w_{i+1,j}^{k+0.5}-2w_{i,j}^{k+0.5}+w_{i-1,j}^{k+0.5}}{h_\eta^2}+\frac{1}{\eta_i}\frac{w_{i+1,j}^{k+0.5}-w_{i-1,j}^{k+0.5}}{2h_\eta}+$$
$$+\frac{w_{i,j+1}^{k}-2w_{i,j}^{k}+w_{i,j-1}^{k}}{h_\xi^2}-\frac{u_{i,j}^{k}+\left|u_{i,j}^{k}\right|}{2}\frac{w_{i+1,j}^{k+0.5}-w_{i,j}^{k+0.5}}{h_\eta}-$$
$$-\frac{u_{i,j}^{k}-\left|u_{i,j}^{k}\right|}{2}\frac{w_{i,j}^{k+0.5}-w_{i-1,j}^{k+0.5}}{h_\eta}-\frac{w_{i,j}^{k}+\left|w_{i,j}^{k}\right|}{2}\frac{w_{i,j+1}^{k}-w_{i,j}^{k}}{h_\xi}-$$
$$-\frac{w_{i,j}^{k}-\left|w_{i,j}^{k}\right|}{2}\frac{w_{i,j}^{k}-w_{i,j-1}^{k}}{h_\xi}, \qquad (26)$$

$$\frac{w_{i,j}^{k+1}-w_{i,j}^{k+0.5}}{0.5\cdot h_\tau}=\frac{w_{i+1,j}^{k+0.5}-2w_{i,j}^{k+0.5}+w_{i-1,j}^{k+0.5}}{h_\eta^2}+\frac{1}{\eta_i}\frac{w_{i+1,j}^{k+0.5}-w_{i-1,j}^{k+0.5}}{2h_\eta}+$$
$$+\frac{w_{i,j+1}^{k+1}-2w_{i,j}^{k+1}+w_{i,j-1}^{k+1}}{h_\xi^2}-\frac{u_{i,j}^{k+0.5}+\left|u_{i,j}^{k+0.5}\right|}{2}\frac{w_{i+1,j}^{k+0.5}-w_{i,j}^{k+0.5}}{h_\eta}-$$
$$-\frac{u_{i,j}^{k+0.5}-\left|u_{i,j}^{k+0.5}\right|}{2}\frac{w_{i,j}^{k+0.5}-w_{i-1,j}^{k+0.5}}{h_\eta}-\frac{w_{i,j}^{k+0.5}+\left|w_{i,j}^{k+0.5}\right|}{2}\frac{w_{i,j+1}^{k+1}-w_{i,j}^{k+1}}{h_\xi}-$$
$$-\frac{w_{i,j}^{k+0.5}-\left|w_{i,j}^{k+0.5}\right|}{2}\frac{w_{i,j}^{k+1}-w_{i,j-1}^{k+1}}{h_\xi}-\frac{\gamma_{i+1,j+1}^{k+1}+\gamma_{i+1,j-1}^{k+1}-\gamma_{i-1,j+1}^{k+1}-\gamma_{i-1,j-1}^{k+1}}{2h_\eta+2h_\xi}, \qquad (27)$$

where u, w are dimensionless velocity projections υ_r and υ_z respectively, η, ξ, τ are dimensionless radial coordinate, linear coordinate and time respectively, h_η, h_ξ, h_τ are steps along the corresponding coordinate axes. These equations are reduced to the form $Ax_{i-1}+Bx_i+Cx_{i+1}=F_i$ and are solved with the tridiagonal matrix algorithm.

We obtain the equation for determining the pressure by differentiating equations (16) and (17) with respect to r and z, and adding them:

$$\Delta p=\rho\left\{\begin{array}{l} v\left(\frac{\partial^2 D}{\partial r^2}+\frac{1}{r}\frac{\partial D}{\partial r}+\frac{\partial^2 D}{\partial z^2}\right)-\frac{\partial D}{\partial t}-u\frac{\partial D}{\partial r}- \\ -w\frac{\partial D}{\partial z}-\left[\frac{\partial u}{\partial r}\right]^2-\left[\frac{\partial w}{\partial z}\right]^2-2\frac{\partial w}{\partial r}\frac{\partial u}{\partial z} \end{array}\right\}, \qquad (28)$$

where $D=\frac{\partial \upsilon_r}{\partial r}+\frac{\partial \upsilon_z}{\partial z}+\frac{\upsilon_r}{r}$. For the equation (28) we also write the difference approximation. The pressure (or rather γ – the dimensionless function corresponding to the relation p/ρ) we shall seek with the Richardson method [8]:

$$\gamma_{i,j}^{s+1}=F\left(\gamma_{i+1,j}^{s},\gamma_{i-1,j}^{s},\gamma_{i,j+1}^{s},\gamma_{i,j-1}^{s}\right) \qquad (29)$$

where s denotes the iteration number. The computation by formula (27) continues, while the difference between values in two adjacent iterations doesn't become less than the preset accuracy ε. Obviously, the equations given have a singularity at the point $r=0$. This obstacle can be bypassed, if we assume $\Delta_r(f)=2\frac{\partial^2 f}{\partial r^2}$ when $r=0$.

The formulas given were implemented as a program in the Matlab environment. The results are shown in the form of graphics in Fig.1,2,3 and 4.

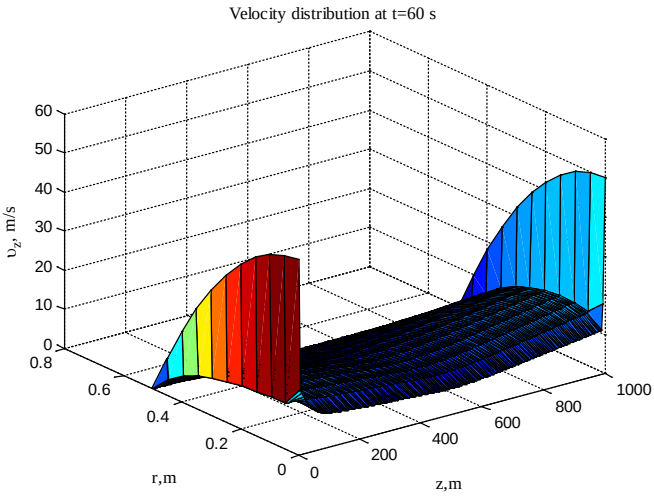

Fig. 1. The velocity υ_z field

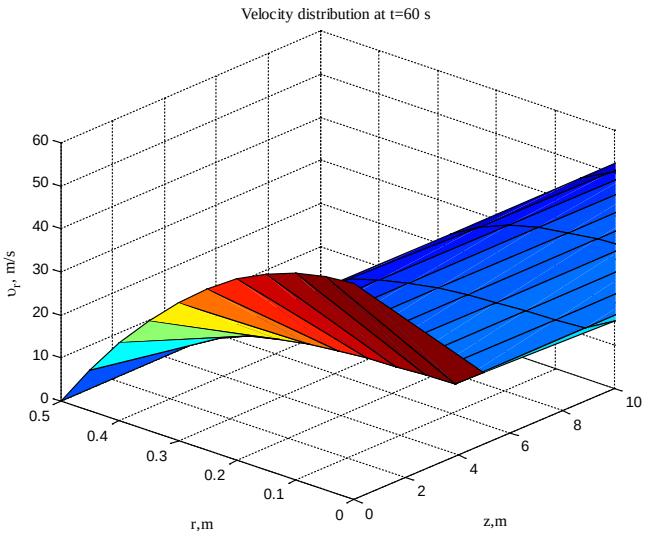

Fig. 2. The velocity υ_z field on the segment $z\in[0,10]$

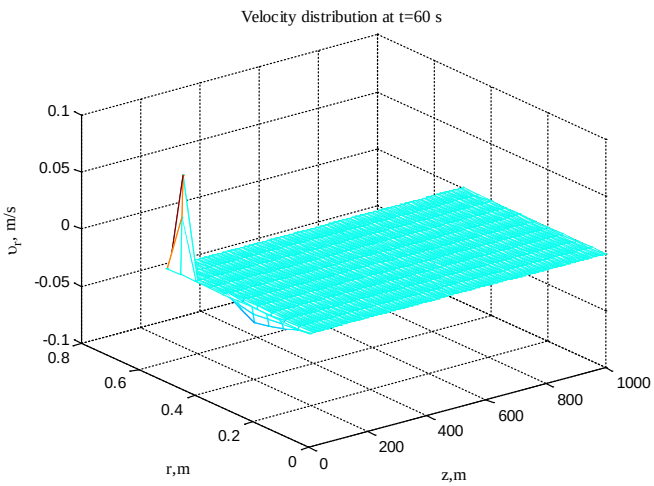

Fig. 3. The velocity υ_r field

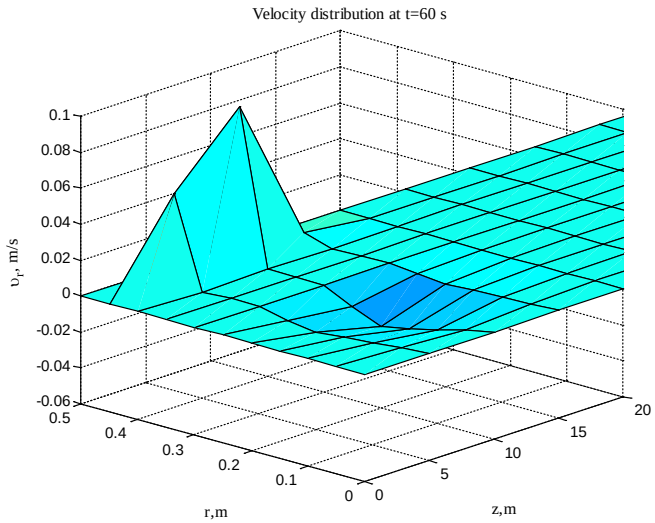

Fig. 4. The velocity υ_r field on the segment $z \in [0,10]$

4. Conclusion

In this paper the mathematical model of the real viscous liquids motion along the horizontal cylindrical pipe is proposed and the implicit difference scheme is built for solving corresponding initial-boundary problems. The scheme was tested on a typical example.

References

1. Charny, I. A. Unsteady motion of a real liquid in pipes (in Russian). – Moscow, 1982
2. Basniev, K. S. Oil and gas hydrodynamics (in Russian). – Moscow-Izhevsk, 2005
3. Nguyen Dang Hoa. Mathematical Modeling and Control of Trunk Pipeline Systems (in Russian). – PhD Diss. In Tech. Sci., Saint Petersburg Polytechnic Univ., 2012
4. Firsov, A. N. Generalized mathematical models and methods for analyzing dynamic processes in distributed systems (in Russian). – Saint Petersburg, 2013 (ch. 5)
5. Vallander, S. V. Lectures on hydroaeromechanics (in Russian). – Saint Petersburg, 2005
6. Slezkin, N. A. Dynamics of a viscous incompressible fluid (in Russian). – Moscow, 1955
7. Ladyzhenskaya, O. A. On the unique solvability in the large of the three-dimensional Cauchy problem for the Navier-Stokes equations in the presence of axial symmetry (in Russian), Zapiski Nauchnikh Seminarov LOMI, 1968, v. 7, p. 155-177
8. Filatov, E. Y., Yasinskiy, F. N. Mathematical modeling of liquid and gas flows: Tutorial / State Educational Institution of Higher Professional education “Ivanovo Power Engineering Institute of V. I. Lenin”. – Ivanovo, 2007 (in Russian)

TRANSFER PROCESSES IN INDUSTRIAL COLUMN APPARATUSES

Chr. Boyadjiev, M. Doichinova, B. Boyadjiev, P. Popova-Krumova
Institute of Chemical Engineering, Bulgarian Academy of Sciences,

chr.boyadjiev@gmail.com

Abstract: *The paper is a presentation of the monography "Chr. Boyadjiev, M. Doichinova, B. Boyadjiev, P. Popova-Krumova, Modeling of Column Apparatus Processes, Springer-Verlag, Berlin Heidelberg, 2016, pp. 313. A new approach to modeling the mass transfer processes in industrial column apparatuses, in the physical approximations of the mechanics of continua, is used for the creation of convection-diffusion and average-concentration models. The models of chemical, absorption, adsorption and catalytic processes are presented.*

Keywords: COLUMN APPARATUSES, NEW MODELS, CHEMICAL PROCESSES, ABSORPTION, ADSORPTION, CATALYTIC PROCESSES

1. Introduction

The modeling and simulation are the main approach for the quantitative description of the mass transfer processes in the chemical, power, biotechnological and other industries [1]. The models of the mass transfer processes are possible to be created on the basis of the physical approximations of the mechanics of continua, where the mathematical point is equivalent to an elementary physical volume, which is sufficiently small with respect to the apparatus volume, but at the same time sufficiently large with respect to the intermolecular volumes in the medium.

The big part of the industrial mass transfer processes are realized in one, two or three phase systems as a result of volume (homogeneous) and surface (heterogeneous) reactions, i.e. mass appearance (disappearance) of the reagents (phase components) in the elementary volumes in the phases or on the its interphase surfaces. As a result, the reactions are mass sources (sinks) in the volume (homogeneous chemical reactions) and on the surface (interphase mass transfer in the cases of absorption, adsorption, catalytic reactions) of the elementary phase volumes.

The volume reactions lead to different concentrations of the reagents in the phase volumes and as a result two mass transfer processes are realized – convective transfer (caused by the movement of the phases) and diffusion transfer (caused by the concentration gradients in the phases). The mass transfer models are a mass balance in the phases, where components are convective transfer, diffusion transfer and volume reactions (volume mass sources or sings). The surface reactions participate as mass sources or sings in the boundary conditions of the model equations.

A fundamental prerequisite for the use of the interphase mass transfer theory is the existence of a theoretical possibility to determine the velocity distribution in the phases and the interphase boundaries (surfaces). In the cases of modeling of the interphase mass transfer processes (absorption, adsorption and catalytic reactions) in column apparatuses, the velocity and the interphase boundaries are unknown and as a result this theory is useful.

The use of the physical approximations of the mechanics of continua for the interphase mass transfer process modeling in industrial column apparatuses [2] is possible if the mass appearance (disappearance) of the reagents on the interphase surfaces of the elementary physical volumes (as a result of the heterogeneous reactions) are replaced by the mass appearance (disappearance) of the reagents in the same elementary physical volumes (as a result of the equivalent homogenous reactions), i.e. the surface mass sources (sinks), caused by absorption, adsorption or catalytic reactions must be replaced with equivalent volume mass sources (sinks).

The new approach to modeling the mass transfer processes in industrial column apparatuses is the creation of the convection-diffusion and average-concentration models.

The convection-diffusion models permit the qualitative analysis of the processes only, because the velocity distribution in the column is unknown. On this base is possible to be obtained the role of the different physical effect in the process and to reject those processes, whose relative influence is less than 1%, i.e. to be made process mechanism identification.

The average-concentration models are obtained from the convection-diffusion models, where average velocities and concentrations are introduced. The velocity distribution effects are introduced by the parameters in the model, which must to be determined experimentally.

2. Convection-diffusion type models

In the general case a multicomponent ($i=1,2,...,i_0$) and multiphase ($j=1,2,3$ for gas, liquid and solid phases) flow in a cylindrical column with radius r_0 [m] and active zone height l [m] will be considered. If F_0 is the fluid flow rate in the column and F_j, $j=1,2,3$ are the phase flow rates [$m^3.s^{-1}$], the parts of the column volume occupied by the gas, liquid and solid phase, respectively, i.e. the phase volumes [m^3] in 1 m^3 of the column volume (hold-up coefficients of the phases), are:

$$\varepsilon_j = \frac{F_j}{F_0}, \quad j=1,2,3, \quad \sum_j^3 \varepsilon_j = 1, \tag{1}$$

The input velocities of the phases in the column u_j^0 [$m.s^{-1}$], $j=1,2,3$ are possible to be defined as:

$$u_j^0 = \frac{F_j}{\varepsilon_j \pi r_0^2}, \quad j=1,2,3; \quad F_0 = \sum_{j=1}^{3} F_j. \tag{2}$$

The physical elementary column volumes contain the elementary phase volumes ε_j, $j=1,2,3$ and will be presented as mathematical points $M(r,z)$ in a cylindrical coordinate system (r,z), where r and z [m] are radial and axial coordinates. As a result, the mathematical point $M(r,z)$ is equivalent to the elementary phase volumes, too.

The concentrations [kg-mol.m^{-3}] of the reagents (components of the phases) are c_{ij}, $i=1,2,...,i_0$, $j=1,2,3$, i.e. the quantities of the reagents (kg-mol) in 1 m^3 of the phase volumes in the column.

In the cases of a stationary motion of fluids in cylindrical column apparatus, $u_j(r,z)$, $v_j(r,z)$, $j=1,2,3$ [$m.s^{-1}$] are the axial and radial velocity components of the phases in the elementary phase volumes.

The volume reactions [kg-mol.$m^{-3}.s^{-1}$] in the phases (homogeneous chemical reactions and heterogeneous reactions, as a volume mass source or sink in the phase volumes in the column) are $Q_{ij}(c_{ij})$, $j=1,2,3$, $i=1,2,...,i_0$. The reagent concentrations in the

elementary phase volumes increase ($Q_{ij} > 0$) or decrease ($Q_{ij} < 0$) and the reaction rates Q_{ij} are determined by these concentrations $c_{ij}(r,z)$ $\left[\text{kg-mol.m}^{-3}\right]$.

The volume reactions lead to different values of the reagent concentrations in the elementary phase volumes and as a result, two mass transfer effects exist – convective transfer (caused by the fluid motion) and diffusion transfer (caused by the concentration gradient).

The convective transfer in column apparatus is caused by a laminar or turbulent (as a result of large-scale turbulent pulsations) flow. In the elementary phase volume around the point *M* (*r*, *z*) in the column, the mass transfer in this volume, as a result of the convection, is $u_j \frac{\partial c_{ij}}{\partial z} + v_j \frac{\partial c_{ij}}{\partial r}$ $\left[\text{kg-mol.m}^{-3}.\text{s}^{-1}\right]$, $j = 1,2,3,$ $i = 1,2,\ldots,i_0$, i.e. convective transfer rate (kg-mol.s^{-1}) in 1 m^3 of the phase volume.

The molecular or turbulent (caused by small-scale turbulent pulsations) diffusive transfer is $D_{ij}\left(\frac{\partial^2 c_{ij}}{\partial z^2} + \frac{1}{r}\frac{\partial c_{ij}}{\partial r} + \frac{\partial^2 c_{ij}}{\partial r^2}\right)$ $\left[\text{kg-mol.m}^{-3}.\text{s}^{-1}\right]$, i.e., diffusive transfer rate (kg-mol.s^{-1}) in 1 m^3 of the phase volume and D_{ij} [m^2.s^{-1}] are the diffusivities of the reagents $(i = 1,2,...,i_0)$ in the phases $(j = 1,2,3)$.

The mathematical model of the processes in the column apparatuses, in the physical approximations of the mechanics of continua, represents the mass balances in the phase volumes (phase parts in the elementary column volume) between the convective transfer, the diffusive transfer and the volume mass sources (sinks). The sum total of these three effects (in the cases of stationary processes) is equal to zero:

$$u_j \frac{\partial c_{ij}}{\partial z} + v_j \frac{\partial c_{ij}}{\partial r} = D_{ij}\left(\frac{\partial^2 c_{ij}}{\partial z^2} + \frac{1}{r}\frac{\partial c_{ij}}{\partial r} + \frac{\partial^2 c_{ij}}{\partial r^2}\right) + Q_{ij}(c_{ij}), \quad (3)$$
$$j = 1,2,3, \quad i = 1,2,\ldots,i_0.$$

The axial and radial velocity components $u_j(r,z)$ and $v_j(r,z)$, $j = 1,2,3$ satisfy the continuity equations

$$\frac{\partial u_j}{\partial z} + \frac{\partial v_j}{\partial r} + \frac{v_j}{r} = 0; \quad z = 0, \quad u_j \equiv u_j(r,0); \quad (4)$$
$$r = r_0, \quad v_j(r_0,z) \equiv 0; \quad j = 1,2,3.$$

The model of the mass transfer processes in the column apparatuses (3) includes boundary conditions, which express a symmetric concentrations distributions $(r = 0)$, impenetrability of the column wall $(r = r_0)$, constant input concentrations c_{ij}^0 and mass balances at the column input $(z = 0)$:

$$r = 0, \quad \frac{\partial c_{ij}}{\partial r} \equiv 0; \quad r = r_0, \quad \frac{\partial c_{ij}}{\partial r} \equiv 0;$$
$$z = 0, \quad c_{ij} \equiv c_{ij}^0, \quad u_j^0 c_{ij}^0 \equiv u_j c_{ij}^0 - D_{ij}\left(\frac{\partial c_{ij}}{\partial z}\right)_{Z_j = 0}, \quad (5)$$
$$j = 1,2,3, \quad i = 1,2,\ldots,i_0.$$

2.1. Column chemical reactor

In the case of one-phase fluid motion [6,7] in the column chemical reactors, the phase index $j = 1,2,3$ is possible to be ignored.

For a two component chemical reaction in the column, the convection-diffusion model (3) has the form:

$$u\frac{\partial c_i}{\partial z} + v\frac{\partial c_i}{\partial r} = D_i\left(\frac{\partial^2 c_i}{\partial z^2} + \frac{1}{r}\frac{\partial c_i}{\partial r} + \frac{\partial^2 c_i}{\partial r^2}\right) - Q_i(c_1,c_2), \quad i = 1,2, \quad (6)$$

where $Q_i(c_1,c_2) = k_i c_1^m c_2^n, \quad i = 1,2.$

2.2. Column physical (chemical) absorber

The convection-diffusion type models of the absorption processes in the gas-liquid systems is possible to be obtained if $j = 1,2$ $(1 = \varepsilon_1 + \varepsilon_2)$, $i = 1,2$. The kinetic terms $Q_{ij}, i = 1,2, j = 1,2$ [kg-mol.m^{-3}s^{-1}] are the interphase mass transfer rates $Q_{1j} = (-1)^j k_0(c_{11} - \chi c_{12})$, $j = 1,2$ in the gas and liquid phases and the chemical reaction rate ($Q_{i2} = -kc_{12}c_{22}, i = 1,2$) in the liquid phase, as volume sources or sinks of the reagents in the phase parts of the elementary (column) volume. As a result:

$$u_1\frac{\partial c_{11}}{\partial z} = D_{11}\left(\frac{\partial^2 c_{11}}{\partial z^2} + \frac{1}{r}\frac{\partial c_{11}}{\partial r} + \frac{\partial^2 c_{11}}{\partial r^2}\right) - k_0(c_{11} - \chi c_{12}),$$
$$u_2\frac{\partial c_{12}}{\partial z} = D_{12}\left(\frac{\partial^2 c_{12}}{\partial z^2} + \frac{1}{r}\frac{\partial c_{12}}{\partial r} + \frac{\partial^2 c_{12}}{\partial r^2}\right) + k_0(c_{11} - \chi c_{12}) - k c_{12}c_{22}, \quad (7)$$
$$u_2\frac{\partial c_{22}}{\partial z} = D_{22}\left(\frac{\partial^2 c_{22}}{\partial z^2} + \frac{1}{r}\frac{\partial c_{22}}{\partial r} + \frac{\partial^2 c_{22}}{\partial r^2}\right) - kc_{12}c_{22},$$

where k_0 [s^{-1}] is the volume interphase mass transfer coefficient, χ - the Henry's number, k - the chemical reaction rate constant. The same models is possible to be used for modeling of the extraction processes if χ is the redistribution factor. In the counter-current absorber $z = z_j$, $j = 1,2$ $(z_1 + z_2 = l)$.

2.3. Column physical (chemical) adsorber

In the adsorption process participate two reagents ($i_0 = 2$), where the first (active component) is in the gas or liquid phase ($i = 1$, $j = 1,2$) and the second (active site) is in the solid phase ($i = 2$, $j = 3$). The adsorption is a process of interphase mass transfer of an active component (AC) from the gas (liquid) volume to the solid interface and a heterogeneous reaction with an active site (AS), due to a physical (Van der Vaals's) or chemical (valence) force.

The convection-diffusion type models of the adsorption processes in the gas (liquid)-solid systems are possible to be obtained if $j = 1,3 = 2,3$ $(1 = \varepsilon_1 + \varepsilon_3 = \varepsilon_2 + \varepsilon_3)$, $i_0 = 2$, where $i = 1$ is for (AC) in the gas (liquid) phase, $i = 2$ is for (AS) in the adsorbent (solid phase). The volume adsorption rate in the case of a solid adsorbent is $Q_3 = b_0 Q_{03}$ [kg-mol.m^{-3}.s^{-1}], where b_0 $\left[\text{m}^2.\text{m}^{-3}\right]$ is m^2 of the inner surface in the solid phase (the surface of the capillaries in the solid phase) in 1 m^3 of the solid phase (adsorbent), Q_{03} $\left[\text{kg-mol.m}^{-2}.\text{s}^{-1}\right]$ – the surface adsorption rate.

A gas adsorption will be considered for convenience, where c_{11} [kg-mol.m^{-3}] is the volume concentration of the AC in the gas phase (elementary) volume, c_{13} [kg-mol.m^{-3}] – the volume concentration of the AC in the void volume of the solid phase (adsorbent), c_{23} [kg-eq.m^{-3}] – the volume concentration of the AS in the solid phase (elementary) volume (1 kg-eq AS in the adsorbent combine 1 kg-mol AC), $1 = \varepsilon_1 + \varepsilon_3$, $u_1 = u_1(r)$ – velocity of the gas phase [m.s^{-1}], $u_3 = 0$ (solid phase is immobile). All concentrations are in kg-mol (kg-eq) in 1 m^3 of the phase (elementary) volume.

2.3.1 Physical adsorption

In the cases of physical adsorption the surface adsorption rate is:

$$Q_{03} = k_1 c_{13} C_{23} - k_2 \frac{c_{23}^0}{b_0}(1 - C_{23}), \quad C_{23} = \frac{c_{23}}{c_{23}^0}. \tag{8}$$

Let us consider a non-stationary gas adsorption in a column apparatus, where the solid phase (adsorbent) is immobile. The convection-diffusion model of this process is possible to be obtained, where the diffusivity of the free AS in the solid phase (adsorbent) volume is equal to zero. If the rate of the interphase mass transfer of the AC from the gas phase to the solid phase is $k_0(c_{11} - c_{13})$ and the process is non-stationary as a result of the free AS concentration decrease, the convection-diffusion model has the form:

$$\begin{aligned}
&\frac{\partial c_{11}}{\partial t} + u_1 \frac{\partial c_{11}}{\partial z} = D_{11}\left(\frac{\partial^2 c_{11}}{\partial z^2} + \frac{1}{r}\frac{\partial c_{11}}{\partial r} + \frac{\partial^2 c_{11}}{\partial r^2}\right) - k_0(c_{11} - c_{13});\\
&\frac{dc_{13}}{dt} = k_0(c_{11} - c_{13}) - b_0 k_1 c_{13}\frac{c_{23}}{c_{23}^0} + k_2 c_{23}^0\left(1 - \frac{c_{23}}{c_{23}^0}\right);\\
&\frac{dc_{23}}{dt} = -b_0 k_1 c_{13}\frac{c_{23}}{c_{23}^0} + k_2 c_{23}^0\left(1 - \frac{c_{23}}{c_{23}^0}\right),
\end{aligned} \tag{9}$$

where t [s] is the time.

2.3.2 Chemical adsorption

In the cases of chemical adsorption the model is

$$\begin{aligned}
&\frac{\partial c_{11}}{\partial t} + u_1 \frac{\partial c_{11}}{\partial z} = D_{11}\left(\frac{\partial^2 c_{11}}{\partial z^2} + \frac{1}{r}\frac{\partial c_{11}}{\partial r} + \frac{\partial^2 c_{11}}{\partial r^2}\right) - k_0(c_{11} - c_{13}),\\
&\frac{dc_{13}}{dt} = k_0(c_{11} - c_{13}) - k\, c_{13} c_{23} = 0, \quad \frac{dc_{23}}{dt} = -k\, c_{13} c_{23},
\end{aligned} \tag{10}$$

where k is the chemical reaction rate constant.

2.4. Heterogeneous catalytic reactor

In a heterogeneous catalytic process participate two reagents, where the first reagent is adsorbed physically (chemically) on the free active sites (AS) of the solid catalytic surface. The reagents concentrations in the gas phase elementary volume are c_{11}, c_{21} [kg-mol.m^{-3}], while in the void elementary volume of the solid phase (catalyst) the concentrations are c_{13}, c_{23}. The concentration of the free AS in the solid (catalytic) phase elementary volume is c_{33} [kg-eq.m^{-3}]. The maximal concentrations of AC and AS are $c_{11}^0, c_{21}^0, c_{33}^0$, where c_{11}^0, c_{21}^0 are input AC concentrations in the gas phase. The volume concentration of the adsorbed AC in the solid phase elementary volume is $c_{33}^0 - c_{33}$ and the catalytic reaction rate is $kc_{23}(c_{33}^0 - c_{33})$. The concentration of AS decreases as a result of the adsorption and increases as a result of the catalytic reaction, because the reaction product does not have adsorption properties.

2.4.1 Physical adsorption mechanism

For a long duration process in the case of physical adsorption mechanism the model has the form:

$$\begin{aligned}
&u_1 \frac{\partial c_{11}}{\partial z} = D_{11}\left(\frac{\partial^2 c_{11}}{\partial z^2} + \frac{1}{r}\frac{\partial c_{11}}{\partial r} + \frac{\partial^2 c_{11}}{\partial r^2}\right) - k_{01}(c_{11} - c_{13});\\
&u_1 \frac{\partial c_{21}}{\partial z} = D_{21}\left(\frac{\partial^2 c_{21}}{\partial z^2} + \frac{1}{r}\frac{\partial c_{21}}{\partial r} + \frac{\partial^2 c_{21}}{\partial r^2}\right) - k_{02}(c_{21} - c_{23});\\
&k_{01}(c_{11} - c_{13}) - b_0 k_1 c_{13}\frac{c_{33}}{c_{33}^0} + k_2 c_{33}^0\left(1 - \frac{c_{33}}{c_{33}^0}\right) = 0;\\
&k_{02}(c_{21} - c_{23}) - kc_{23}(c_{33}^0 - c_{33}) = 0;\\
&-b_0 k_1 c_{13}\frac{c_{33}}{c_{33}^0} + k_2 c_{33}^0\left(1 - \frac{c_{33}}{c_{33}^0}\right) + kc_{23}(c_{33}^0 - c_{33}) = 0;
\end{aligned} \tag{11, 12}$$

2.4.2 Chemical adsorption mechanism

In the cases of chemical adsorption mechanism the last model has the form:

$$\begin{aligned}
&k_{01}(c_{11} - c_{13}) = k_{13} c_{13} c_{33}; \quad k_{02}(c_{21} - c_{23}) = kc_{23}(c_{33}^0 - c_{33});\\
&k_{13} c_{13} c_{33} = kc_{23}(c_{33}^0 - c_{33}).
\end{aligned} \tag{13}$$

2.5. Qualitative analysis of the models

The qualitative analysis of the convective-diffusion models will be illustrated with the case of a complex chemical reaction:

$$\begin{aligned}
&u\frac{\partial c_i}{\partial z} = D_i\left(\frac{\partial^2 c_i}{\partial z^2} + \frac{1}{r}\frac{\partial c_i}{\partial r} + \frac{\partial^2 c_i}{\partial r^2}\right) - k_i c_1^m c_2^n;\\
&r = 0, \quad \frac{\partial c_i}{\partial r} \equiv 0; \quad r = r_0, \quad \frac{\partial c_i}{\partial r} \equiv 0;\\
&z = 0, \quad c \equiv c_i^0, \quad u^0 c_i^0 \equiv u c_i^0 - D_i\frac{\partial c_i}{\partial z}, \quad i = 1,2,
\end{aligned} \tag{14}$$

using generalized variables:

$$\begin{aligned}
&r = r_0 R, \quad z = lZ, \quad u(r) = u(r_0 R) = u^0 U(R),\\
&\tilde{u}(r) = \tilde{u}(r_0 R) = U(R),\\
&c_i(r,z) = c_i(r_0 R, lZ) = c_i^0 C_i(R,Z) \quad (i = 1,2), \quad \varepsilon = \left(\frac{r_0}{l}\right)^2,
\end{aligned} \tag{15}$$

where r_0, l, u^0, c_i^0 $(i = 1,2)$ are the characteristic (inherent) scales (maximal or average values) of the variables. The introduction of the generalized variables (15) leads to:

$$\begin{aligned}
&U\frac{\partial C_i}{\partial Z} = \mathrm{Fo}_i\left(\varepsilon\frac{\partial^2 C_i}{\partial Z^2} + \frac{1}{R}\frac{\partial C_i}{\partial R} + \frac{\partial^2 C_i}{\partial R^2}\right) - \mathrm{Da}_i C_1^m C_2^n;\\
&R = 0, \quad \frac{\partial C_i}{\partial R} \equiv 0; \quad R = 1, \quad \frac{\partial C_i}{\partial R} \equiv 0;\\
&Z = 0, \quad \mathrm{C}_i \equiv 1, \quad 1 \equiv U - \mathrm{Pe}_i^{-1}\frac{\partial C_i}{\partial Z};\\
&\mathrm{Fo}_i = \frac{D_i l}{u_0 r_0^2}, \quad \mathrm{Da}_i = \theta^{i-1}\mathrm{Da}_i^0, \quad \mathrm{Pe}_i = \frac{u_0 l}{D_i},\\
&\mathrm{Da}_i^0 = \frac{k_i l}{u_0}\left(c_1^0\right)^{m-1}\left(c_2^0\right)^n, \quad \theta = \frac{c_1^0}{c_2^0}; \quad i = 1,2,
\end{aligned} \tag{16}$$

where Fo, Da and Pe are the Fourier, Damkohler and Peclet numbers, respectively.

2.5.1. Comparison qualitative analysis

If all equations in a model are divided by the dimensionless parameter, which has the maximal order of magnitude, all terms in the model equations will be classified in three parts:

1. The parameter is unity or its order of magnitude is unity, i.e. this mathematical operator represents a main physical effect;

2. The parameter's order of magnitude is 10^{-1}, i.e. this mathematical operator represents a small physical effect;

3. The parameter's order of magnitude is $\le 10^{-2}$, i.e. this mathematical operator represents a very small (negligible) physical effect and has to be neglected, because it is not possible to be measured experimentally.

2.5.2. Pseudo-first-order reactions

In the cases of big difference between inlet concentrations of the reagents $\left(c_1^0 \gg c_2^0\right)$ in the chemical reactor model, the problem is possible to be solved in zero approximation with respect to the very small parameter $\theta\left(0=\theta\le 10^{-2}\right)$ and as a result $Da_2 = 0, C_2 \equiv 1$. Very often $m = 1$ and from (1.16) follows:

$$
\begin{aligned}
&U\frac{\partial C}{\partial Z} = \mathrm{Fo}\left(\varepsilon\frac{\partial^2 C}{\partial Z^2}+\frac{1}{R}\frac{\partial C}{\partial R}+\frac{\partial^2 C}{\partial R^2}\right)-\mathrm{Da}\,C;\quad \varepsilon=\mathrm{Fo}^{-1}\mathrm{Pe}^{-1};\\
&R=0,\quad \frac{\partial C}{\partial R}\equiv 0;\quad R=1,\quad \frac{\partial C}{\partial R}\equiv 0;\\
&Z=0,\quad \mathrm{C}\equiv 1,\quad 1\equiv U-\mathrm{Pe}^{-1}\frac{\partial C}{\partial Z};
\end{aligned}
\tag{17}
$$

where $C = C_1, \mathrm{Da} = \mathrm{Da}_1^0$ and model of column apparatuses with pseudo-first-order chemical reaction is obtained.

2.5.3. High-column model

For high columns ε is a very small parameter and the problem (1.18) is possible to be solved in zero approximation with respect to $\varepsilon\left(0=\varepsilon\le 10^{-2}\right)$, i.e. $\mathrm{Pe}^{-1}\le 10^{-2}\,\mathrm{Fo}$ and for $\mathrm{Fo}\le 1$ the next very small parameter is Pe^{-1} $\left(0=\mathrm{Pe}^{-1}\le 10^{-2}\right)$.

2.5.4. Effect of the chemical reaction rate

When fast chemical reactions take place $\left(\mathrm{Da}\ge 10^2\right)$, the terms in in the chemical reactor model must be divided by Da and the approximation $0=\mathrm{Da}^{-1}\le 10^{-2}$ has to be applied (model is diffusion type).

2.5.5. Effect of the average velocity

In the cases of big values of the average velocity $\left(0=\mathrm{Fo}\le 10^{-2}\right)$, from the convection-diffusion type model is possible to obtain a convection type model when putting $\mathrm{Fo}=0$.

2.6. Calculation problems

The solutions of the model equations lead to different calculation problems as solution of set of equations in two systems of coordinates and the presence of small parameters at the highest derivates.

2.7. Models applications

The convection-diffusion models are applied for theoretical analysis of the "back mixing effect" and the modeling of the scale effect, circulation zones, and airlift apparatuses.

3. Average-concentration type models

The average-concentration model will be presented on the bases of the convection-diffusion model of the one-phase system in the case of pseudo-first-order chemical reaction:

$$
\begin{aligned}
&u\frac{\partial c}{\partial z} = D\left(\frac{\partial^2 c}{\partial z^2}+\frac{1}{r}\frac{\partial c}{\partial r}+\frac{\partial^2 c}{\partial r^2}\right)-kc;\\
&r=0,\quad \frac{\partial c}{\partial r}\equiv 0;\quad r=r_0,\quad \frac{\partial c}{\partial r}\equiv 0;\\
&z=0,\quad c\equiv c^0,\quad u^0c^0\equiv uc^0-D\frac{\partial c}{\partial z}.
\end{aligned}
\tag{18}
$$

The average values of the velocity and concentration at the column cross-sectional area in one-phase systems are:

$$
\bar{u}=\frac{2}{r_0^2}\int_0^{r_0} r u(r)\,dr,\quad \bar{c}(z)=\frac{2}{r_0^2}\int_0^{r_0} r c(r,z)\,dr. \tag{19}
$$

The functions $u(r), c(r,z)$ can be presented with the help of the average functions:

$$
u(r)=\bar{u}\tilde{u}(r),\quad c(r,z)=\bar{c}(z)\tilde{c}(r,z), \tag{20}
$$

where $\tilde{u}(r)$ and $\tilde{c}(r,z)$ represent the radial non-uniformity of the velocity and concentration and satisfy the following conditions:

$$
\frac{2}{r_0^2}\int_0^{r_0} r\,\tilde{u}(r)\,dr=1,\quad \frac{2}{r_0^2}\int_0^{r_0} r\,\tilde{c}(r,z)\,dr=1. \tag{21}
$$

The introduction of the average values of the velocity and concentration in the convection-diffusion model leads to the average concentration model:

$$
\begin{aligned}
&\alpha\bar{u}\frac{d\bar{c}}{dz}+\frac{d\alpha}{dz}\bar{u}\bar{c}=D\frac{d^2\bar{c}}{dz^2}-k\bar{c};\\
&z=0,\quad \bar{c}(0)=c^0,\quad \frac{d\bar{c}}{dz}=0,
\end{aligned}
\tag{22}
$$

where

$$
\alpha(z)=\frac{2}{r_0^2}\int_0^{r_0} r\tilde{u}(r)\tilde{c}(r,z)\,dr \tag{23}
$$

represents effect of the radial non-uniformity of the velocity.

The use of the generalized variables

$$
\begin{aligned}
&r=r_0R,\quad z=lZ,\quad u(r)=\bar{u}U(R),\quad \tilde{u}(r)=\frac{u(r)}{\bar{u}}=U(R),\\
&c(r,z)=c^0C(R,Z),\quad \bar{c}(z)=c^0\bar{C}(Z),\\
&\tilde{c}(r,z)=\frac{c(r,z)}{\bar{c}(z)}=\frac{C(R,Z)}{\bar{C}(Z)},\quad \bar{C}(Z)=2\int_0^1 RC(R,Z)dR,\\
&\alpha(z)=\alpha(lZ)=A(Z)=2\int_0^1 RU(R)\frac{C(R,Z)}{\bar{C}(Z)}dR,
\end{aligned}
\tag{24}
$$

leads to:

$$
\begin{aligned}
&A(Z)\frac{d\bar{C}}{dZ}+\frac{dA}{dZ}\bar{C}=\mathrm{Pe}^{-1}\frac{d^2\bar{C}}{dZ^2}-\mathrm{Da}\,\bar{C};\\
&Z=0,\quad \bar{C}=1,\quad \frac{d\bar{C}}{dZ}=0,
\end{aligned}
\tag{25}
$$

where Pe and Da are the Peclet and Damkohler numbers, respectively:

$$
\mathrm{Pe}=\frac{\bar{u}l}{D},\quad \mathrm{Da}=\frac{kl}{\bar{u}}. \tag{26}
$$

The case of parabolic velocity distribution (Poiseuille flow) will be presented as an example:

$$
u=\bar{u}\left(2-2\frac{r^2}{r_0^2}\right),\quad \bar{u}=u^0,\quad U(R)=2-2R^2. \tag{27}
$$

The use of the velocity distribution permits to obtain the function $A(Z)$. The result obtained shows, that the function $A(Z)$ for Fo = 0.1, Da = 1 can be presented as linear approximation $A=a_0+a_1Z$ ($a_0=1, a_1=0.254$). As a result, the model assumes the form:

$$
\begin{aligned}
&(a_0+a_1Z)\frac{d\bar{C}}{dZ}+a_1\bar{C}=\mathrm{Pe}^{-1}\frac{d^2\bar{C}}{dZ^2}-\mathrm{Da}\,\bar{C};\\
&Z=0,\quad \bar{C}=1,\quad \frac{d\bar{C}}{dZ}=0.
\end{aligned}
\tag{28}
$$

3.1. Effect of the velocity radial non-uniformity

In the cases of absence of radial non-uniformity of the velocity distribution at the column cross-sectional area (plug flow cases) $u=\overline{u}, U(R)\equiv 1$ and $A(Z)\equiv 1$, i.e. the radial non-uniformity of the velocity distribution leads to $A(Z)>1$.

The equation can be modified as

$$\frac{d\overline{C}}{dZ}=\left[A(Z)\right]^{-1}\left[Pe^{-1}\frac{d^2\overline{C}}{dZ^2}-(Da+\frac{dA}{dZ})\overline{C}\right], \qquad (29)$$

i.e. the radial non-uniformity of the velocity distribution leads ($A(Z)$ > 1) to a decrease of the axial gradient of the average concentration $\left(d\overline{C}/dZ\right)$ and the conversion degree, because the conversion degree is possible to be presented as $G=\overline{C}(0)-\overline{C}(1)$.

3.2. Model parameters identification

The solution of the convection-diffusion model permits to $C(Z_n,R)$ be obtained for different $Z_n=0.1n, n=1,2,...,10$ and the average concentrations:

$$\overline{C}(Z_n)=2\int_0^1 RC(Z_n,R)dR, \quad n=1,...,10. \qquad (30)$$

As a result it is possible to obtain "artificial experimental data" for different values of Z:

$$\begin{aligned}&\overline{C}^m_{\exp}(Z_n)=(0.95+0.1B_m)\overline{C}(Z_n),\\ &m=1,...10, \quad Z_n=0.1n, \quad n=1,2,...,10,\end{aligned} \qquad (31)$$

where $0\le B_m\le 1, m=1,...,10$ are obtained with a generator of random numbers. The obtained artificial experimental data are used for illustration of the parameters' (a_0, a_1) identification in the average concentrations models by minimization of the least-squares functions for different values of Z:

$$\begin{aligned}&Q_n(a_{0n},a_{1n})=\sum_{m=1}^{10}\left[\overline{C}(Z_n,a_{0n},a_{1n})-\overline{C}^m_{\exp}(Z_n)\right]^2,\\ &Z_n=0.1n, \quad n=1,3,5.\end{aligned} \qquad (32)$$

These parameter values are used for the calculations of the average concentration in the model. The obtained values $\overline{C}(Z_n,a_{0n},a_{1n})$, $Z_n=0.1n$, $n=1,3,5$ (the points) are compared (Fig. 1) with the "exact" function of the average concentration $\overline{C}(Z)$ (the line). From Fig. 1 it is evident that the experimental data, obtained in a short column ($Z=0.1$) with real diameter, are useful for the model parameters identification.

Similar results are obtained in the cases of the co-current and counter-current physical (chemical) absorption, non-stationary physical (chemical) adsorption, gas (liquid) – solid catalytic reactions in the cases of physical (chemical) adsorption mechanism.

4. Conclusions

The convection-diffusion and average-concentration models are used for the qualitative and quantitative analysis of the homogeneous chemical reactions, co-current and counter-current physical (chemical) absorption, non-stationary physical (chemical) adsorption, gas (liquid) – solid catalytic reactions in the cases of physical (chemical) adsorption mechanism. In all these cases it is used an approximation, according to which the radial non-uniformity of the axial velocity component does not change along the column height, i.e. the radial velocity component is equal to zero. This approach is not effective for very high columns, where the axial velocity component decreases along the column height. In these cases ($u_j=u_j(r,z), v_j=v_j(r,z), j=1,2,3$) will be proposed new type models.

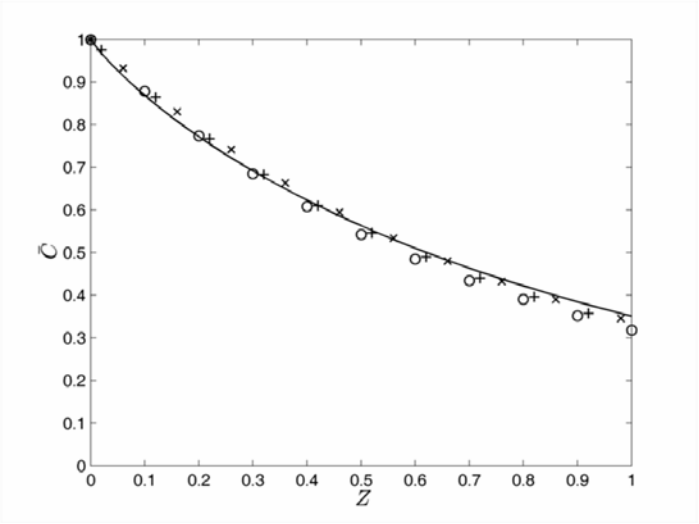

Fig. 1 *Average concentration* $\overline{C}(Z)$ *for* $\mathrm{Fo}=0.1, \mathrm{Da}=1, \varepsilon=10^{-1}, \mathrm{Pe}^{-1}=0.01$: *line – average concentration (24) after solution of (17);*
○ *– solution of (28)* $\overline{C}(Z,a_{01},a_{11})$, $Z=0.1$, $a_{01}=1$, $a_{11}=0.3519$ *;*
\+ *– solution of (28)* $\overline{C}(Z,a_{03},a_{13})$, $Z=0.3$, $a_{03}=1$, $a_{13}=0.2707$ *;*
× *– solution of (28)* $\overline{C}(Z,a_{05},a_{15})$, $Z=0.5$, $a_{05}=1$, $a_{15}=0.2162$.

5. References

[1] Chr. Boyadjiev, "Theoretical Chemical Engineering. Modeling and simulation", Springer-Verlag, Berlin Heidelberg, 2010, pp. 594.

[2] Chr. Boyadjiev, M. Doichinova, B. Boyadjiev, P. Popova-Krumova, "Modeling of Column Apparatus Processes", Springer-Verlag, Berlin Heidelberg, 2016, pp. 313.

MODEL ADHESION WEAR OF FRICTION SURFACE

МОДЕЛЬ АДГЕЗИОННОГО ИЗНОСА ПОВЕРХНОСТИ ТРЕНИЯ

Candidate of Science, associate Professor. Shalygin M.G.
Faculty of Mechanical and Technical – Bryansk State Technical University, Russia

Abstract: *The article deals with forming the adhesive bond of bodies at the crystal lattice level. There is offered a mathematical model for determining the adhesion wear. There are carried out laboratory tests for model validation. There is found that the amount of adhesive wear is nonline-arly dependent on the surface roughness inclination angle.*
KEYWORDS*: FRICTION, WEAR, ADHESION, MATEMATICS MODELING*

1. Introduction

Adhesion of steel surfaces is usually described in terms of the dispersion forces. Many existing adhesion models do not take into account the molecules adhesion within the solid body and the presence of irregularities on the parts surfaces. In the process of friction machine parts are exposed to adhesive wear. Moreover, in general, the amount of adhesive wear depends on the number of surface interacting cycles (n). Work [2] is dedicated to determining adhesive wear at individual surface contact (n = 1). Approaching the surfaces of two bodies at a distance forms adhesive bond FB3 (Fig. 1).

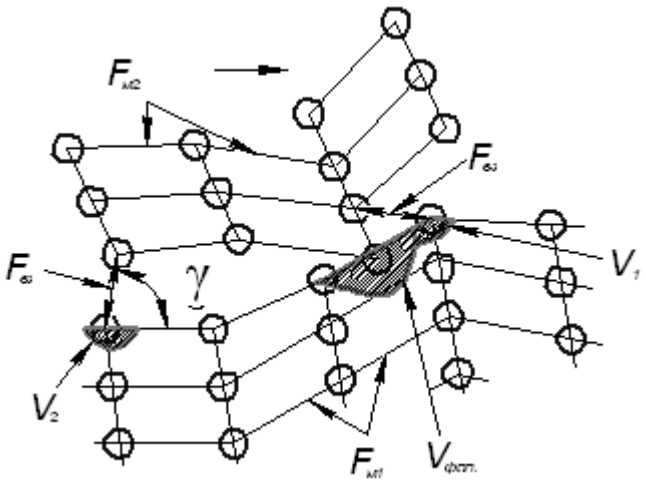

Fig. 1 Surfaces interaction during the adhesion at the nanoscale

There is also an intermolecular interaction in the volume of the forces themselves FM.. In-termolecular force and adhesion force can be determined by relationships proposed in work [1].

2. Results and Discussions

Let us assume that body 2 has the highest possible intermolecular force FM2=>max and ad-hesive wear of the body is not possible. Then, upon application of the shear load to body 2 there occurs adhesive wear of body 1, which visually represents the tension load on the surface.

Let us assume that the volume of the unit adhesive tear-out is determined by the intermo-lecular interaction force in the body FM. Then it is required to define vectors l, forming the vol-ume of tear-out. For a body having a crystal structure the vector direction can be determined by the shape of the unit cell, and the vector value is determined by the interplay of the two neigh-bouring molecules in the chosen direction. For example, steel, whose basic structure is austenite, the direction and the number of vectors that determine the amount of tear-out.

Thus, the vectors defining the scope of a single tear-out are located in three mutually per-pendicular planes, the angle between them is 45 degrees. The task of determining the scope of a single tear-out is reduced to determining the figure volume bounded by vectors l.

In order to build a mathematical model let us number the molecules on which vectors l are directed and assign the vector an index of the molecule to which it is directed. We note in par-ticular that vectors l1…l8 lie on the surface of the body, vectors l9…l13 are directed from the sur-face deep into the body. Let us construct a three-dimensional body model, built on top of 18 vec-tors in three-dimensional space. Assume that the body is an ellipsoid of revolution.

Approximately volume of the figure bounded by 13 vectors can be determined by the de-pendence

$$V = \frac{1}{12}[l_{10}(l_1 + l_9)(l_8 + l_2) + l_{13}(l_7 + k_9)(l_8 + l_6) + \\ + l_{12}(l_5 + l_9)(l_6 + l_4) + l_{11}(l_3 + l_9)(l_4 + l_2)]$$

From practice it is known that adhesion is carried out by digging to a depth significantly greater than the intermolecular distance of two neighbouring molecules. For this reason, we can-not say that the adhesive wear occurs to a depth greater than the intermolecular distance in the unit cell. Molecule located inside the body volume, communicates with a larger number of neighbouring molecules kk,, than a molecule located on the surface body and having a certain number of uncompensated bonds v1. Moreover, generally the number of possible neighbouring molecules k=kk+v1 is defined from the crystal lattice of the body.

The numerical value of the vectors l is by factors determining adhesion tension load. At the same time it should be noted that the actual surface profiles have irregularities such as roughness and subroughness. Thus, the adhesive bond FB3 is formed on surfaces disposed in relation to each other at a predetermined angle γ. The vector value l depends on the angle volume γ, because part of the body volume disposed closest to the top of asperity easier yields to tension load. Then the expression for l has the form

$$l_i = \left| \frac{v_1 F_{вз}}{k F_м G} tg\gamma \right|$$

where G - is shear modulus; k – is the possible number of neighbouring molecules; $k_k = k - v_1$ – is the actual number of neighbouring molecules.

It should be noted that the vectors directed deep into the body have the number of neigh-bouring molecules which is equal to the total number of possible molecules, $k = k_k$, then for vectors disposed on the surface

$$l_i = \left| \frac{F_{вз}}{F_м G} tg(F_{вз}, F_м) \right|,$$

aimed deep into the body

$$l_i = \left| \frac{v_1 F_{вз}}{k F_м G} tg(F_{вз}, F_м) \right|.$$

Formulas for calculating these parameters is given in works [1].

3. CONCLUSION

In order to test this theory, the experimental study of samples was conducted on the installation SAV10. Before the experiment samples of steel 1045 (*Ra* = 0.025) were purified by polar and non-polar solvent. In order to fix the surface before the test (2a) samples were examined under an optical microscope at a magnification 10000 fold.

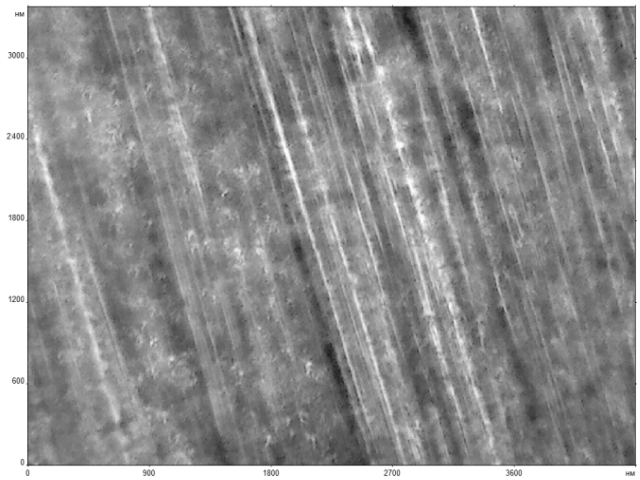

a)

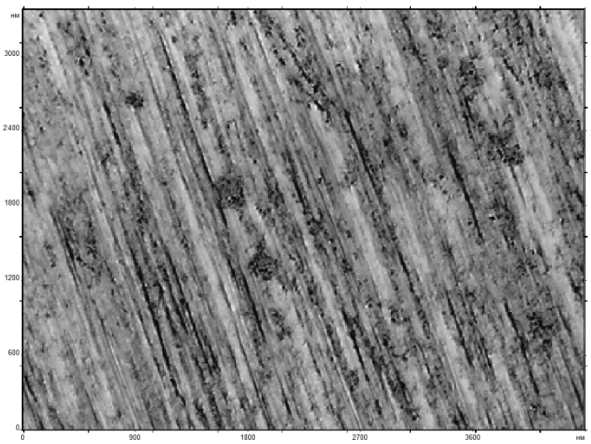

b)

Fig. 2. The surface of steel 45:
a) before forming the adhesive cut-away; b) after forming the adhesive tear-out.

Adhesive bond was considered formed when sample 2 is not detached from specimen 1 by gravity. Sample 2 was connected to a force sensor, sample 1 was rigidly secured to the mounting surface. By applying a force to the sensor sample 2 was displaced. Adhesive bond was considered broken at a time when there was a displacement of the sample relative to the other, then the surface of the samples was investigated under the microscope (Fig. 2b). The resulting dark spots were considered tear-out, formed as a result of adhesive wear.

The surface area and the wear-out depth were determined by 10 stains on 6 surface shots, after which the obtained values were averaged. The volume of tear-out is calculated as half of the ellipsoid volume

$$V = \frac{2}{3}\pi abc$$

where a, b, c - the ellipsoid axis.

According to the above-mentioned relationships there was counted the volume of single tear-out based on the conditions that the tested steel has austenitic structure $k = 18$, the shear modulus of steel $G=79\cdot10^9$ Pa, the distance between the centres of the particles $r = 3.495$ *nm* [3], compensated distance $z_0=2.86$ Å [2], Hamaker's constant $A_{\mu}=45\cdot10^{-24}$ J [3].

The initial data, the results of calculations and experiments are given in Table 1.

Table 1: Determination of adhesive tear-out volume

Calculated parameter	l_2	l_4	l_6	l_8	l_9	V, x10^5
Calculated, nm	59,651	59,94	59,65	59,94	16,57	1,241
Experiment, nm	54,43	66,30	54,43	66,30	16,65	1,258

Thus, there is a proximity of experimental and theoretical calculations. By theoretical expressions there were plotted the dependency graphs of the wear vector length l on the irregularities angle γ (Fig. 3a) and the number of possible neighbouring molecules k (Fig. 3b).

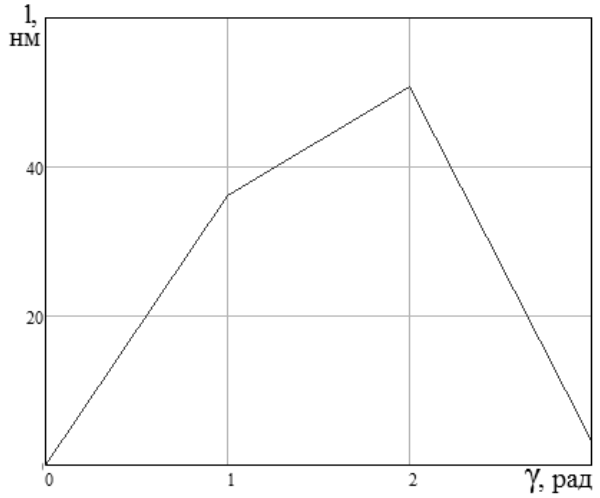

a)

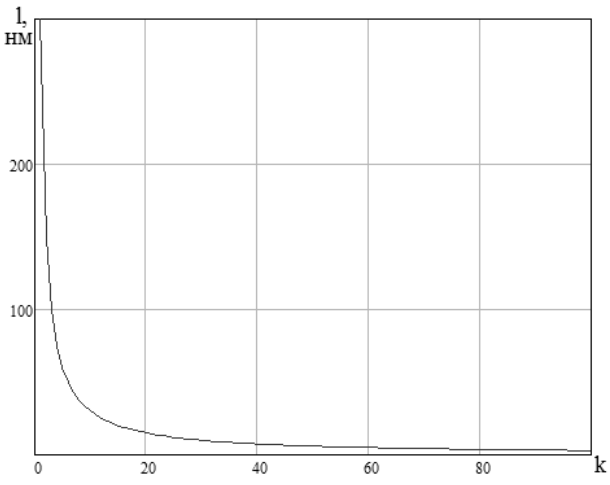

b)

Fig. 3 Dependence of the wear vector length on:
a) the inclination angle of irregularities γ to the adhesive bond (if $k = k_k$);
b) number of possible neighbouring molecules k (for $\gamma = 68^0$).

As can be seen from Fig. 5, vector l increases, if angle $\gamma = 0^0 \ldots 115^0$ and decreases with angles $\gamma = 116^0 \ldots 180^0$. With the increasing number of possible neighbouring molecules wear is re-

duced, which means that the larger molecules the unit cell contains and the smaller the distance is between them, then it is less prone to adhesion. Using proposed in work [1, 4] model of adhesive wear there is calculated an equation for determining the scope of a single adhesive tear-out. In accordance with the model of adhesive wear volume depends nonlinearly on the profile inclination angle and the crystal structure of the steel. In future, using the methods suggested in the works, it is possible to obtain a general expression for the determination of a single adhesive tear of steel with any structure.

4. REFERENCES

[1] Suslov A.G., Poroshin V.V., Shalygin M.G. Adhesive wear of the friction surfaces at the level of subroughness. // Friction & lubrication in machines and mechanisms, 2015, no. 7, pp. 29-31.

[2] Shalygin MG, Kokunov VA, Lukaviy AP, Elovikov AB Deformation and adhesive wear of friction surfaces nanoroughness martensitic steels. // Assembly in machine building, instrument making, 2017, no. 2. pp. 79-81.

[3] Suslov A.G., Shalygin MG, Kokunov VA, Lukaviy AP, Elovikov AB A model of adhesive wear based the inclination angle of the protrusion of the profile unevenness. // Fundamental research, 2015, no. 12. Part 6. pp. 1144-1148.

[4] Shalygin M.G. Modeling of wear of roughness of friction surfaces subservient. // Construction and road machines, 2016, no. 3, pp. 42-44.

DEVELOPMENT OF AUTOMATED QUALITY CONTROL SYSTEMS AND METHOD FOR ABSOLUTE PRESSURE SENSORS

Dr. Tech. Sci. A.V. Markov
Baltic State Technical University «VOENMEH» named after D.F. Ustinov, Saint Petersburg, Russia.

E-mail: markov-av@maill.ru

Abstract: *The article reviews concept of quality control systems of absolute gas pressure measuring instruments. Structure of quality control system is proposed. Development ways of method for control validity improvement of absolute pressure measuring instruments are overviewed.*

Keywords: QUALITY CONTROL SYSTEM, CONTROL AUTOMATION, CONTROL VALIDITY, ABSOLUTE PRESSURE SENSOR.

1. Introduction

Current practice of absolute pressure measurement is making higher requirements to accuracy, automation and productivity of quality control systems. It is noteworthy that in most of the cases these requirements are conflicting in such a way that improvement of some characteristics is achieved by decreasing of others. For example, increasing of system functional capabilities, accompanied by it complexity growth, decrease reliability caused by increase of element failure rate. That is why development of quality control system should be supported by continuous searching of compromise between implemented properties, technical capabilities and economic efficiency.

Development of measurement techniques, continuous improvement of constructive, technological and functional characteristics of measuring equipment, large-scale implementation of information technology leads to change of control operations content, increase of it complexity and responsibility and as a consequence leads to new heightened requirements to quality control systems.

Main metrological problem of absolute pressure sensors control system development was and remains problem of it systematic accuracy improvement with keeping high productivity of control operations.

2. System structure

Analysis of requirements to absolute pressure sensors quality control system structure was done based on the assumption that it main quality parameters are: metrological characteristics (range, accuracy, speed), stability of indications, measuring- equipment reliability. Analysis indicated that achieving of acceptable accuracy and productivity should include several standard instruments of pressure measuring, than can provide precise and reliable joint measuring by various methods [1, 2]. Based on requirements to accuracy and reliability of measurement, structure of automated system for absolute pressure sensors quality control should consist of [3, 4]: automated system of air pressure values setting (ASPS), containing automated pressure control unit and reference frequency pressure sensor; receiver; reference deadweight manometer (Fig. 1). By ASPS in the working cavity of receiver and controlled instrument, absolute pressure is set with limit of error 20 Pa in the range of 0,7 to 100kPa and 0,015% in the range of 100 to 285 kPa. This allows to use ASPS as a precision instrument for absolute pressure sensor quality control. Reference frequency pressure sensor needs in periodical verification. For this purpose in the structure of automated system for absolute pressure sensors quality control included reference deadweight manometer with the following limit of error: 7 Pa in the range of 0,7 to 100kPa and 0,005% in the range of 100 to 720 kPa.

3. Control method

Practical application of proposed structure of absolute pressure sensors quality control system require improve of control method. The reason for this is that existing methods and guidelines are not always taking into account automated character of control and also requirements to accuracy of controlled instruments quite difficult to provide by enough accurate reference measuring instruments included into automated quality control system. Validity of control instruments have to be ensured by complication of control operations organization, by introduction of strict acceptance limits, by complication of technical means [5, 6].

It is important to note that lack of accuracy of reference measuring instruments reflected in the verification methods of working pressure measuring instruments MM (measurement method) 2124-90 SSEUM (state system for ensuring the uniformity of measurements) «Manometers, vacuum meters, mano-vacuum meters, pressure gauges, draught meters and draught and pressure gauges indicating and recording. Verification method». Regulatory documents are proposing to use stricter acceptance limit than measurement error in technical passport of controlled instrument. Value of acceptance limit is calculated based on statistical model that provides require control validity with error ratio between reference and controlled instruments $\alpha_p \leq 0{,}5$ in accordance with MM 187-86 SSEUM «Validity and requirements to measurement instruments verification method» and MM 188-86 SSEUM «Measurements instruments. Setting of parameters values for verification methods».

It is proposed to adhere following condition during periodical calibration of pressure sensor ASPS and control of absolute pressure sensor:

$$(\Delta_0/D)100 \leq \alpha_p \gamma, \qquad (1)$$

where Δ_0 – limit of absolute permissible error of reference instrument; D – scale range of calibratable (controlled) absolute pressure measurement instrument; α_p – ratio between limit of permissible error of reference instrument and limit of intrinsic permissible error of calibratable (controlled) absolute pressure measurement instrument; γ – limit of intrinsic permissible error of instrument as a percentage of standardized value. This changes statistical approach to reference measure selection in the quality of ASPS during control of pressure sensor allowing selection of α_p with higher value ($\alpha_p \leq 0{,}5$). Herewith high quality of control is provided by introduction of so-called acceptance limit $\Delta_{ac.}$, which is less than limit of intrinsic permissible error $\Delta_{max.}$ of calibratable (controlled) absolute pressure measurement instrument.

$$\Delta_{ac.} < \Delta_{max.}. \qquad (2)$$

Absolute pressure sensors quality control systems of proposed in the article structure include two reference instruments with different principles of measurement. ASPS simulate air pressure which is measured by control instruments. Availability of deadweight manometer which implements direct method of pressure measurement allows to provide high validity of metrological characteristics of graduated and calibrated absolute pressure measurement instruments.

Within proposed concept automated and high-productivity precision systems for absolute pressure measurements instruments quality control can be created. These systems allow collection of mass data, comparison of results of periodical verification and control of measurement instruments, analysis of failure root causes, calculation of metrological validity value and prompt correction of verification intervals.

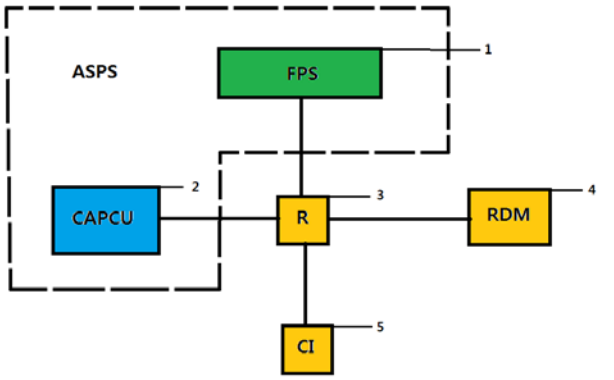

Fig. 1*. System structure: 1 - frequency pressure sensor; 2 - containing automated pressure control unit; 3 – receiver; 4 - reference deadweight manometer; 5 - controlled instrument*

References

[1] Markov A.V. Problems and ways of absolute pressure sensors quality control systems modernization. Scientific journal «Age of Quality» № 4, 2014. – p. 30-32. (in Russian)

[2] Markov A.V. Concept of measuring instruments of absolute pressure sensors quality control systems. Scientific journal «Age of Quality» № 1, 2015. – p. 34-35. (in Russian)

[3] Loparev V.K., Markov A.V., Stepanyan N.M., Dryuk V.A. Structure of automatic verification stand of air pressure measuring instruments. // Information technologies on transport. Collection of research papers, Saint-Petersburg: Polytechnics, 2003. – p. 220-222. (in Russian)

[4] Markov A.V. Problems of metrological assurance for measuring instruments. // 61 scientific-technical conference abstracts dedicated to Day of Radio, Saint Petersburg Electrotechnical University "LETI", 2006. – p. 226-228. (in Russian)

[5] Loparev V.K., Markov A.V., Spiridonov E.I., Stepanyan N.M. Organization of frequency pressure sensor with ratio of error of verifiable and reference instruments. // Methods of applied mathematics in transport systems: issue 6, Collection of research papers, Saint-Petersburg: Saint Petersburg State University of Water Communications, 2002. – p. 137-139. (in Russian)

[6] Loparev V.K., Markov A.V., Petrov V.M., Stepanyan N.M. Selection of reference manometer accuracy characteristics, used during verification of frequency pressure sensor. // Methods of applied mathematics in transport systems: issue 7, Collection of research papers, Saint-Petersburg: Saint Petersburg State University of Water Communications, 2002. – p. 198-199. (in Russian)

MATHEMATICAL MODELLING OF THE OSCILLATING BODY SUBMERGED IN THE LIQUID AT THE PRESENCE OF THE INITIAL AND CONSTANTLY ACTING DISTURBANCES

Dr. Vasily V. Maximov.[1,2], Elena A. Krylatykh.[3],
Chief Scientific Secretary, JSC "Oceanpribor", St. Petersburg, Russia [1]
Professor, SPbSUPTD, St. Petersburg, Russia[2]
Researcher, Khrulev Military Academy of Logistics, St. Petersburg, Russia[3]

wmaximov@mail.ru

Abstract: *The problem of the rigid body oscillations, submerged in the liquid of the uniform depth, as the problem of the potential theory is concerned. Small oscillations of the body and disturbances caused by the presence of a body in a liquid are studied. The problem is solved by the Green's-function method. The solution for the velocity potential is obtained in the form of a system of integral equations with a real kernel.*

Keywords: LIQUID OF UNIFORM DEPTH, BODY, DISTURBANCE, VELOCITY POTENTIAL, GREEN FUNCTION, INTEGRAL EQUATION

1. Introduction

Of great practical interest is the study of oscillations of hydroacoustic transducers and antennas placed in a layer of liquid with boundaries. We consider this problem as the initial-boundary value problem of potential theory.

Let a solid body be immersed in a liquid bounded from above by a free surface, from below - by a horizontal bottom. The liquid is assumed to be perfectly incompressible, and its motion is irrotational. We choose the Cartesian coordinate system *Oxyz* as follows: the axes *Ox, Oy* lie in the horizontal plane coinciding with the free surface of the liquid in the unperturbed state, the axis *Oz* is directed vertically upwards. The problem of the oscillations of a body in a liquid under these assumptions is nonlinear [1]. In this paper we consider the case of small oscillations of a liquid and a body.

2. Formulation of the problem

In the linear case [2], the perturbed motion of the liquid is described by means of a harmonic function $\Phi = \Phi(x, y, z, t)$, satisfying the following boundary and initial conditions:

$$\frac{1}{g}\frac{\partial^2\Phi}{\partial t^2} + \frac{\partial\Phi}{\partial z} = -\frac{1}{\rho g}\frac{\partial p_0}{\partial t} = P(x,y,t), \qquad z = 0,$$

$$\frac{\partial\Phi}{\partial z} = 0, \qquad z = -H,$$

$$\frac{\partial\Phi}{\partial n} = V_n - \frac{\partial\varphi_\infty}{\partial n}, \qquad (x,y,z) \in S,$$

$$\lim_{R\to\infty}\Phi = 0, \qquad \lim_{R\to\infty}\nabla\Phi = 0, \qquad R = \sqrt{x^2+y^2},$$

$$\Phi = F_1(x,y,t), \qquad z = 0, \qquad t = t_0,$$

$$\frac{\partial\Phi}{\partial t} = F_2(x,y,t), \qquad z = 0, \qquad t = t_0.$$

Here we have adopted the following notation: Φ is the velocity potential of the disturbed motion of the liquid; φ_∞ is potential of the system of incoming waves; p_0 is pressure applied to the free surface; ρ is the density of the liquid; g is the acceleration due to gravity; H is the depth of the liquid layer; S - position of the body surface in the static state; n is the normal to S, directed into the interior of the liquid; V_n is the projection of the velocity of points on the surface of the body on the normal; F_j, $j = 1,2$ are known functions.

3. Construction of the Green's function

Bearing in mind the use of the formula for the theory of harmonic functions [3], we construct a function G corresponding to the wave motion of a liquid caused by the action of a source placed at a point $N = (\xi, \eta, \zeta)$ from $t = \tau$. The function G everywhere, except the point $M = (x, y, z)$, is harmonic and satisfies the following conditions:

$$\frac{\partial^2 G}{\partial t^2} + \frac{\partial G}{\partial z} = 0, \qquad z = 0,$$

$$\frac{\partial G}{\partial z} = 0, \qquad z = -H,$$

$$\lim_{R\to\infty} G = 0, \quad \lim_{R\to\infty}\nabla G = 0,$$

$$G = \frac{\partial G}{\partial t} = 0, \quad z = 0, \quad t = \tau.$$

Let us construct the function G. Let

$$G = \frac{1}{r} + \frac{1}{r_1} + B(M,t;N,\tau),$$

$$r = \sqrt{(x-\xi)^2 + (y-\eta)^2 + (z-\zeta)^2}, \quad r_1 = \sqrt{R_0^2 + (z-\zeta')^2},$$

$$R_0 = \sqrt{(x-\xi)^2 + (y-\eta)^2}, \quad \zeta' = -(2H + \zeta),$$

here $B = B(M,t;N,\tau)$ is a function to be determined.

By this representation we have

$$\frac{\partial B}{\partial z} = 0, \qquad z = -H.$$

The function B satisfies the condition at $z = 0$

$$\frac{\partial^2 B}{\partial t^2} + g\frac{\partial B}{\partial z} = -\frac{\partial}{\partial z}\left(\frac{1}{r} + \frac{1}{r_1}\right) = \frac{\partial}{\partial\zeta}\left(\frac{1}{r_1} - \frac{1}{r}\right).$$

By the equality of [3]

$$\left(\frac{1}{r_1} - \frac{1}{r}\right)\Big|_{z=0} = -\int_0^\infty (\exp(\zeta s) - \exp(\zeta' s))J_0(sR_0)ds,$$

where $J_0(x)$ is the Bessel function of zero order, the condition at $z = 0$ becomes:

$$\frac{\partial^2 B}{\partial t^2} + g\frac{\partial B}{\partial z} = 2g\int_0^\infty s\exp(-Hs)\operatorname{ch} s(H+\zeta)J_0(sR_0)ds.$$

Now for the harmonic function B we obtain the following representation:

$$B=\int_0^\infty sT(t,s)\exp(-Hs)\operatorname{ch}s(H+\zeta)\frac{\operatorname{ch}s(H+z)}{\operatorname{ch}sH}J_0(sR_0)ds,$$

in which the function $T=T(t,s)$ satisfies equation

$$\frac{\partial^2 T}{\partial t^2}+\sigma^2 T=2g,\qquad \sigma^2=gs\operatorname{th}sH$$

and the initial conditions

$$2+sT(\tau,s)=0,\qquad \frac{\partial T(\tau,s)}{\partial t}=0.$$

The solution of this problem has the form:

$$T(t,s)=-\frac{2}{s}(1+\operatorname{cth}sH)\cos\sigma(t-\tau)+\frac{2}{s}\operatorname{cth}sH.$$

Consequently, for the function B we obtain the following representation:

$$B=2\int_0^\infty[-(1+\operatorname{cth}sH)\cos\sigma(t-\tau)+\operatorname{cth}sH]\cdot$$

$$\cdot\exp(-Hs)\operatorname{ch}s(H+\zeta)\frac{\operatorname{ch}s(H+z)}{\operatorname{ch}sH}J_0(sR_0)ds.$$

4. The solution of the problem

Now we turn to the solution of the main problem. Let us consider an area τ_Σ, that is bounded by a surface Σ consisting of the following parts: the surface of the body *S*, the surface S_R of the cylinder of radius *R* with the *z*-axis, the circle S_1 in the plane $z=0$, and the circle S_2 in the plane $z=-H$.

In the domain τ_Σ we apply to the functions $\frac{\partial\Phi}{\partial t}$ and *G* the formula for the theory of harmonic functions:

$$\frac{1}{4\pi}\iint_\Sigma\left(G\frac{\partial^2\Phi}{\partial t\partial n}-\frac{\partial\Phi}{\partial t}\frac{\partial G}{\partial n}\right)d\sigma=\begin{cases}\frac{1}{2}\frac{\partial\Phi}{\partial t}, M\in\Sigma\\ \frac{\partial\Phi}{\partial t}, M\in\tau_\Sigma\end{cases},$$

Where $\bar n$ is the unit vector of the outer normal to the surface Σ at the point *N*, over which the integration takes place.

Using the boundary conditions at the bottom and at infinity ($R\to\infty$), we obtain:

$$\frac{1}{4\pi}\iint_{\zeta=0}\left(G\frac{\partial^2\Phi}{\partial t\partial\xi}-\frac{\partial\Phi}{\partial t}\frac{\partial G}{\partial\zeta}\right)d\xi d\eta+$$

$$+\frac{1}{4\pi}\iint_S\left(\frac{\partial\Phi}{\partial t}\frac{\partial G}{\partial n}-G\frac{\partial^2\Phi}{\partial t\partial n}\right)d\sigma=\begin{cases}\frac{1}{2}\frac{\partial\Phi}{\partial t}, M\in S\\ \frac{\partial\Phi}{\partial t}, M\in\tau_\infty\end{cases},$$

where τ_∞ is the region outside *S* between the planes $z=0$ and $z=-H$, $\bar n$ is the outer normal to *S*.

Integrating the last equation with respect to *t*, we obtain:

$$\frac{1}{4\pi}\iint_{\zeta=0}\int_{t_0}^t\left(G\frac{\partial^2\Phi}{\partial t\partial\xi}-\frac{\partial\Phi}{\partial t}\frac{\partial G}{\partial\zeta}\right)dtd\xi d\eta+$$

$$+\frac{1}{4\pi}\int_{t_0}^t\iint_S\left(\frac{\partial\Phi}{\partial t}\frac{\partial G}{\partial n}-G\frac{\partial^2\Phi}{\partial t\partial n}\right)d\sigma dt=\begin{cases}\frac{1}{2}\Phi\big|_{t_0}^t, M\in S\\ \Phi\big|_{t_0}^t, M\in\tau_\infty\end{cases}.$$

Let us consider the integral

$$\int_{t_0}^t\left(G\frac{\partial^2\Phi}{\partial t\partial\zeta}-\frac{\partial\Phi}{\partial t}\frac{\partial G}{\partial\zeta}\right)dt=\int_{t_0}^t\left(G\frac{\partial^2\Phi}{\partial t\partial\zeta}+\frac{\partial\Phi}{\partial t}\frac{\partial^2 G}{\partial t^2}\right)dt.$$

As

$$\frac{d}{dt}\left(G\frac{\partial\Phi}{\partial\zeta}+\frac{1}{g}\frac{\partial\Phi}{\partial t}\frac{\partial G}{\partial t}\right)=G\frac{\partial^2\Phi}{\partial t^2}+\frac{1}{g}\frac{\partial\Phi}{\partial t}\frac{\partial^2 G}{\partial t\partial\zeta}+\frac{\partial G}{\partial t}P,$$

we get:

$$\int_{t_0}^t\left(G\frac{\partial^2\Phi}{\partial t\partial\zeta}-\frac{\partial\Phi}{\partial t}\frac{\partial G}{\partial t}\right)dt=\left(G\frac{\partial\Phi}{\partial\zeta}+\frac{1}{g}\frac{\partial\Phi}{\partial t}\frac{\partial G}{\partial t}\right)\Big|_{t_0}^t-\int_{t_0}^t P\frac{\partial G}{\partial t}dt.$$

Setting now in the last equation $t=\tau$ and taking into account the initial conditions imposed on *G* and $\frac{\partial G}{\partial t}$, we have the equalities:

$$-\frac{1}{4\pi}\iint_{\zeta=0}\left\{\left(G\frac{\partial\Phi}{\partial\zeta}+\frac{1}{g}F_2\frac{\partial G}{\partial t}\right)\Big|_{t=t_0}+\int_{t_0}^t P\frac{\partial G}{\partial t}dt\right\}d\xi d\eta+$$

$$+\frac{1}{4\pi}\int_{t_0}^\tau\iint_S\left(\frac{\partial\Phi}{\partial t}\frac{\partial G}{\partial n}-G\frac{\partial^2\Phi}{\partial t\partial n}\right)d\sigma dt=\begin{cases}\frac{1}{2}\Phi\big|_{t_0}^\tau, M\in S\\ \Phi\big|_{t_0}^\tau, M\in\tau_\infty\end{cases}. \qquad (1)$$

The potential of the velocity at the initial instant of time $t=t_0$, $\Phi(\mathrm{M},t_0)$ is the solution of the problem:

$$\left.\begin{aligned}\frac{\partial^2\Phi}{\partial x^2}+\frac{\partial^2\Phi}{\partial y^2}+\frac{\partial^2\Phi}{\partial z^2}=0\\ \Phi(x,y,0,t_0)=F_1(x,y)\\ \frac{\partial\Phi}{\partial z}=0, z=-H\\ \Phi\to0,\nabla\Phi\to0,R\to\infty\end{aligned}\right\}.$$

Let us represent the function $F_1(x,y)$ in the form of a Fourier integral:

$$F_1(x,y)=\frac{1}{4\pi^2}\int_{-\pi}^{\pi}\int_0^\infty sA(s,\vartheta)\exp(-is(x\cos\vartheta+y\sin\vartheta)dsd\vartheta$$

$$A(s,\vartheta)=\int_{-\infty}^{\infty}\int_{-\infty}^{\infty}F_1(x,y)\exp(is(x\cos\vartheta+y\sin\vartheta)dxdy,$$

by means of which the solution of the problem for the potential Φ would be:

$$\Phi(\mathrm{M},\mathrm{t}_0)=\frac{1}{4\pi^2}\int_{-\pi}^{\pi}\int_0^\infty sA(s,\vartheta)\frac{\operatorname{ch}s(H+z)}{\operatorname{ch}sH}\exp(is(x\cos\vartheta+y\sin\vartheta))dsd\vartheta.$$

Let us find the derivative of the potential:

$$\left.\frac{\partial\Phi}{\partial z}\right|_{z=0}=\frac{1}{4\pi^2}\int_{-\pi}^{\pi}\int_0^\infty sA(s,\vartheta)\operatorname{th}sH\exp(-is(x\cos\vartheta+y\sin\vartheta))dsd\vartheta.$$

The lower row in equation (1) determines the form of the potential $\Phi(\mathrm{M},\tau),\mathrm{M}\in\mathrm{S}$ at each point of the region occupied by the liquid, and the upper row leads to the equation for finding the velocity potential of the disturbed liquid motion on the surface *S*. This equation has the form:

$$\Phi(\mathrm{M},\tau)=\frac{1}{2\pi}\int_{t_0}^\tau\iint_S\frac{\partial\Phi}{\partial t}\frac{\partial G}{\partial n}d\sigma dt-\frac{1}{2\pi}\int_{t_0}^\tau\iint_S\frac{\partial^2\Phi}{\partial t\partial n}Gd\sigma dt+\beta(M,\tau),$$

$$\beta(\mathrm{M},\tau)=-\frac{1}{2\pi}\iint\limits_{\zeta=0}\left\{\left(\mathrm{G}\frac{\partial\Phi}{\partial\zeta}+\frac{1}{g}\mathrm{F}_2\frac{\partial G}{\partial t}\right)\Big|_{t=t_0}+\int\limits_{t_0}^{\tau}P\frac{\partial G}{\partial t}dt\right\}d\xi d\eta+\Phi(M,t_0).$$

If we take the boundary condition on the surface *S* of the body into account explicitly, then we can obtain some consequences from this equation. This condition can be written as:

$$\frac{\partial^2\Phi}{\partial t\partial n}=\sum_{j=1}^{6}\gamma_j\frac{\partial u_j}{\partial t}-\frac{\partial^2\varphi_\infty}{\partial t\partial n},$$

where $(u_1,u_2,u_3)=\overline{\mathrm{V}}$ is the linear velocity of the body, $(u_4,u_5,u_6)=\overline{\omega}$ is the angular velocity of the body, $(\gamma_1,\gamma_2,\gamma_3)=\overline{n}$ is the normal to its surface *S*, $(\gamma_4,\gamma_5,\gamma_6)=(\overline{r}-\overline{r}_0)\times\overline{n}$, $\overline{r}=(x,y,z)$ is the radius vector of the point *M*, $\overline{r}_0$ is the radius vector of the center of gravity of the body in the static state.

Now we can put an additive expression for the velocity potential:

$$\Phi=\sum_{j=0}^{7}\Phi_j(M,\tau).$$

The functions $\Phi_j, j=0\div7,$ are solutions of the following integral equations:

$$\Phi_0(M,\tau)=\frac{1}{2\pi}\int\limits_{t_0}^{\tau}\iint\limits_{S}\frac{\partial\Phi_0}{\partial t}\frac{\partial G}{\partial n}d\sigma dt+\frac{1}{2\pi}\int\limits_{t_0}^{\tau}\iint\limits_{S}G\frac{\partial^2\varphi_\infty}{\partial n\partial t}d\sigma dt,$$

$$\Phi_j(M,\tau)=\frac{1}{2\pi}\int\limits_{t_0}^{\tau}\iint\limits_{S}\frac{\partial\Phi_j}{\partial t}\frac{\partial G}{\partial n}d\sigma dt-\frac{1}{2\pi}\int\limits_{t_0}^{\tau}\iint\limits_{S}G\gamma_j\frac{\partial u_j}{\partial t}d\sigma dt,$$

$$j=1\div6;$$

$$\Phi_7(M,\tau)=\frac{1}{2\pi}\int\limits_{t_0}^{\tau}\iint\limits_{S}\frac{\partial\Phi_7}{\partial t}\frac{\partial G}{\partial n}d\sigma dt+\beta(M,\tau).$$

Let us represent the function *G* as follows:

$$G=\frac{1}{r}+\frac{1}{2\pi}\int\limits_{-\pi}^{\pi}\int\limits_{0}^{\infty}\exp(-(z+\zeta+2H)s-is[(\mathrm{x}-\xi)\cos\vartheta+(\mathrm{y}-\eta)\sin\vartheta])dsd\vartheta+$$

$$+\frac{1}{\pi}\int\limits_{-\pi}^{\pi}\int\limits_{0}^{\infty}[\mathrm{cth\,sH}-(1+\mathrm{cth\,sH})\cos\sigma(\mathrm{t}-\tau)]\times$$

$$\times\exp(-Hs)\,\mathrm{ch}\,s(H+\zeta)\frac{\mathrm{ch}\,s(H+z)}{\mathrm{ch}\,sH}\exp(-is[(\mathrm{x}-\xi)\cos\vartheta+(\mathrm{y}-\eta)\sin\vartheta])\,\mathrm{dsd}\,\vartheta.$$

We transform with the help of this expression the resulting integral equations. As a result, we will have:

$$\Phi_0(M,\tau)=\frac{1}{2\pi}\iint\limits_{S}\frac{\partial}{\partial n}\left(\frac{1}{r}\right)\Phi_0(N,\tau)d\sigma-$$

$$-\frac{1}{2\pi}\iint\limits_{S}\frac{\partial}{\partial n}\left(\frac{1}{r}\right)\Phi_0(N,t_0)d\sigma+\frac{1}{2\pi}\iint\limits_{S}\frac{1}{r}\frac{\partial\varphi_\infty}{\partial n}\Big|_{t_0}^{\tau}d\sigma+N_0(M,\tau),$$

$$j=1\div6,$$

$$\Phi_j(M,\tau)=\frac{1}{2\pi}\iint\limits_{S}\frac{\partial}{\partial n}\left(\frac{1}{r}\right)\Phi_j(N,\tau)d\sigma-$$

$$-\frac{1}{2\pi}\iint\limits_{S}\frac{\partial}{\partial n}\left(\frac{1}{r}\right)\Phi_j(N,t_0)d\sigma-\frac{1}{2\pi}[\mathrm{u}_j(\tau)-u_j(t_0)]\iint\limits_{S}\frac{1}{r}\frac{\partial\varphi_\infty}{\partial n}\Big|_{t_0}^{\tau}d\sigma+N_j(M,\tau),$$

$$\Phi_7(M,\tau)=\frac{1}{2\pi}\iint\limits_{S}\frac{\partial}{\partial n}\left(\frac{1}{r}\right)\Phi_7(N,\tau)d\sigma-$$

$$-\frac{1}{2\pi}\iint\limits_{S}\frac{\partial}{\partial n}\left(\frac{1}{r}\right)\Phi_7(N,t_0)d\sigma+N_7(M,\tau).$$

Here the following notation is adopted:

$$N_j(M,\tau)=-\frac{1}{4\pi^2}\int\limits_{t_0}^{\tau}\int\limits_{-\pi}^{\pi}\int\limits_{0}^{\infty}\{\exp(-(z+H)s)\tilde{H}_j(s,\vartheta,t)+$$

$$+2\exp(-Hs)[1-(1+\mathrm{th}\,sH)\cos\sigma(t-\tau)]\times$$

$$\times\mathrm{ch}\,s(H+z)H_j(\mathrm{s},\vartheta,\mathrm{t})\}\exp(-\mathrm{is}(\mathrm{xcos}\,\vartheta+\mathrm{ysin}\,\vartheta))\,\mathrm{dsd}\,\vartheta\,\mathrm{dt},$$

$$j=0\div7;$$

$$\tilde{H}_0(s,\vartheta,t)=-\iint\limits_{S}\exp(-(\zeta+H)s+is(\xi\cos\vartheta+\eta\sin\vartheta))\times$$

$$\times\left\{\begin{array}{c}\dfrac{\partial\varphi_\infty}{\partial n\partial t}+s\dfrac{\partial\Phi_0}{\partial t}[i\cos\vartheta\cos(n,\xi)+\\+i\sin\vartheta\cos(n,\eta)-\cos(n,\zeta)]\end{array}\right\}d\sigma,$$

$$H_0(s,\vartheta,t)=-\iint\limits_{S}\exp(is(\xi\cos\vartheta+\eta\sin\vartheta))\frac{\mathrm{ch}\,s(H+\zeta)}{\mathrm{sh}\,sH}\times$$

$$\times\left\{\begin{array}{c}\dfrac{\partial^2\varphi_\infty}{\partial n\partial t}+s\dfrac{\partial\Phi_0}{\partial t}[i\cos\vartheta\cos(n,\xi)+\\+i\sin\vartheta\cos(n,\eta)+\mathrm{th}\,s(\zeta+H)\cos(n,\zeta)]\end{array}\right\}d\sigma,$$

$$\tilde{H}_j(s,\vartheta,t)=-\iint\limits_{S}\exp(-(\zeta+H)s+is(\xi\cos\vartheta+\eta\sin\vartheta))\times$$

$$\times\left\{\begin{array}{c}\gamma_j(N)\dfrac{\partial u_j}{\partial t}-s\dfrac{\partial\Phi_j}{\partial t}[i\cos\vartheta\cos(n,\xi)+\\+i\sin\vartheta\cos(n,\eta)-\cos(n,\zeta)]\end{array}\right\}d\sigma,$$

$$H_j(s,\vartheta,t)=-\iint\limits_{S}\exp(is(\xi\cos\vartheta+\eta\sin\vartheta))\frac{\mathrm{ch}\,s(H+\zeta)}{\mathrm{sh}\,sH}\times$$

$$\times\left\{\begin{array}{c}\gamma_j(N)\dfrac{\partial u_j}{\partial t}-s\dfrac{\partial\Phi_j}{\partial t}[i\cos\vartheta\cos(n,\xi)+\\+i\sin\vartheta\cos(n,\eta)+\mathrm{th}\,s(\zeta+H)\cos(n,\zeta)]\end{array}\right\}d\sigma,$$

$$\tilde{H}_7(s,\vartheta,t)=-s\iint\limits_{S}\exp(-(\zeta+H)s+is(\xi\cos\vartheta+\eta\sin\vartheta))(\Phi_7)_{\mathrm{t}}\times$$

$$\times[i\cos\vartheta\cos(n,\xi)+$$

$$+i\sin\vartheta\cos(n,\eta)-\cos(n,\zeta)]d\sigma,$$

$$H_7(s,\vartheta,t)=-s\iint\limits_{S}\exp(is(\xi\cos\vartheta+\eta\sin\vartheta))\frac{\mathrm{ch}\,s(H+\zeta)}{\mathrm{sh}\,sH}\times$$

$$\times\frac{\partial\Phi_7}{\partial t}[i\cos\vartheta\cos(n,\xi)+$$

$$+i\sin\vartheta\cos(n,\eta)+\mathrm{th}\,s(\zeta+H)\cos(n,\zeta)]d\sigma.$$

Functions $\tilde{H}_j(s,\vartheta,t)$ and $H_j(s,\vartheta,t)$ are functions of Kochin [1]. If the body is completely immersed in a liquid, these functions can be calculated using the values of the potential corresponding to the motion of the body in an unbounded liquid. All the resulting integral equations have the general form:

$$\Phi_j(M,\tau)=\frac{1}{2\pi}\iint\limits_{S}\frac{\partial}{\partial n}\left(\frac{1}{r}\right)\Phi_j(N,\tau)\,\mathrm{d}\,\sigma+f_j(M,\tau),\ \ j=0\div7.$$

The kernel of this equation $K(M,N)=\frac{1}{2\pi}\frac{\partial}{\partial n}\left(\frac{1}{r}\right)$ is real, and τ plays the role of a parameter. As its approximate solution, we can take that solution which is obtained by substituting the value of the potential corresponding to the motion of a body in an unbounded liquid under the integral sign.

Conclusion

The above solution allows to determine the velocity and pressure at any point occupied by liquid, both in the near and far zones.

The solution of the obtained system of integral equations (with the known functions of Kochin) can be carried out numerically using the known standard procedures [4, 5]. In this case, quantitative assessments of the transformation of the initial wave can be obtained by introducing a solid body immersed in a liquid with an invariable geometry into it.

References

1. Kochin, N.Ye. Collected Works. V.2, Moskwa-Leningrad.: izd-vo AN SSSR, 1949 (in Russian).
2. Aleshkov, Yu. Z. Theory of waves on the surface of a heavy liquid. Leningrad.: izd-vo LGU, 1981(in Russian).
3. Koshlyakov, N. S., Gliner, E. B., Smirnov, M. M. Equations in partial derivatives of mathematical physics. Moskva.: Vysshaya Shkola, 1970 (in Russian).
4. Tikhonov, A.N., Goncharskiy, A.V., Stepanov, V.V., Yagola, A.G. Numerical methods for solving ill-posed problems. Moskva.: Nauka, 1990 (in Russian).
5. Manzhirov, A.V., Polyanin, A. D. Methods for solving integral equations: a reference book. Moskva.: Faktorial, 1999 (in Russian).

PARAMETRIC ANALYSIS OF SURFACES OF ACOUSTO-ELECTRONIC RESONATORS USING NI LABVIEW AND SCANNING PROBE MICROSCOPY

Ph.D. V.V. Spiridonov

Baltic State Technical University «VOENMEH» named after D.F. Ustinov, Saint Petersburg, Russia

E-mail: spiridonov-vlad@yandex.ru

Abstract: *The article describes the results of analysis of the two acoustic electronic resonators performed using the scanning probe microscope and the software developed in the graphical integrated development environment LabVIEW with the machine vision module NI LabVIEW Vision. The most important surface parameters were measured and analyzed, and the corresponding conclusions were made regarding possible defects and compliance with the reference performance indicators of the two resonators.*

Keywords: QUALITY, RESONATORS, MACHINE VISION, HISTOGRAM EQUALIZATION, LABVIEW

1. Introduction

Today, acousto-electronic devices are widely used in radio-electronic devices, including mobile communication devices, radar systems, and radio navigation equipment. Among huge variety of acousto-electronic devices, one of the most promising are SAW resonators which operate on the basis of Surface Acoustic Waves. These resonators are highly sensitive, and can efficiently detect and handle complex signals in real-time or near real-time [1]. However, accuracy and sensitivity of SAW resonators strongly depend on the quality and geometry of their surfaces.

In this paper, surfaces of the two acousto-electronic SAW resonators were analyzed using a scanning probe microscope, NI LabVIEW Vision library, and the special LabVIEW-based software developed at BSTU VOENMEH.

2. Analysis workflow

To acquire images of the resonator surfaces, the special test equipment based on Nanoeducator, a popular scanning probe microscope (SPM), is used. The information acquired from the Nanoeducator is saved as an SPM frame, which is a two-dimensional array (matrix) of integers *Z [i, j]*. Each pair of indices *<i, j>* corresponds to a certain point of the surface within the scanned area. Coordinates of the surface points are calculated by multiplying the corresponding index by the distance between the points at which the data was acquired. SPM-frames are visualized by as two-dimensional (2D) and three-dimensional (3D) brightness-based images, which are convenient for edge detection. For 2D visualization, each point *Z = f (x, y)* of the surface is mapped with a hue of a certain color depending on the height of the surface item at that point. For 3D visualization, the whole image of the surface is generated in the axonometric perspective using pixels or lines. To ensure efficient coloring of 3D images and highlight even the smallest items on the surfaces, a point light source located above the surface was used.

To facilitate and speed up the image processing, as well as to filter out unwanted ("noisy") particles on the background and along the image border, it is necessary to binarize the image using local thresholds and/or apply corresponding particle filters. Image binarization in LabVIEW can be performed with the **IMAQ Threshold** component from NI Vision library [2]. The simplified program code of the algorithm is shown in Fig. 1.

Before the analysis, the image should be equalized using histogram alignment and the transformation function, which can be derived from a histogram of the original image. Assume that a given image with the first histogram is equalized using the following equation:

$$s = T(r) = \int_0^r p_r(w)dw, \quad (1)$$

where $p_r(r)$ and $p_z(r)$ are the original and target probability-density functions of brightness respectively, and w is the brightness.

If we assume that the target image is available, then its brightness levels could also be aligned using the conversion function:

$$v = G(z) = \int_0^z p_z(w)dw, \quad (2)$$

where $p_r(r)$ and $p_z(r)$ are the original and target probability-density functions of brightness respectively, and w is the brightness.

Therefore, the inverse transformation $z = G^{-1}(v)$ would restore the original levels, with $p_s(s)$ and $p_v(v)$ being identical uniform densities, since the equations (1) and (2) mutually ensure uniform density regardless of the nature of the probability-density function under the integral sign. Thus, if we replace v in the inverse transformation with the inverse levels s obtained from the original image, the resulting levels $z = G^{-1}(s)$ will have the desired probability-density function $p_z(z)$. If we assume that $G^{-1}(s)$ is a single-value function, the high-level algorithm can be described as follows [3]:

1. Align the brightness levels of the original image using equation (1).
2. Determine the desired brightness probability-density function and obtain the transformation function $G(z)$ using equation (2).
3. Perform the inverse transformation $z = G^{-1}(s)$ of the image to the brightness levels of the image with the histogram aligned in Step 1.

The proposed algorithm is implemented in the LabVIEW environment using NI Vision library (Fig. 2).

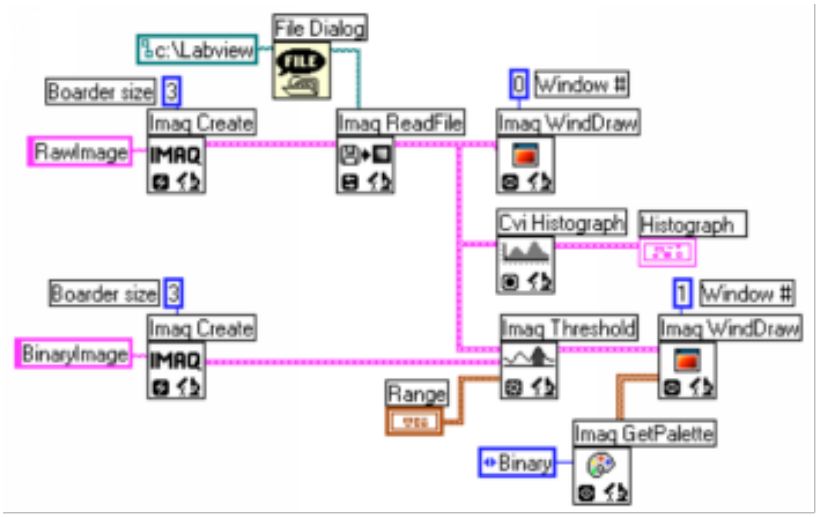

***Fig. 1**. Simplified program code of the image binarization algorithm*

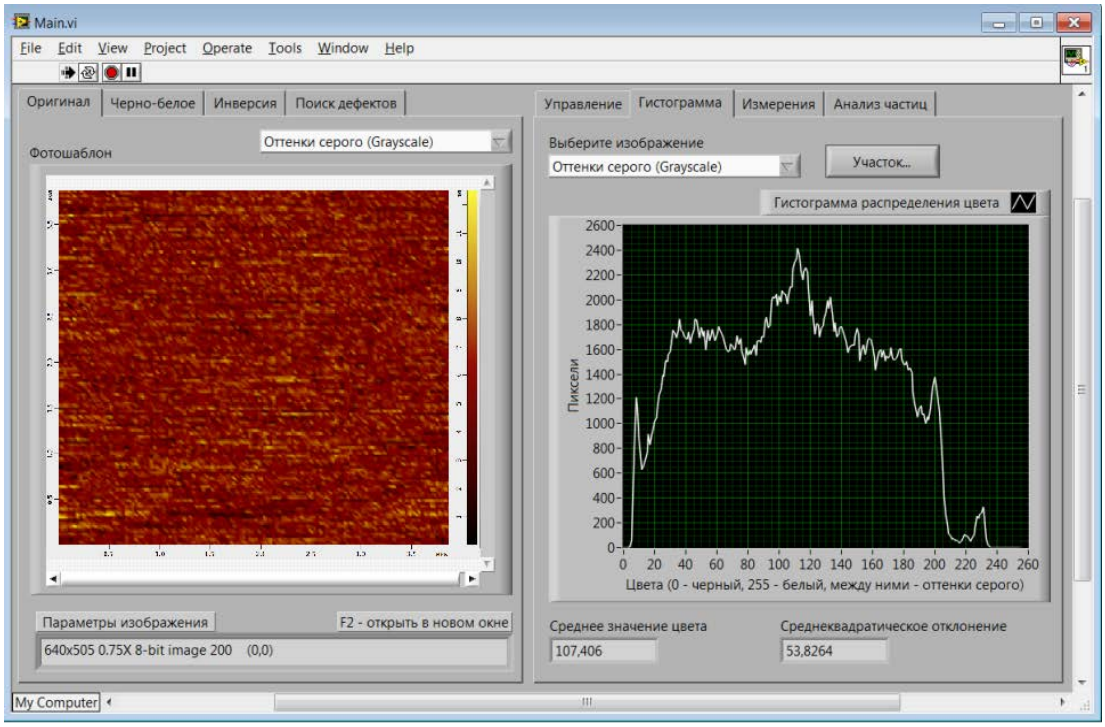

***Fig. 2**. Screenshot of the developed LabVIEW-based software*

3. Toolkit used for analysis

To analyze the images acquired from the scanning probe microscope, a software tool developed in the LabVIEW environment using the NI LabVIEW Vision library was used.

The software itself is a virtual instrument (VI) consisting of the two parts - the Front Panel and the Block Diagram. The Front Panel implements the graphical user interface, while the Block Diagram implements the internal logic of the software (its source code) [4, 5].

The software provides the following key features:

1. Operations with images in four main formats (BMP, JPEG, PNG, TIFF)
2. Image transformation: negative image, decomposition into color channels (Red, Green, Blue), grayscale image, binary image, inverted binary image
3. Measurement of distances between the two user-defined points, as well as any rectangular and annular areas in the image
4. Image calibration (setting up of a reference distance for scaling)
5. Calculation of the basic statistical parameters of a surface
6. Histograms of brightness, both for the whole image and for any user-defined area, as well as the calculation of the average brightness and standard deviation
7. Particle ("blob") analysis of the image and calculation of numerous particle parameters (length, height, area, center of gravity, etc.).

4. Results of the analysis

The following resonators were analyzed (Fig. 3 and Fig. 4):

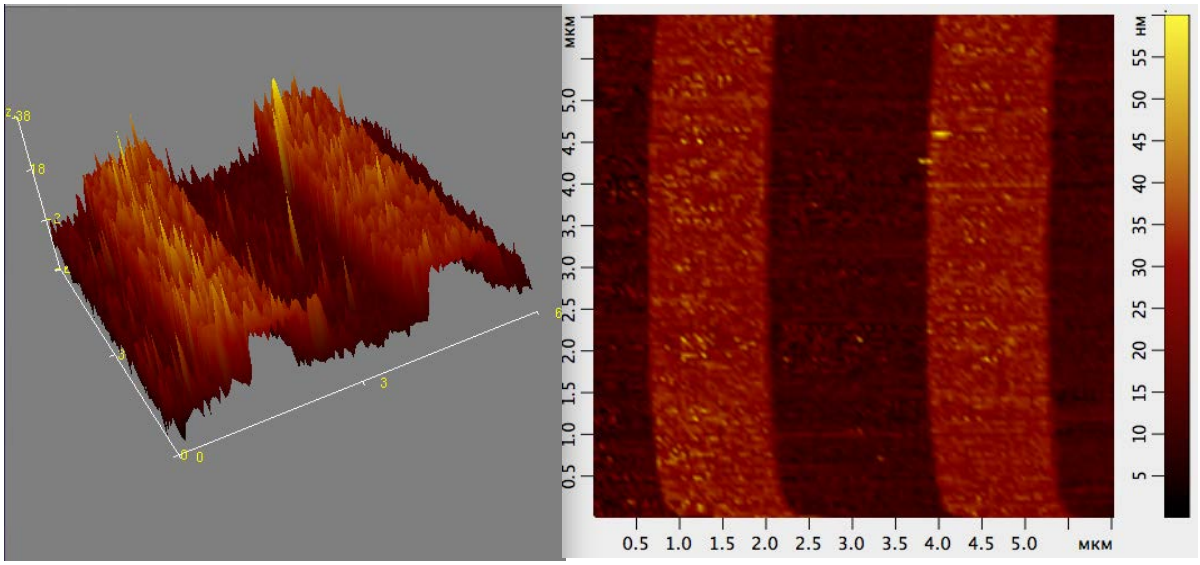

Fig. 3*. Resonator #1 (3D and 2D views)*

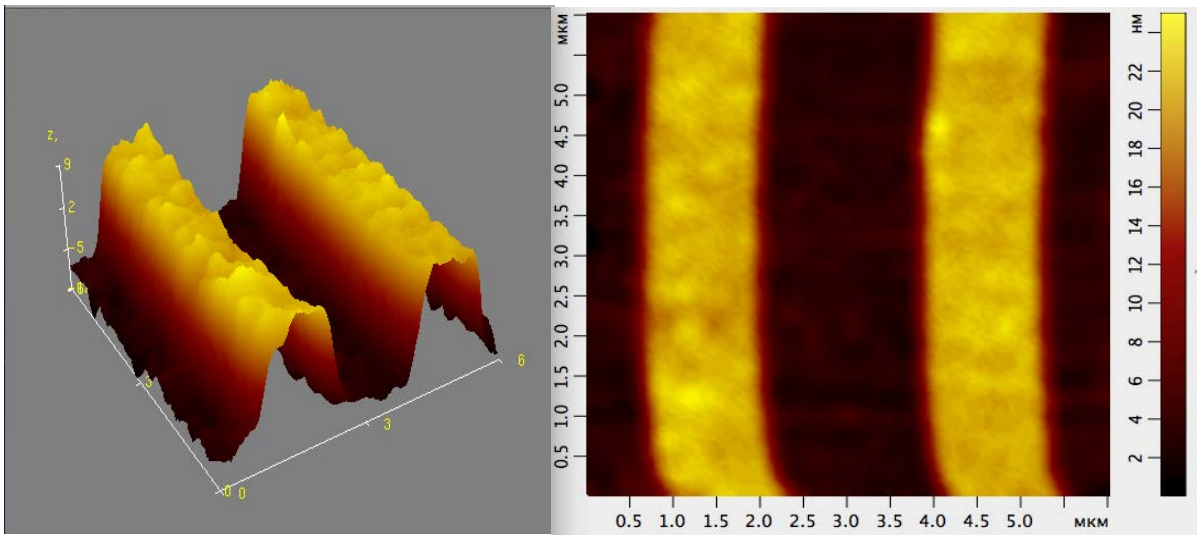

Fig. 4*. Resonator #2 (3D and 2D views)*

These resonators normally should have the reference characteristics listed in Table 1.

Table 1: Reference parameters of the two acousto-electronic resonators

Parameter name and its measurement unit	Short designation	Reference value for Resonator #1	Reference value for Resonator #2
Transformation range, g	D_g	± 25	± 50
Sensitivity threshold, g	E_g	0.3	0.6
Min. non-linearity of transfer characteristics, %	E	5	5
Conversion frequency range, Hz	F	50	75
Supply voltage, V	U_{in}	5	5
Max. amplitude of the output signal, V	U_{out}	1	1

The actual statistical values obtained during the analysis are summarized in Table 2.

Table 2: Statistical values of surfaces of the two acousto-electronic resonators

Parameter	Resonator #1	Resonator #2
Average unevenness	481.13 nm	513.40 nm
Minimum unevenness	19.61 nm	0.00 nm
Maximum unevenness	1000.00 nm	1000.00 nm
Median unevenness	498.04 nm	498.04 nm
Asymmetry	-0.576	0.349
Excess	6.03	1.84
Surface area	$10.18 * 10^{-9}$ m^2	$8.63 * 10^{-9}$ m^2
Projection area	$9.88 * 10^{-9}$ m^2	$8.40 * 10^{-9}$ m^2
Slope θ	0.24 degrees	0.38 degrees
Slope φ	-142.83 degrees	-140.07 degrees

5. Conclusions

Based on the obtained results, the following conclusions can be made:

1. Despite that Resonator #1 is characterized by a smaller absolute height difference than Resonator #2, the standard deviation of the unevenness heights of Resonator #1 is much larger than that of the Resonator #2, which indicates an uneven distribution of these heights on the surface of Resonator #1. Thus, the surface of Resonator #2 demonstrates higher irregularities, but at the same time it is much smoother and does not have any sharp peaks.
2. The values of asymmetry of surfaces of the both resonators are very different. This indicates that Resonator #1 demonstrates deeper cavities (negative asymmetry), i.e. its surface is rather "porous", while Resonator #2 shows sharp peaks without numerous cavities.
3. The values of the excess of surfaces of the both resonators are also different. This means that the surface profile of Resonator #1 features *elongated and narrow* peaks ("barbs") and cavities (Excess > 3), while Resonator #2 has *wider and low-sloped* peaks and cavities (Excess < 3).
4. Based on the above three conclusions, the quality of the surface of Resonator #2 is significantly higher than that of Resonator #1, and can be characterized as symmetric and smooth thanks to the absence of sharp peaks ("barbs") and sharp cavities ("pores"). The observed deviations may lead to deviations in the operating frequency of Resonator #1 compared to the reference values.

References

[1] Acousto-electronic devices. Terms and definitions / Acoustic wave devices. Terms and definitions [Text]: *International Standard GOST 28170-89 - 1989. - Introduction. 1991-01-01. Moscow: Publishing house of standards*, 2007.

[2] Y.V. Wisilter. Processing and analysis of digital images with examples on LabVIEW and IMAQ Vision [Text]: *Moscow: DMK Press, 2007* - 464 p.

[3] V.V. Spiridonov. Analysis and implementation of the micro-level defects detection method [Text]: *Materials of the 67th Scientific and Practical Conference SPBGETU LETI - SPBGETU LETI*, 2012 - 189 p.

[4] System for automated visual inspection for the engineering instrumentation industry [Text]: *Certificate of state registration of the computer program No.2014610514* / V. V. Spiridonov.

[5] V.V. Spiridonov. Key segmentation methods of grayscale images in modern machine vision systems [Text]: *Materials of the III All-Russian Scientific and Technological Conference "Basic Principles of Ballistic Design"* – Publishing house of BSTU "VOENMEH", 2012, Vol.2 - 428 p.

AUTOMATION OF THE QUALIMETRIC METHOD OF SELECTING LAYOUT SOLUTION OF THE PUMPING EQUIPMENT FOR NPPS

postgraduate student, chair I2, G.S. Vinogradova.
Baltic State Technical University "Voenmeh" D.F.Ustinov, Saint-Petersburg, Russian Federation

E-mail: vinogradovag@mail.ru

Abstract. *Discusses qualitative methods of evaluation the layout of pumping equipment implemented in the software. There are various methods of processing expert assessments, analysis has shown that the evaluation of pumping equipment design results for nuclear facilities the best in terms of accuracy, the complexity and time-consuming method is the weighted average expert assessments. On the basis of this method, the technique of choosing the optimal layout decision of several options in the design of new equipment. Implementation of the developed algorithm in a dedicated software allows to automate and optimize the process of selecting the layout in the technical design stage of pumping equipment.*

Key words: AUTOMATION, QUALITY, LAYOUT SOLUTION, SYSTEM OF SUPPORT OF DECISION-MAKING

1. Introduction

The share of electricity generated by nuclear power plants (NPPs) grows annually, contracts are signed for the construction of nuclear power units both in Russia and abroad. The State Atomic Energy Corporation ROSATOM has developed road maps, the strategic goals of which are the construction of 16 power units in Russia until 2020 and 38 power units in other countries until 2030. High competition in the world market in design and construction of NPP units defines strict requirements for the quality of the product. In order to increase the competitiveness of Russian products, in this case the project of NPP unit, the developers are trying to reduce the commissioning time of each new NPP unit, but with the shortening of the NPP unit commissioning time, the quality, reliability and safety of Russian NPP projects should be at the required level.

Modern technologies allow to design of new generation nuclear power plants with WWER-1000 and WWER-1200 reactors. One of the most important elements of the NPP reactor facility is the pumping equipment of the primary circuit - the main circulation pump (MCP). This equipment has the same high requirements for safety and reliability, as well as for the reactor plant. The MCP is a complex technical system. Proceeding from the definition of the technical system [1] it follows that in order to perform the given functions, it must have a certain structure and relative arrangement of units, that is, the technical system must have the appropriate layout solution.

2. Description of the qualimetric method of selecting layout solution

Layout solution of pumping equipment is a set of design works to justify the relative location of nodes, systems and shape of pump. It is during the definition of the layout solution the entire structure of the future pump is created. When choosing a layout solution, it is determined not only the appropriate location of its devices and assemblies, but also determines the optimal sizes and shapes of the surfaces of parts, the choice of materials that meet the technical and economic requirements specified in the technical specification (TS). The volume of the pump depends on its weight, the space occupied by it in the engine room, and transport costs. The general design trend is the desire to reduce the dimensions of the structure with the optimal layout.

When designing the equipment an important issue is the problem of ensuring the quality indicators specified in the technical specification (TS), taking into account resource limitations. The choice of characteristics of the future design is a task that can be classified not only as relating to reliability engineering and engineering technology [2], but also to decision theory [3, 4].

At the initial stage of the design of pumping equipment, especially in the design of new structures, where there is no sufficient statistical data to evaluation the quality of layout decision and approving it for further development decision, the decision-maker evaluates the layout solution under conditions of non-stochastic uncertainty. To solve this problem, the author proposes to apply the developed qualimetric methed [5, 6], implemented in special software. The software is developed in Visual Studio 2015 in C ++ [7].

The essence of the methodology is the application of the method of expert assessments and taking into account risks by the Savage criterion. The software belongs to the class of decision support systems (DSS) [8, 9, 10], and implements the algorithm of work, shown in Fig 1.

3. Description of software operation

The window application of the program allows the user to enter the initial value of the parameters provided by the technical specification and normative documents, Fig. 2.

The First stage based on the data entered, as well as the results of calculations that depend on these data, the parameters of the technical system being designed, the program selects the layouts appropriating to the requirements set by the user from the relational database used in the program. Further, with any result of this sample, the program allows to determine the optimal layout for the technical system being designed, Fig. 3.

If in the course of the selection the program finds several, appropriating to the requirements, layouts, then according to the developed algorithm of the qualimetric method, the user is invited to enter the data of the experts' questionnaires and their estimates for the layouts selected by the program at the first stage.

If only one layout solution satisfy the requirements of the technical specification, then the program offers it for approval, as an optimal one, without expert analysis.

If there are no layouts in the database that satisfy the requirements of the technical specification, the means of the program provides for the compilation of new layout solutions from the replenishable device databases for the designed technical system

The second stage, expert analysis is implemented in the program as follows. The user defines a set of quality indicators, by selecting the number of these indicators from one to twelve.

The user selects the set of quality indicators from the most relevant indicators for a designing technical system or by entering their own.

Also, the user can save the selected sets of quality indicators in the program database.

For each set of quality indicators, there is a database of experts with rank rankings included in this set of quality indicators, which the user can complement with new experts and their rankings of quality indicators. From among these experts an expert commission is drawn up, which may include from three to ten experts. When adding each expert to the commission, the

concordance coefficient is calculated. On the basis of significance of the concordance coefficient, at the level of significance selected by the user, the consistency of the opinions of experts selected to the commission is determined.

When the program determines the inconsistency of the opinions of experts, the program will not allow expert analysis until the commission is re-elected, Fig. 4.

.

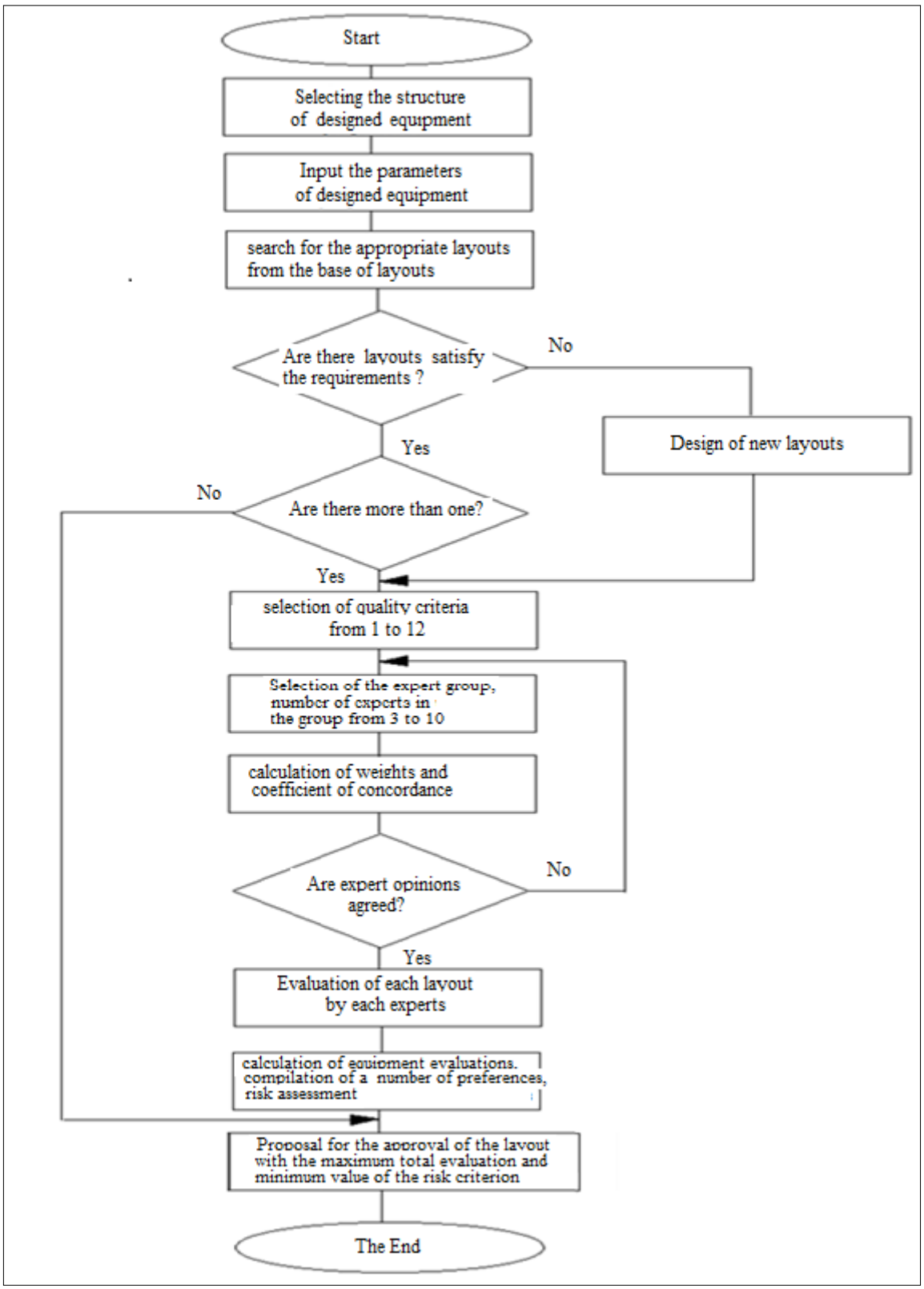

Fig.1*. Algorithm of software operation*

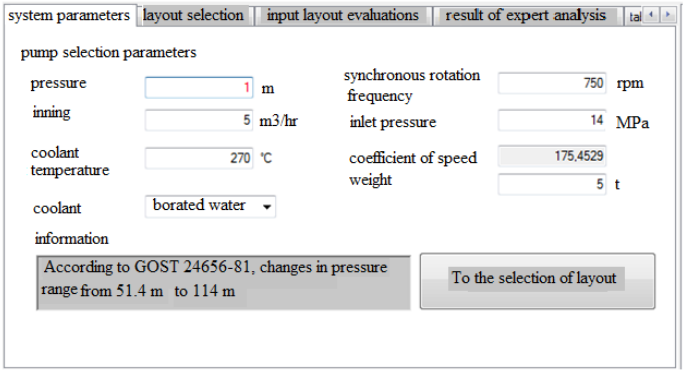

Fig.2. *The input window for the parameters of the technical specification.*

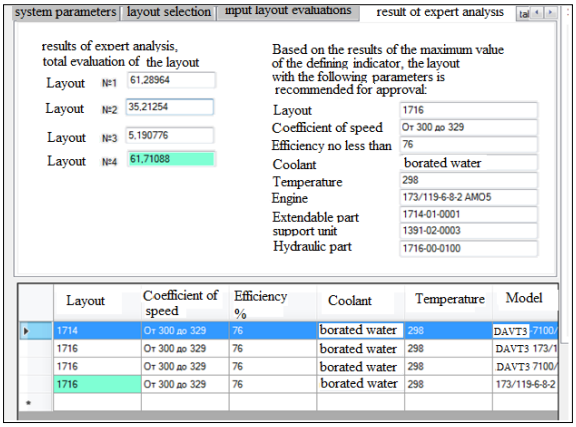

Fig.3.*Result of selecting the optimal layout solution*

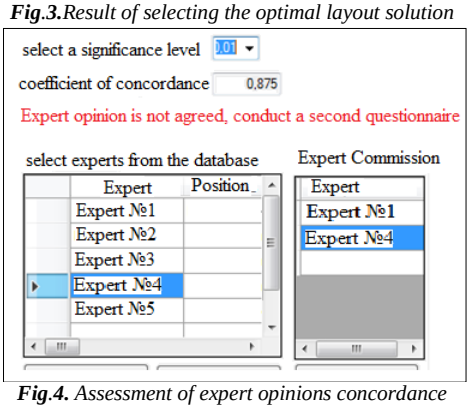

Fig.4. *Assessment of expert opinions concordance*

4. Conclusions

The implementation of the developed qualimetric method in specialized software allows to automate and optimize the selection process of the layout solution at the stage of technical design of pumping equipment for nuclear power plants. The use of special software ensures verification of the project, reduces the risk of approving a suboptimal layout, reduces design costs, allows to ensure the required quality of pumping equipment, which in turn increases the competitiveness of the Russian project of NPP unit.

References

[1] Kirillov N. P. Class characteristics and the definition of "technical systems" // Aerospace instrumentation, No. 8, 2009.

[2] Aristov A. I., Volkov P. N., Dubicki, L. G. etc. Maintainability of the machines. - Moscow: "machine building",1975, 368p.

[3] Fedoseev V. V., Garmash A. N., etc. Economic-mathematical methods and applied models: the textbook / under the editorship of V. Fedoseev, V. Moscow: YUNITI , 1999. 391c.

[4] Castles S. A. Tolstopiatenko AV, Cheremnykh Yu. N. Mathematical methods in Economics: textbook/ Moscow: Business and Service, 2009. 384 p.

[5] Vinogradova G.S., Markov A.V. Evaluating and selecting a layout decision in the design of pump equipment for nuclear facilities taking into account the competence of the experts' – Moscow, "Quality and Life" issue 2, 2016

[6] Vinogradova G.S., Markov A.V. An algorithm of design prototype selection at the stage of engineering development of nuclear facility pumping equipment – Irkutsk, “Proceedings of Irkutsk state technical university” issue 9,2016

[7] Kernighan B., Ritchie D., The C programming language \ translation from English., 3rd ed, St. Petersburg "Nevsky Dialect", 2001, 352p.

[8] Kondakov A. I., CAD technical processes: textbook for higher educational institutions – Moscow, Akademia, 2007, 272p.

[9] Larichev O.I., Petrovskiy A.B., Support system of decision-making. Current state and prospects of their development.//Results of science and technology. Technical Cybernetics. VINITI, 1987

[10] Barnes A.D., Shcherbina O.A. Systems analysis and modern information technologies // Proceedings of the Crimean Academy of sciences.- Simferopol: SONAT,2006

PRODUCTION OF BORON CARBIDE BASED SANDBLASTING NOZZLE by USING LOW PRESSURE POWDER INJECTION MOLDING METHOD and MODELING of PRODUCTION PARAMETERS via ARTIFICIAL NEURAL NETWORK

S. Hartomacıoğlu. PhD.[1], H.O.Gülsoy. PhD.[2], A. Onat. PhD.[1],
Faculty of Mechanical Engineering – Marmara University, Turkey [1]
Faculty of Metallurgy and Materials Engineering– Marmara University, Turkey [2]
selimh@marmara.edu.tr

Abstract: *In this study boron carbide based sandblasting nozzles were produced by Low Pressure Powder Injection Molding (LPPIM) method, and wear behaviors of the nozzles were examined. The addition powder, addition ratio and sintering temperature were used as input parameters while density, micro hardness and wear rate were used as output parameters in the experimental design. This study consists of 3 steps: 1) production of standard samples and characterization, 2) modeling of proses parameters using Artificial Neural Network (ANN) method, 3) selection of nozzle material and production of nozzle, and testing. As a results of this study, ANN method can be used for modeling of process parameters of powder injection molding since the average value of the prediction error is below 7%, and boron carbide based products can be produced by using LPPIM method.*

Keywords: LOWER PRESSURE POWDER INJECTION MOLDING, ARTIFICIAL NEURAL NETWORK, BORON CARBIDE

1. Introduction

Powder injection molding is a novel process, which combines plastic injection molding and conventional powder metallurgy (PM) technologies. This technique combines the advantages of the plastic injection molding with the material versatility of the traditional powder metallurgy, producing highly complex part of small size, tight tolerance, and low production cost. The process overcomes the shape limitation of traditional powder compaction, the cost of machining, the productivity limits of isostatic pressing and slip casting, and the defect and tolerance limitations of conventional casting. The PIM process is composed of four sequential steps; mixing of the powder and organic binder, injection molding, debinding (binder removal), and sintering [1].

Sandblasting (abrasive blasting, as a surface treatment method) is often applied in the field of Mechanical Engineering, Ship Building Engineering, Chemical Industry, etc. Sandblasting is widely used for surface strengthening, surface modification, surface clearing, and rust removal, surface smoothing or surface roughening, corrosion removal. The blasting could be considered as a technique of abrasive machining; this method is based on the effects generated at the contact of the abrasive particles transported by means of the compressed air jet with the workpiece surface. Sandblasting nozzle is the most critical component and worn by repeated impact of the abrasive particle. The sandblasting operation is shown in Figure 1.

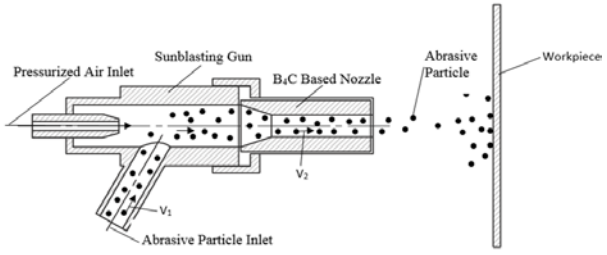

Fig. 1 The working principle of sandblasting operation

The literature review carried out in detail on the subject indicated that, B_4C nozzles are produced by post-hot pressing (HP) and hot isostatic pressing (HIP) techniques [1-5]. These techniques are not economical and not suitable for mass production. The production of B_4C nozzles will become fast and economic by the PIM method. As a result, in the production of B_4C based blast nozzle, aim is to enhance wear resistance and reduce the cost. For enhance of wear resistance and reducing the cost of production B_4C nozzle, the additive materials (SiC, C, TiC, Cu, CrB_2, etc.) were used [2-19].

In this study, B_4C + SiC / Y_2O_3 / TiB_2 composites based sandblast nozzles produced by LPPIM method were investigated and the wear properties of the nozzle materials were examined using sandblasting cabinet testing. Metallographic techniques were employed to sintered sandblast nozzles samples to investigate the sintering behaviors. Density, hardness and erosive wear properties of the sintered products were evaluated in sintered condition. Abrasive air-jet nozzles made of boron carbide with high relative density and excellent wear resistance provides a longer life compared with those made of other materials.

2. Materials and Method

In this study, commercially available B_4C powder (ABSCI Co, UK for base material and SiC, TiB_2 and Y_2O_3 powders (H.C. Stack, Germany) were used for additive powders. Some properties of base powder and additive powders were listed in Table 1.

Table 1: *Some properties of the main powder and additive powders*

Powders	Manufacturer	Average Grain Size	Powder Shape
B_4C	Absco Co.	D_{50}: 14 µm , %98,19 B_4C	Angular
SiC	Almatis Co.	D_{50}: 1.1 µm	Angular
TiB_2	H.C. Stack	D_{50}: 2 µm	Angular
Y_2O_3	H.C. Stack	D_{50}: 1.7 µm	Angular

For molding the mixing powders, binder materials and their rates must be defined. The primary required the binder is to allow flow of the particles into the cavity. Paraffin Wax (PW), Carnauba Wax (CW), Polypropylene (PP) and Stearic Acid (SA) were selected for binder system. Some properties of binder system components are shown in Table 2.

Table 2: *Some properties of the binder system components*

Binder Type	**Density (g/cm^3)**	**Melting Point ^{o}C**
Paraffin Wax (MERC)	0.9	90
Carnauba Wax (MERC)	0.97	112
Polypropylene (MERC)	0.89	161
Stearic Acid (MERC)	0.85	73

Firstly, amount of additive was adjusted and each mixture was blended in a Turbula mixer for 1 hour. The feedstock was prepared using binder system and blended powders by hand at 175 ºC. The

powder loading in this mixture was 55 vol%. The feedstocks were injected at 10 bar custom made vertical injection molding machine to produce samples and sandblasting nozzles. In the injection molding step, barrel temperature was 140 ºC, the mold temperature 35-40 ºC, and cycle time was 15 second. The sandblast nozzle design is shown in Figure 2. After injection molding step, solvent and thermal debinding process was performed. In the solvent debinding step, the products were placed into heptane at 70 ºC for 8 hours. Thermal debinding process was performed under Argon atmosphere using debinding furnace at different temperature range. After debinding process and pre-sintering process, the sintering process was performed under Argon atmosphere at 2000 ºC, 2100 ºC and 2200 ºC using special designed furnace with graphite resistant. The special designed high temperature furnace is shown in Figure 3. Finally, the cooling stage with based on the furnace's thermal inertias was used.

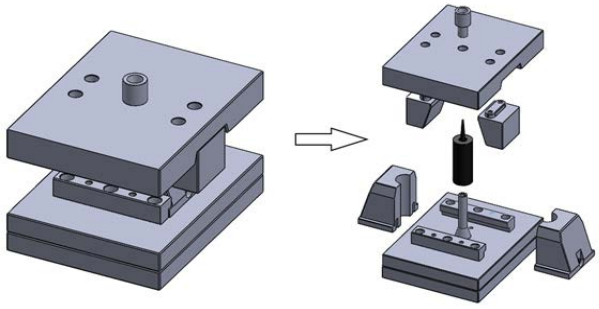

Fig. 2 ***Design of the nozzle mold***

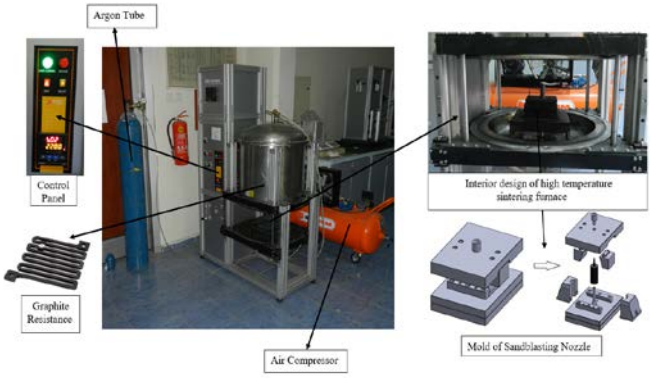

Fig. 3 ***A special designed high temperature sintering furnace***

The densities of the sintered samples and nozzles were measured by using of the Archimedes water-immersion method. The micro-hardness tests were conducted using a Shimadzu-HMV tester under 98.1N load. The wear tests were done using Sandblasting device. In the sand blasting test apparatus, air pressure was set 6 bar, and flow rate is set up 225 m^3/min. SiC powders were used as erodent abrasive and size of particle was between 180-212 µm (80 mesh). The sandblast cabinet test was done for 10 hours, and the weight loss was measured for every hour.

After experimental studies, the results of experimental studies were modelled by using artificial neural networks (ANN) method. In the ANN step, the multilayer perceptron (MLP) was used as ANN topology. MLP consists three layer: 1) input layer, 2) hidden layer, 3) output layer. Each layer consists of neurons named process element. In the Figure 4, view of biological neuron and artificial neuron are shown.

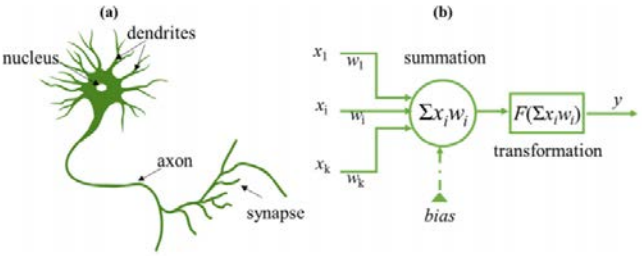

Fig. 4 ***Biological and artificial neuron [20]***

The MLP structure were build and trained in Neurosolutions software environment. In the training step, the mean-square-error (MSE) was used as evaluation performance of structure. In the prediction step, the mean absolute error (MAE) was used as evaluation performance of ANN structure. The neural network structure of the experimental study is shown in Figure 5.

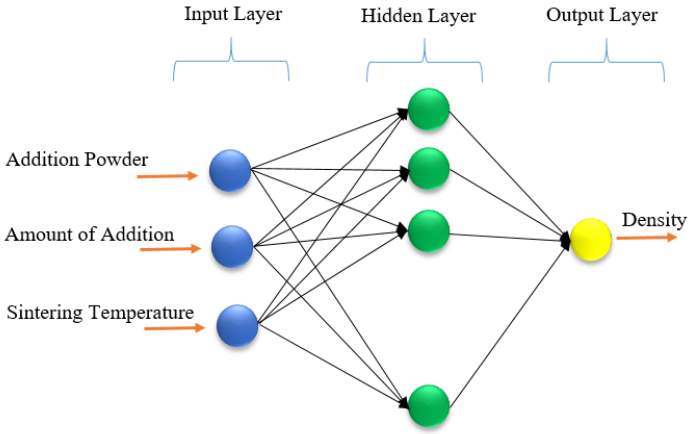

Fig. 5 ***the ANN structure of experimental study***

In the experimental design, full factorial distribution was used. The input variables of the study were amount of additive powder, additive powder, and sintering temperature. The input variables and their levels are listed in Table 2. The output variables of the study were density, micro-hardness and wear rate. Firstly, the full factorial experimental study was performed and then the ANN model was developed using the experimental results. Firstly, the results of experimental study were normalized from 0 to 1, and normalized data set was randomly divided into two groups of 75% training and 25% testing. After training and testing steps of ANN, the optimal ANN structure was determined. Using the ANN structure, the new results were predicts using new input variable levels. In the prediction stage, the values of amount of additional powder and sintering temperature were 0-32wt.% and 2000-2300 ºC, respectively.

Table 3: *Input and output variables of experimental study*

Factors	**1**	**2**	**3**	**4**	**5**	**6**
A: Amount of Additional Powder	0	2	4	8	12	16
B: Additive Powder	TiB_2	Y_2O_3	SiC			
C: Sintering Temperature	2000	2100	2200			

3. Results and Discussion

In the ANN development steps, the effect of change in neuron number of hidden layer on error was shown in Figure 6. Each neural network structure was trained 3 times in 60000 epochs. In the training step, total of 50 different network types were used, and the optimal network structure giving the minimal error was selected from these. The test operation was conducted by using the optimal

ANN structure, and the value of mean absolute error (MAE) was calculated and illustrated in Figure 7. In the optimal ANN structure, the SigmoidAxon was used as transfer function, Momentum (step size:0.1, momentum rate: 0.7) was used as learning rule, neuron number of 22 was defined as hidden layer at 60 000 epoch. As a results of ANN training and testing stage, it is calculated that the average error value is 7.75%.

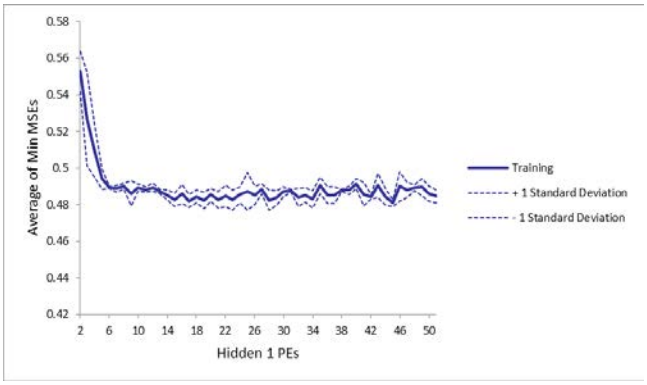

Fig. 6 ***Changing of MSE according to the number of neurons of hidden layer***

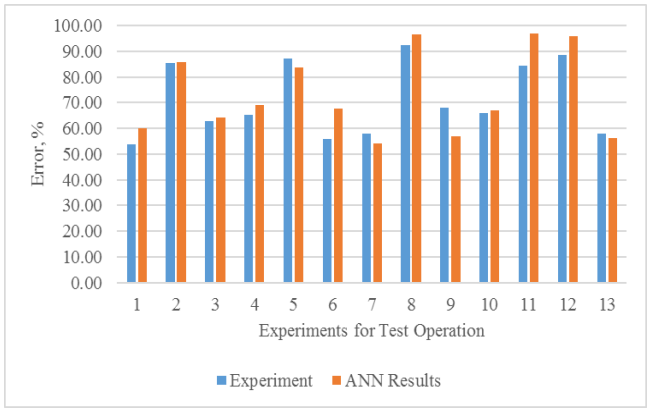

Fig. 7 ***The value of MEA in the test steps of ANN***

New results were predicted using amount of additive powder (0-32wt.%) and sintering temperature (2000 - 2300 ºC) by using the optimal ANN structure. Predicted results were shown in Figure 8, 9 and 10 according to additive powder.

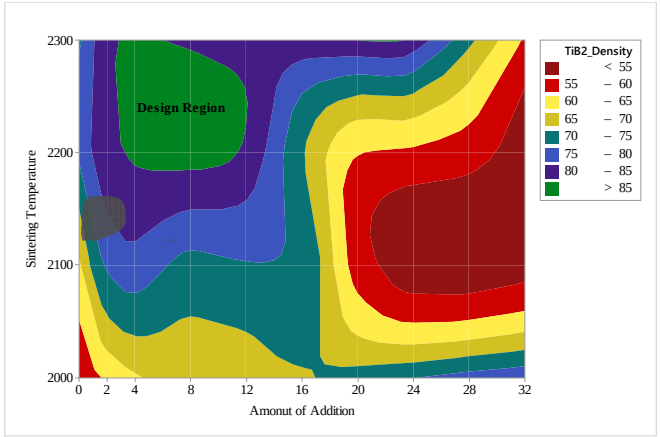

Fig. 8 ***Predicted results of composites with TiB_2 additive***

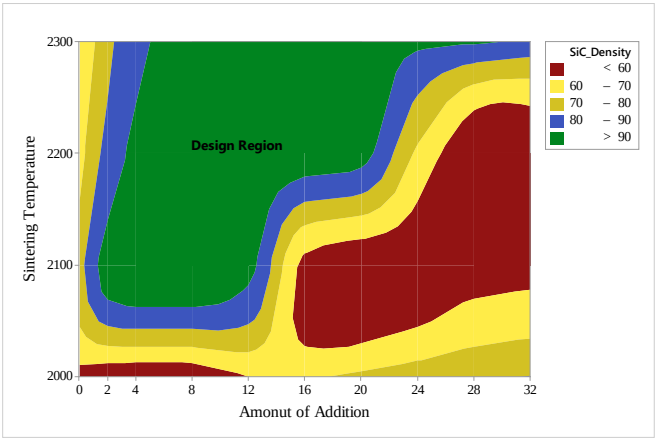

Fig. 9 ***Predicted results of composites with SiC additive***

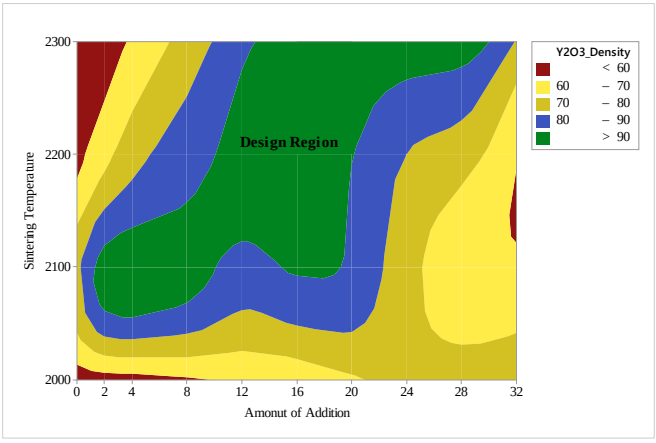

Fig. 10 ***Predicted results of composites with Y_2O_3 additive***

In the Figure 8, 9 and 10, the dark green area was defined as design region for production of B_4C based sandblasting nozzles. The sandblasting nozzle materials were selected from these design areas with high density listed in Table 4 and the nozzles were produced using the optimal experimental conditions.

Table 4: *Selected sandblasting nozzles materials and the properties*

#	Composite	Sint. Temp.	%, Density	Hardness
A0	B_4C	2200 °C	58.00%	8.58
A1	8% TiB_2 + 92% B_4C	2200 °C	90.27%	15.23
A2	8% SiC + 92% B_4C	2200 °C	96.11%	17.21
A3	12% SiC + 88% B_4C	2200 °C	96.64%	18.48
A4	16% SiC + 84% B_4C	2200 °C	96.03%	19.42
A5	4% Y_2O_3 + 96% B_4C	2100 °C	96.93%	14.43
A6	16% Y_2O_3 + 84% B_4C	2200 °C	94.05%	16.95

After the nozzle production, the wear tests were conducted using sandblasting cabinet test equipment (pressure: 6 bar, erodent abrasive: SiC, Time: 10h). The test results were shown in Figure 11.

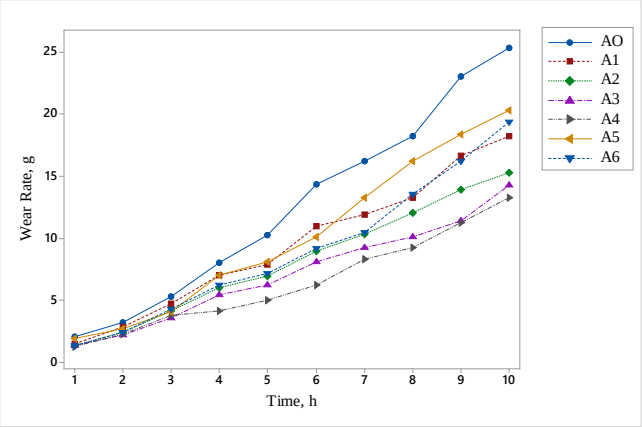

Fig. 11 ***Wear rate of nozzle***

From the Figure 11, the highest amount of wear occurred in the A0 nozzle, the least amount of wear occurred in the A4 nozzle.

4. Conclusion

The main objective of this study is to produce B_4C based sandblasting nozzles via low pressure powder injection molding method (LPPIM). As a results of this study, boron carbide products can be produced by LPPIM method, and ANN method can be used for modeling of production parameter of B4C products. The addition of TiB_2, SiC, and Y_2O_3 on B_4C composite provides significant improvement physical and mechanical properties compare with monolithic B_4C sintered same conditions.

5. Acknowledgements

This work is support by TUBITAK (The Scientific and Technical Research Council of Turkey-Grand: 213M196) and Scientific Research Project Program of Marmara University (Grand: **FEN-K-110117-0019**).

6. References

[1] Momber, As., (2008) Blast Cleaning Technology. Springer, Hamburg, Germany

[2] D. Jianxin, 'Wear behaviors of ceramic nozzles with laminated structure at their entry', Wear, Vol: 266, p30-36, 2009

[3] Sogabe, T., Matsuda, T., Kuroda, K., Hirohata, Y., Hino, T. (1995) Preparation of B_4C-Mixed Graphite by Pressureless Sintering and Its Air Oxidation Behaviour. Pergamon, Carbon Vol. 33(12), 1783-1788

[4] Sigl, L.S. (1998) Processing and Mechanical Properties of Boron Carbide Sintered with TiC. Journal of the European Ceramic Society, 18, 1521-1529

[5] Levin, L., Frage, N., Dariel, M.P. (2000) A Novel Approach for the Preparation of B_4C-Based Cermets. International Journal of Refractory Metals & Hard Materials, 18, 131-135

[6] Skorokhod, VI.V. Krstic, V.D. (2000) Processing, Microstructure, and Mechanical Properties of B4C-TiB_2 Particulate Sintered Composites 1. Pressureless Sintering and Microstructure Evolution. Powder Metallurgy and Metal Ceramics, 39, 7-8

[7] Lee, H., Speyer, R.F. (2002) Hardness and Fracture Toughness of Pressureless-Sintered Boron Carbide (B_4C). Journal of American Ceramic Society, 85(5), 1291-1293

[8] Lee, H., Speyer, R.F. (2003) Pressureless Sintering of Boron Carbide. Journal of American Ceramic Society, 86(9), 1468-1471

[9] Frage, N., Levin, L., Dariel, M.P. (2004) the Effect of the Sintering Atmosphere on the Densification of B_4C Ceramics. Journal of Solid State Chemistry, 177, 410-414

[10] Zorzi, J.E., Perottoni, C.A., Jornada, J.A.H. (2005) Hardness and Wear Resistance of B_4C Ceramics Prepared with Several Additives. Materials Letters, 59, 2932-2935

[11] Roy, T.K., Subramanian, C., Suri, A.K. (2006) Pressureless Sintering of Boron Carbide. Ceramic International, 32, 227-233

[12] Baharvandi, H.R., Hadian, A.M., Abdizadeh, A. (2006) Investigation on Addition of ZrO_3-3 mol% Y_2O_3 Powder on Sintering Behaviour and Mechanical Properties of B_4C. Journal of Materials Science, 41(16), 5269-5272

[13] Baharvandi, H.R., Hadian, A.M., Alizadeh, A. (2006) Processing and Mechanical Properties of Boron Carbide-Titanium Diboride Ceramics. Applied Composite Materials, 13, 191-198

[14] Goldstain, A., Yeshurun, Y., Goldenberg, A. (2007) B_4C/Metal Boride Composites Derived from B_4C/Metal Oxide Mixtures. Journal of the European Ceramic Society, 27, 695-700

[15] Mashhadi, M., Taheri-Nassaj, E., Sglavo, V.M., Sarpoolaky, H., Ehsani, N. (2009) Effect of Al Addition on Pressureless Sintering of B_4C. Ceramic International, 35, 831-837

[16] Mashhadi, M., Taheri-Nassaj, E., Sglavo, V.M. (2010) Pressureless Sintering of Boron Carbide. Ceramic International, 36, 151-159

[17] Wei, R., Zhang, Y., Gong, H., Jiang, Y., Zhang, Y. (2013) The Effect of Rare-Earth Oxide Additives on the Densification of Pressureless Sintering B_4C ceramics. Ceramic International, 29, 6449-6452

[18] Li, X., Jiang, D., Zhang, J., Lin, Q., Chen, Z., Huang, Z. (2014) Pressureless Sintering of Boron Carbide with Cr_3C_2 as Sintering Additive. Journal of European Ceramic Society, 34, 1073-1081

[18] Jianxin, Yihua, F., Zeliang, D., Peiwei, S. (2003) Wear behavior of ceramic nozzles in sand blasting treatments. Journal of the European Ceramic Society, 23, 323-329

[19] Jianxin, D. (2005) Erosion wear of boron carbide ceramic nozzles by abrasive air jets. Materials Science and Engineering: A, 408, 227-233

[20] Yan, Z., Kim, Y., Hara, S., Shikazona, N., 'Prediction of Ya0.6Sr0.4Co0.2Fe0.8O3 cathode microstructures during sintering: Kinetic Monte Carlo (KMC) simulations calibrated by artificial neural networks, Journal of Power Sources, 346, (2017) 103-112

MODELING OF THE EFFECTS OF THREEFOLD TYPE RHVT AND SIX CASCADE TYPE RHVT ON THE PERFORMANCE OF COUNTER FLOW RHVTS BY FUZZY LOGIC APPROACH

Assist. Prof. Dr. Yusuf Yılmaz[*], Res. Asst. Sadık Ata[**], Assist. Prof. Dr. Kevser Dincer[*],Assist. Prof. Dr. Gürol Önal[*], Assist. Prof. Dr. Ali Serhat Ersoyoğlu[*]

[*]*Selcuk University, Department of Mechanical Engineering, Konya*
***KTO Karatay University, Department of Mechanical Engineering, Konya*

Abstract*—In this study, performances of Ranque-Hilsch Vortex Tubes (RHVTs) were modeled under three different situations based on inlet pressure and the ratio of mass flow rate of the cold stream to the mass flow rate of the inlet stream (ξ) by fuzzy logic approach. 1st situation is the conventional RHVT. 2nd situation is the threefold cascade type RHVT. Here three RHVTs were used. 3rd situation deals with the six cascade type RHVT. In this case, six RHVTs were used. Input-output parameters were described by Rule Based Mamdani Type Fuzzy (RBMTF) with if-then rules. The performance parameters are the difference between the hot and cold stream temperatures (ΔT), the cold flow fraction (ξ), inlet pressure conditions. The comparison between experimental data and RBMTF is done by using statistical methods like absolute fraction of variance (R^2). The actual values and RBMTF results indicated that RBMTF can be successfully used for the analysis of performance RHVTs.*

***KEYWORDS*— RANQUE-HILSCH, VORTEX TUBE, FUZZY LOGIC MODELLING**

1. Introduction

Vortex tube is a simple device, which can separate an incoming compressed gas stream of uniform temperature into two streams one warmer than the inlet stream and the other Colder than the inlet stream. Such separation of the gaseous ßuid stream into two different streams of higher and lower temperatures is referred to as temperature (energy) separation effect. Ranque invented the vortex tube and Þrst reported about energy separation. Later Hilsch published systematic experimental results of this effect. Since then, this phenomenon has attracted many scientists. Various theories have been proposed to explain this phenomenon from experimental, analytical and numerical studies. Hilsch suggested that the expansion of air from high pressure near the wall to low pressure near the axis generates a velocity gradient in radial direction, which results in transfer of kinetic energy by the viscous force from the inner ßuid layers to the outer ßuid layers [1].

Working principle of the counterflow RHVT can be defined as follows. Compressible fluid, which is tangentially introduced into the vortex tube from nozzles, starts to make a circular movement inside the vortex tube at high speeds, because of the cylindrical structure of the tube, depending on its inlet pressure and speed. Pressure difference occurs between tube wall and tube center because of the friction of the fluid circling at high speeds. Speed of the fluid near the tube wall is lower than the speed at the tube center, because of the effects of wall friction. As a result, fluid in the center region transfers energy to the fluid at the tube wall, depending on the geometric structure of the vortex tube. The cooled fluid leaves the vortex tube from the cold output side, by moving towards an opposite direction, compared to the main flow direction, after a stagnation point. Heated fluid leaves the tube in the main flow direction from the other endRHVTs are used, among others, for cooling, heating, drying and snow production [2]. In the existing literature, there have been many investigations [3-5] about RHVT performance.One of the methods to determine the effects of the parameters on RHVT performance is fuzzy logic method.

In this study, Ranque-Hilsch vortex tube (RHVT) was investigated experimentally for the best performance of 3 differentsituations. 1st situation is the conventional RHVT. 2nd situation is the threefold cascade type RHVT. Here three RHVTs were used. 3rd situation deals with the six cascade type RHVT. In this case, six RHVTs were used. When the entire test results under Pi = 360 kPa and Pi = 400 kPa pressure conditions are compared, it is found that the best performance occurs at the 3rd situation. Also in this study, Rule-based Mamdani-type fuzzy modeling used to evaluate performance of RHVT. Performance parameters are difference between the hot and cold stream temperatures (ΔT), the cold flow fraction (ξ), inlet pressure conditions (P_i). Study includes fuzzification of input variables, representation of fuzzy set with 9 linguistic variables, formation of rule basis and a comparison between output values obtained by experiments and by calculation based on generated rules and RBMTF technique.

2. Materials and Methods

The fuzzy subsets theory was introduced by Zadeh in 1965 as an extension of the set theory by the replacement of the characteristic function of a set by a membership function, whose values range from 0 to 1. RBMTF is basically a multi-valued logic that allows intermediate values to be defined between conventional evaluations like yes/no, true/false, black/white, large/small, etc [6].

Fuzzification is the initial process of a fuzzy model where fuzzy subsets of universal set of fuzzy variable are constructed. If there is no data, intuition and experience can be used in fuzzification process. By simply looking at the distribution of data of each variable the obvious clusters can be seen and fuzzified. If there is available data initially the dataset is portioned into two sets; calibration (training) and verification (testing). Calibration set is used for fuzzification and constructing the fuzzy rules. Verification set is used for testing the accuracy of the model set [7].

The general structure of the fuzzy logic modeling consists of four components: fuzzification, fuzzy rule base, fuzzy output engine, and defuzzification. Fuzzification converts each piece of input data to degrees of membership by lookup in one or more several membership functions The central fuzzy rule base is the concept of the fuzzy If-Then rule, which is a mathematical interpretation of the linguistic If-Then rule. Membership functions are used to retranslate the fuzzy output into a crisp value. This technique is known as defuzzification and can be performed using several methods. There are many defuzzification methods such as centre of gravity or centroid, bisector area, mean of maxima, leftmost maximum, rightmost maximum, etc [8]. In this study, we applied the most widely used centre of gravity technique.

The aim of this study is tomodel RHVT performance for 3 different situations by using fuzzy logic. 1st situation is the conventional RHVT: the RHVT in the literature, in this situation classical RHVT is taken into account. One RHVT was used in the classic RHVT. Inlet pressure selected was 360 kPa and 400 kPa. 2nd situation is the threefold cascade type RHVT. Here three RHVT were used. The inlet pressure values of the first RHVT were 360 kPa and 400 kPa.3rd situation deals with the six cascade type of RHVT. In this case, six RHVTs were used. All of the RHVTs, the inlet pressures (P_i) were 360 kPa and 400 kPa [9]. With the aid of experimental data, RHVT performances at different situations in terms of difference between the hot and cold stream temperatures (ΔT), the cold flow fraction (ξ) were modeled with Rule-Based Mamdani-Type Fuzzy (RBMTF) modeling technique. RBMTF was designed using MATLAB fuzzy logic toolbox. In the developed RBMTF system, output parameter difference between the hot and

cold stream temperatures (ΔT)was determined using inlet parameters the cold flow fraction (ξ) and inlet pressure conditions. Hereafter the rules, which are used to detect the behavior of the fuzzy logic controller and the relationship between system's input and output, are determined. As a result of these rules, every value obtained from the experimental study is also determined by fuzzy logic too.

3. Results and Discussion

Vortex tubes are classified into two groups according to their flow characteristics: counter flow RHVT and parallel flow RHVT. The efficiency of parallel flow RHVT is low. For this reason, in this study the counter flow RHVT was used. The cold flow fraction (ξ) is an important parameter in the counter flow RHVT. The cold flow fraction is defined as the ratio of the mass flow rate of the cold stream to the mass flow rate of the inlet stream [9]. The aim of this study with the aid of experimental data, RHVT performances in terms of difference between the hot and cold stream temperatures (ΔT), the cold flow fraction (ξ) were modeled with fuzzy logic modeling technique. In the developed RBMTF system, output parameters ΔT was determined using inlet parameters ξ and P_i.

Figs. 1-2 show comparison of experimental data with RBMTF for the variation of cold flow fraction with inlet pressure of difference between the hot and cold stream temperatures (P_i = 360-400 kPa; ξ = 0.1-0.9). From a comparison of the experimental results with the results of the fuzzy logic study, one can see that the results are quite compatible (Figs. 1-2).

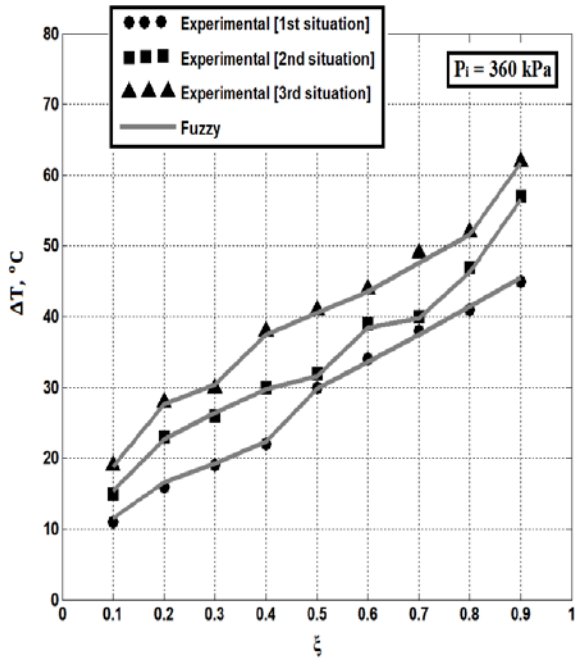

Fig. 1 *Comparison of experimental data with RBMTF in terms of performances of classic RHVT (1st situation), threefold cascade type RHVT (2nd situation) and six cascade type RHVT (3rd situation) under 360 kPa inlet pressure operating conditions.*

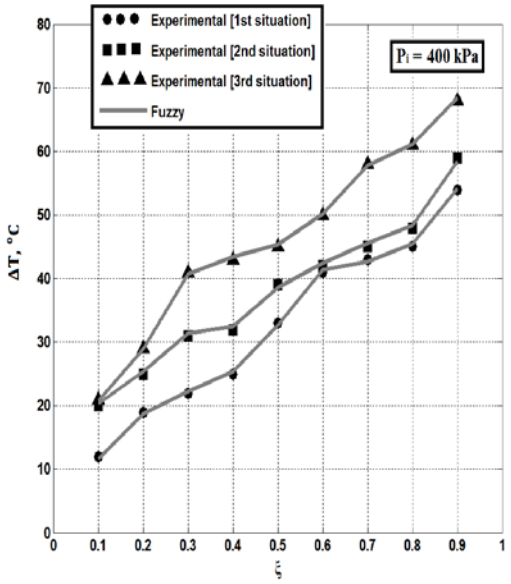

Fig. 2 *Comparison of experimental data with RBMTF in terms of performances of classic RHVT (1st situation), threefold cascade type RHVT (2nd situation) and six cascade type RHVT (3rd situation) under 400 kPa inlet pressure operating conditions.*

These figures present that;

- The performances of the classic RHVT, the performances of threefold type RHVT and the performances of six cascade type RHVT increase with the ratio ξ.
- When the entire test results under P_i = 360 kPa and P_i = 400 kPa pressure conditions are compared, it is found that the best performance occurs at the 3rd situation. Moreover, the performance of the 3rd situation at P_i = 400 kPa pressure is higher than that at P_i = 360 kPa (Figs 1-2).

In this study, fuzzy logic is also used for prediction. The 48 cold flow fraction values between 0.15-0.85 which are not obtained from experimental work for difference between the hot and cold stream temperatures are predicted by fuzzy logic method. Figs. 3-4 show the comparison of experimental data with fuzzy prediction for the variation of cold flow fraction with inlet pressure conditions of difference between the hot and cold stream temperatures.

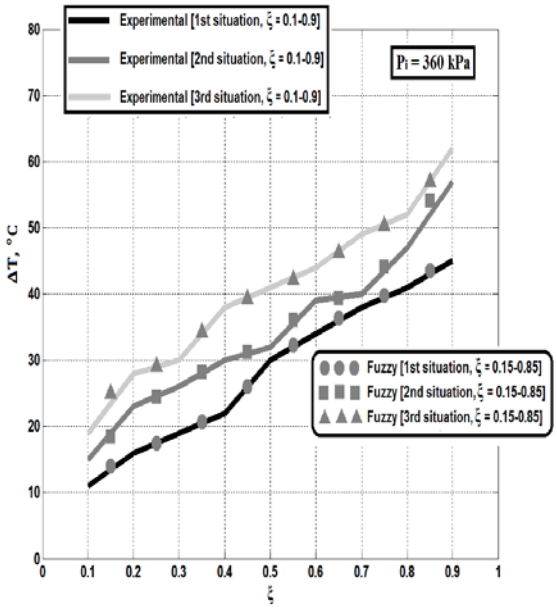

Fig. 3*Comparison of experimental data with fuzzy predict for different cold flow fraction (ξ) values under 360 kPa inlet pressure operating conditions.*

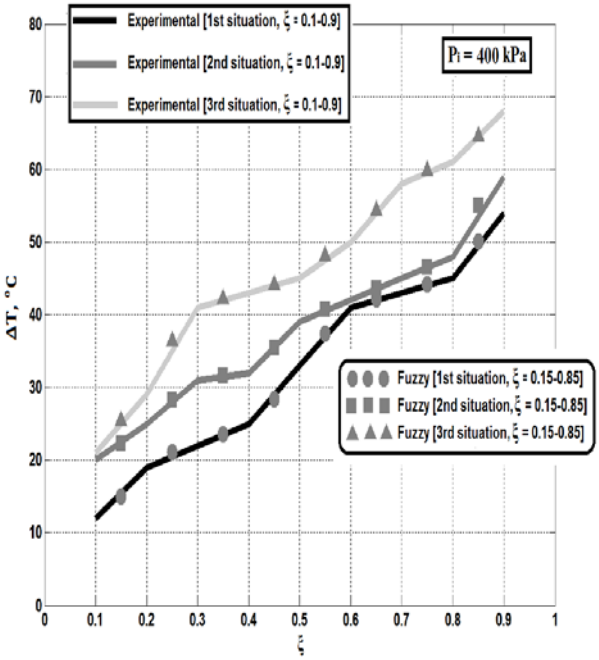

Fig. 4*Comparison of experimental data with fuzzy predict for different cold flow fraction (ξ) values under 400 kPa inlet pressure operating conditions.*

These figures present that;

- The difference between the hot and cold stream temperature value predicted by RBMTF for 2nd situation and the cold flow fraction = 0.75 is higher than the temperature value from the results of the experimental work for 2nd situation and the cold flow fraction = 0.7, but less than the temperature value from the results of the experimental work for the 2nd situation and the cold flow fraction = 0.8

- The difference between the hot and cold stream temperature value predicted by RBMTF for 3rd situation and the cold flow fraction = 0.25 is higher than the temperature value from the results of the experimental work for 3rd situation and the cold flow fraction = 0.2, but less than the temperature value from the results of the experimental work for the 3rdsituation and the cold flow fraction = 0.3 (Figs. 3-4).

The comparison between experimental data and fuzzy logic is done using statistical methods such as the coefficient of multiple determination (R^2) are defined as follows, where n is the number of data patterns, $y_{p,m}$ indicates the predicted, $t_{m,m}$ is the actual value of one data point m, and $\bar{t}_{m,m}$is the mean value of all actual data points [6]. When Table 1 is observed, it is found that actual values and the values from fuzzy technique are very close to each other.

$$R^2 = 1 - \frac{\sum_{m=1}^{n}(t_{m,m} - y_{p,m})^2}{\sum_{m=1}^{n}(t_{m,m} - \bar{t}_{m,m})^2} \quad (1)$$

Table 1. *Comparison of the actual and RBMTF results for difference between the hot and cold stream temperatures (ΔT)*

INLET PRESSURE	**ΔT, °C**
	R^2
360 kPa	98.05%
400 kPa	97.89%

4. Conclusions

In this study, RHVT performances at different situations in terms of difference between the hot and cold stream temperatures (ΔT) were experimentally investigated. With this study, it has been found that when the performance of the cascade type RHVT is compared with that of the classic RHVT, the performance of the cascade type RHVT becomes higher than that of its classic counterpart. The best performance obtained at six cascade type RHVT (3rd situation). With the aid of experimental data, RHVT performances at different situations in terms of difference between the hot and cold stream temperatures (ΔT), the cold flow fraction (ξ) were modeled fuzzy logic technique. In the developed RBMTF system, output parameters ΔT was determined using inlet parameters ξ and P_i. Every value obtained from the experimental study is also determined by fuzzy logic too. The comparison between fuzzy logic and experimental data is done using statistical methods. R^2 is calculated under 360 kPa-400 kPa inlet pressure operating conditions 98.05% and 97.89% respectively. The actual values and RBMTF results indicated that RBMTF can be successfully used for the specification RHVT performances at different situations.

5. References

[1] Yılmaz, Y., Berber, A., Dincer, K., Özen, D.N., Baskaya, Ş. “”Rule-Based Mamdani Type Fuzzy Modeling of Exergy Analysis Performances of Counter Flow Ranque-Hilsch Vortex Tubes With Different Geometric Constructions For Aluminum”, Academic Journal of Science, 1(3), 75-88, 2012.

[2] Dincer, K., Tasdemir, S., Baskaya, S., Uysal, B.Z. “Modeling of the effects of length to diameter ratio and nozzle number on the performance of counterflow Ranque–Hilsch vortex tubes using artificial neural networks”, Applied Thermal Engineering, 28, 2380-2390, 2008.

[3] Niknam, P.H., Mortaheb, H.R., Mokhtarani, B. “Numerical Investigation of a Ranque–Hilsch Vortex Tube Using a Three-Equation Turbulence Model”, Chemical Engineering Communications, DOI: 10.1080/00986445.2016.1155989, 2016.

[4] Dincer, K., Baskaya, S., Uysal, B.Z., Ucgul, I., “Experimental investigation of the performance of a Ranque–Hilsch vortex tube with regard to a plug located at the hot outlet”, International Journal of Refrigeration, 32, 87-94, 2009.

[5] Behera, U., Paul, P.J., Dinesh, K., Jacob, S. “Numerical investigations on flow behaviour and energy separation in Ranque–Hilsch vortex tube”, International Journal of Heat and Mass Transfer, 51, 6077-6089, 2008.

[6] Onal, G., Dincer, K., Yayla, S., Yılmaz, Y., Ersoyoğlu, A.S. “Pt/C Coating for Proton Exchange Membrane Fuel Cell (PEMFC) and Rule-Based Mamdani-Type Fuzzy Modeling of PEMFC Performance,” International Journal of Mining, Metallurgy & Mechanical Engineering, 3(3), 122-128, 2015.

[7] Selvi, Ö. “Traffic Accident Prediction Based On Fuzzy Logic Approach For Safer Urban Environment, Case Study: İzmir Metropolitan Area”, PhD Thesis, İzmir Instıtute of Technology, İzmir, 2009.

[8] Bozokalfa, G. “Artificial Neural Networks and Fuzzy Logic Models For Cooling Load Prediction”, MSc Thesis, İzmir Instıtute of Technology, İzmir, 2005.

[9] Dincer, K., “Experimental investigation of the effects of threefold type Ranque-Hilsch vortex tube and six cascade type Ranque-Hilsch vortex tube on the performance of counter flow Ranque-Hilsch vortex tubes”, International Journal of Refrigeration, 34, 1366-1371, 2011.

COMPUTER AIDED ANALYSIS OF KINEMATICS AND KINETOSTATICS OF SIX-BAR LINKAGE MECHANISM THROUGH THE CONTOUR METHOD

Prof.Asoc.Dr. Likaj R. [1], Prof.Asoc.Azem Kycyku*, MSc. Qelaj M[1], Prof.Ass.Dr. Bajrami X[1].

Faculty of Mechanical Engineering – University of Prishtina "Hasan Prishtina", Kosovo [1]

azem.kycyku@uni-pr.edu (*corresponding author),

Abstract: *In this paper is presented a six-bar linkage mechanism of the pump for oil extrusion. In this mechanism are introduced higher kinematic pairs. Dimensions and other incoming links are adopted as necessary. For the six-bar linkage mechanisms is carried out the kinematic analysis and for all linkages are shown the displacement, velocity and acceleration. The analysis is performed by Math Cad software, while kinetostatic analysis is carried out using Contour Method, comparing results of two different software's Math CAD and Working Model. The simulation parameters are computed for all points of the contours of mechanism*

Keywords: *MECHANISM, CONTOUR, DISPLACEMENT, VELOSITY, ACCELARATION*

1. Introduction

This paper has been completed using Math Cad and Working Model software's. In this paper is presented a six-bar linkage ABCD and a simple crank mechanism DEF as shown in the figure below. Firstly, in this mechanism is determined DF_y and θ_5. Derivative DF_y represents the speed of the slider F. From the given picture $0.1 \le \theta_2 \le 360^o$ should be determined. The masses are adopted, since the moments of inertia need to calculate. The kinematic part of the paper will be completed by finding the velocities and accelerations of each point ***A, B, C, D, E, F*** for the centres from C_1 to C_6. In this way are determined the angular accelerations and velocities of the linkages 2, 3, 4 and 5. Whereas for the kinetostatic part will be determined the reaction forces of the points: $X_A, Y_A, X_B, Y_B, X_C, Y_C, X_D, Y_D, X_E, Y_E, X_F, Y_F, N=X_{F6}$ and M_{tr} which are acting on the leading link 2. In the picture are shown 5 bodies: ***AB, BC*** right triangle, rod ***EF***, slider bar ***F***.

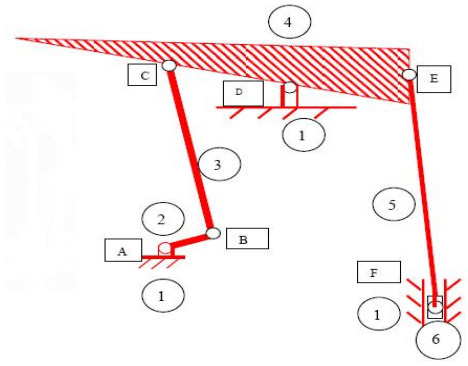

Fig. 1 *Six bar-linkage mechanism ABCDEF*

Given data:

$$\left|\begin{array}{l}\theta_2 = 0.5\deg ...360[\deg], \omega_2 = 2, r_2 = 1.7 \\ r_3 = 6.9, r_{4a} := 4.2, r_D = \sqrt{4.2^2 + 6.4^2}, \alpha = 56.725\end{array}\right| .....(1)$$

Determination of angle α of r_D with x_1: Linkage I

$$\left|\vec{r_2} + \vec{r_3} + \vec{r_{4a}} = \vec{r_D}\right| .....(2)$$

From then designed outline at x and y we have the following initial conditions:

$$\left|\begin{array}{l}r_2 \cdot \cos(\theta_2) + r_3 \cdot \cos(\theta_3) + r_{4a} \cdot \cos(\theta_4) = r_D \cdot \cos(\alpha) \\ r_2 \cdot \sin(\theta_2) + r_3 \cdot \sin(\theta_3) + r_{4a} \cdot \sin(\theta_4) = r_D \cdot \sin(\alpha)\end{array}\right| ..... (3)$$

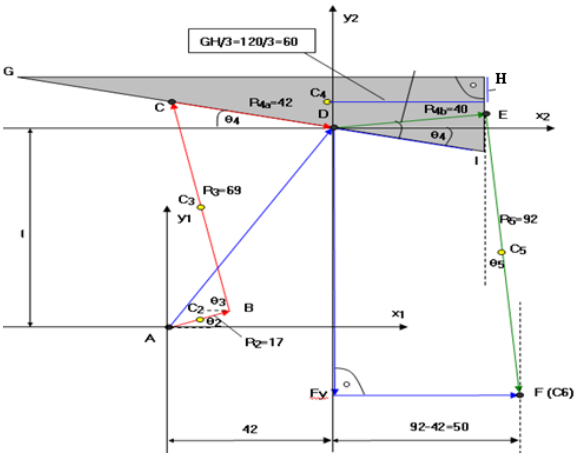

Fig. 2 *Four-bar linkage ABCD and crank mechanism DEF*

As shown in the Figure 2, there are 14 unknown sizes, 12 equations for the first four bodies, $dy(x, y)$ for the slider 14 equations.

2. The analysis of the positions, velocities and accelerations of six-bar linkage mechanism

In the figure 3 is presented the velocity plan for the points A, B, C and D. Also are presented angular velocities and angular accelerations for the points A, B and C. After finding the velocities and accelerations of these points, the displacements, velocities and accelerations of these points with angles θ_3 and θ_4 in function of θ_2 are shown graphically. Outline is shown in this form:

$$\left|\theta_3 = 180[\deg], \theta_4 = 90[\deg]\right| ..... (3)$$

The vector equation without the **contour I** is:

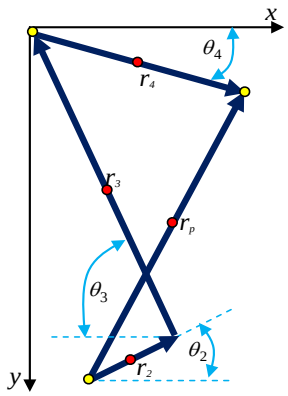

Fig. 3 *Velocity plan for the points A, B and C*

$$\left| \begin{pmatrix} r_2\cos(\theta_2) \\ r_2\sin(\theta_2) \\ 0 \end{pmatrix} + \begin{pmatrix} r_3\cos(\theta_3) \\ r_3\sin(\theta_3) \\ 0 \end{pmatrix} + \begin{pmatrix} r_4\cos(\theta_4) \\ r_4\sin(\theta_4) \\ 0 \end{pmatrix} = \begin{pmatrix} r_p\cos(\alpha) \\ r_p\sin(\alpha) \\ 0 \end{pmatrix} \right| \quad (4)$$

$$\left| \begin{aligned} &Zgj(\theta_2) = Find(\theta_3, \theta_4), \\ &\theta_3 = 104.18[\text{deg}], \theta_4 = -3.96[\text{deg}], \beta = 59.48[\text{deg}] \\ &\omega_3 = \frac{d}{d\theta_2}\theta_3(\theta_2)\cdot\omega_2, \omega_4 = \frac{d}{d\theta_2}\theta_4(\theta_2)\cdot\omega_2 \\ &\varepsilon_3 = \frac{d^2}{d{\theta_2}^2}\theta_3(\theta_2)\cdot{\omega_2}^2, \varepsilon_4 = \frac{d^2}{d{\theta_2}^2}\theta_4(\theta_2)\cdot{\omega_2}^2 \end{aligned} \right| \quad \text{.....(5)}$$

After calculation of the values by Math Cad software, in the following are shown graphically the values of positions, velocities and accelerations respectively for $\theta_3, \omega_3, \varepsilon_3$ and $\theta_4, \omega_4, \varepsilon_4$:

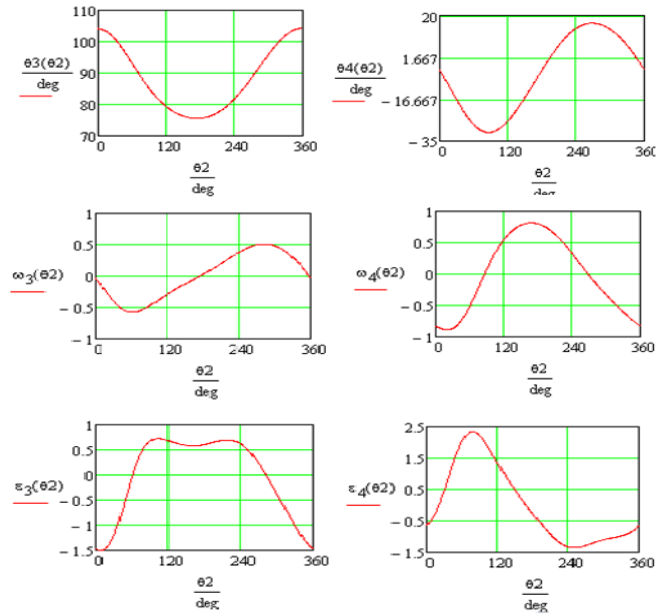

Fig. 4 *Diagrams for positions, velocities and accelerations*

2.1 Position of the point B

The position of the point B is calculated in direction of x and y :

$$\left| \begin{aligned} &x_B = r_2\cdot\cos(\theta_2), y_B = r_2\cdot\sin(\theta_2) \\ &v_{Bx} = -r_2\cdot\sin(\theta_2)\cdot\omega_2, v_{By} = r_2\cdot\cos(\theta_2)\cdot\omega_2 \\ &v_B = \sqrt{v_{Bx}(\theta_2)^2 + v_{By}(\theta_2)^2} = 10.03[cm/s] \end{aligned} \right| \quad \text{..... (6)}$$

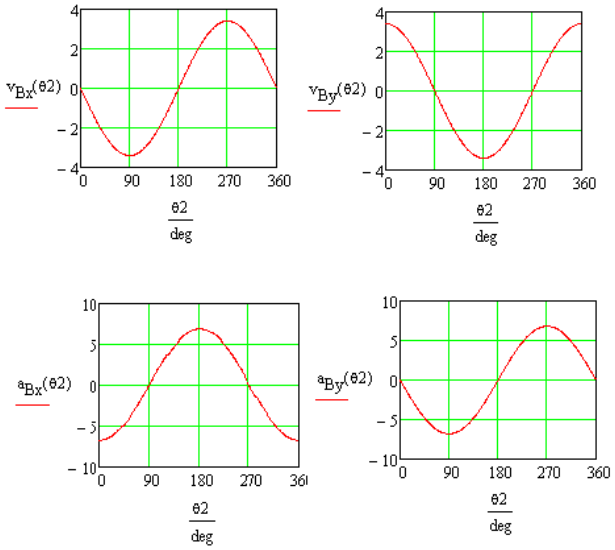

Fig. 5 *The position diagrams for the position equations of the point B in direction of x and y*

$$\left| \begin{aligned} &a_{Bx} = -r_2\cdot\cos(\theta_2)\cdot\omega_2^2, v_{By} = -r_2\cdot\sin(\theta_2)\cdot\omega_2^2 \\ &a_B = \sqrt{a_{Bx}(\theta_2)^2 + a_{By}(\theta_2)^2}\,[cm/s^2] \end{aligned} \right| \quad \text{..... (7)}$$

Angular velocity and acceleration for the point B:

$$\left| \begin{aligned} &\omega_4 = \frac{d}{d\theta_2}\theta_4\cdot\omega_2, \varepsilon_4 = \frac{d^2}{d{\theta_2}^2}\theta_4\cdot{\omega_2}^2 \\ &\omega_4 = -0.87[\text{deg}], \varepsilon_4 = 0.45[\text{deg}^2] \end{aligned} \right| \quad \text{..... (8)}$$

3. The equations for position (displacement), velocity and acceleration of the point C

In the following is shown the displacement of point C, along with velocities and accelerations which are presented graphically by the diagrams via Math Cad program:

$$\left| \begin{aligned} &x_c = 0\, y_c = r_2\cdot\cos(\theta_2) + r_3\cdot\sin(\theta_3(\theta_2)) \\ &v_{cx} = 0, v_{cy} = r_2\cdot\sin(\theta_2) + r_3\cdot\cos(\theta_3(\theta_2)) \\ &v_c = v_{cy}(\theta_2); {}_c\, a_{cx}(\theta_2) = 0 \\ &a_{cy} = (-r_2\cdot\sin(\theta_2) - r_3\cdot\cos(\theta_3(\theta_2)))\cdot\omega^2 \\ &a_c = a_{cy}(\theta_2) \end{aligned} \right| \quad \text{..... (9)}$$

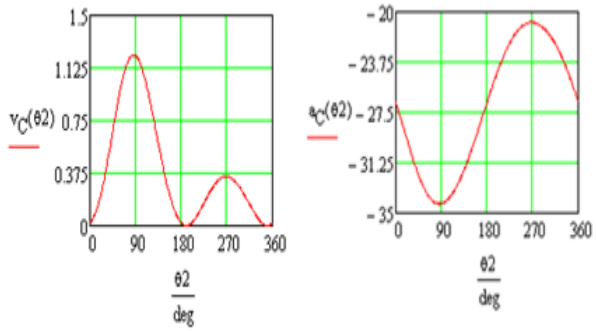

Fig. 6 *Velocities and acceleration of point C*

3.1 The expression for the middle point of the bars AB, BC and CD

In the following are extracted the displacement for the middle position of the bars AB, BC and CD and other displacement which belong to these bars. Are also presented the velocities and accelerations of these bars and their diagrams separately:

$$\left|\begin{array}{l} AB: \\ x_{c2}=\frac{r_2}{2}\cos(\theta_2);\ y_{c2}=\frac{r_2}{2}\sin(\theta_2) \\ a_{xc2}=\frac{-r_2}{2}\sin(\theta_2)\cdot\omega^2;\ a_{yc2}=\frac{r_2}{2}\cos(\theta_2)\cdot\omega^2 \end{array}\right| \quad \text{.....(9)}$$

$$\left|\begin{array}{l} BC: \\ x_{c3}=\frac{r_3}{2}\cos(\theta_3(\theta_2));\ y_{c3}=\frac{r_3}{2}\sin(\theta_3(\theta_2)) \\ a_{xc2}=\frac{-r_3}{2}\sin(\theta_3(\theta_2))\cdot\omega_2^2;\ a_{yc3}=\frac{r_3}{2}\cos(\theta_3(\theta_2))\cdot\omega_2^2 \end{array}\right| \quad \text{...(10)}$$

$$\left|\begin{array}{l} CD: \\ x_{c4}=\frac{r_4}{2}\cos(\theta_4(\theta_2));\ y_{c4}=\frac{r_3}{2}\sin(\theta_4(\theta_2)) \\ a_{xc4}=\frac{-r_4}{2}\sin(\theta_4(\theta_2))\cdot\omega_2^2;\ a_{yc4}=\frac{r_4}{2}\cos(\theta_4(\theta_2))\cdot\omega_2^2 \end{array}\right| \quad \text{..(11)}$$

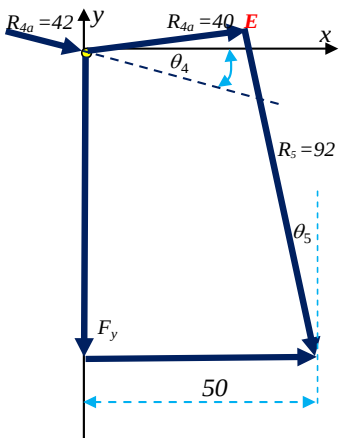

Fig. 7 *Crank mechanism*

3.2 The equations for position (displacement), velocity and acceleration of the point E

For the point ***E*** of Crank Mechanism determined the displacement, and in the following pictures are shown velocities and accelerations in the direction ***x*** and ***y***:

$$\left|\begin{array}{l} x_E=r_{4b}\cos(\theta_4(\theta_2));\ y_E=r_{4b}\sin(\theta_4(\theta_2)) \\ x_E=-r_{4b}\sin(\theta_4(\theta_2))\cdot\omega_2;\ y_E=r_{4b}\cos(\theta_4(\theta_2))\cdot\omega 2 \\ a_{Ex}=-r_{4b}\cos(\theta_4(\theta_2))\cdot\omega_2^2;\ a_{Ey}=-r_{4b}\sin(\theta_4(\theta_2))\cdot\omega_2^2 \end{array}\right| \quad \text{.. (12)}$$

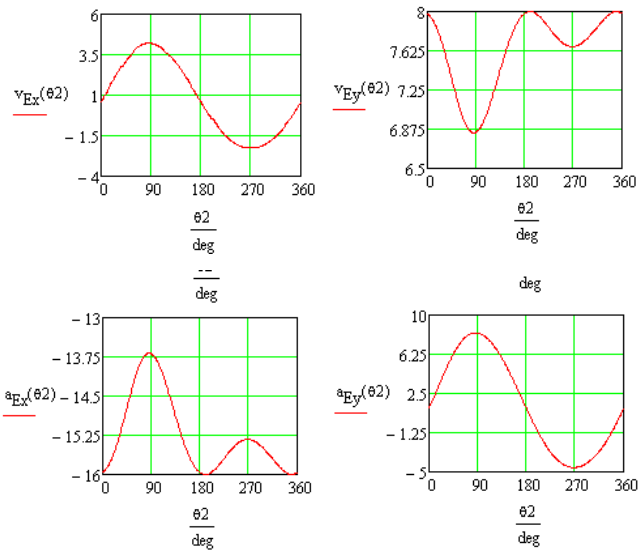

Fig. 8. *Diagrams of the velocities and acceleration for the E*

4. Kinetostatic analysis of the six-bar linkage mechanism

For the kinetostatic part will be presented the kinetostatic analysis of six-bar linkage mechanism by Math Cad software. Moments of inertia, masses of bodies are used in the following:

$$\left|\begin{array}{l} m_2=10;m_3=15;m_4=20;m_5=15;m_6=5;g=9.807 \\ J_{C2}=\frac{1}{2}\cdot m_2\cdot {r_2}^2;J_{C3}=\frac{1}{2}\cdot m_3\cdot {r_3}^2 \\ J_{C4}=\frac{1}{12}\cdot m_4(2.4^2-1.2^2);J_{C5}=\frac{1}{12}\cdot m_5\cdot {r_5}^2 \end{array}\right| \quad \text{. (13)}$$

Linkage I:

The equilibrium conditions for the point A are equal to zero. Six linkages are used for the kinetostatic analysis. For the first linkage are given the following equilibrium conditions $\boldsymbol{X_A, Y_A}$ and $\boldsymbol{X_B, Y_B}$ for the middle points of the linkage AB, point C2 and for the body mass $\boldsymbol{m_2}$.

$$\left|\begin{array}{l} X_A-X_B=m_2\cdot a_{xc2}(\theta_2);Y_A-Y_B=m_2\cdot a_{yc2}(\theta_2) \\ M_{tr}=Y_A\frac{r_2}{2}\cos(\theta_2)-X_A\frac{r_2}{2}\cos(\theta_2)+ \\ \qquad Y_B\frac{r_2}{2}\cos(\theta_2)-X_B\frac{r_2}{2}\sin(\theta_2) \end{array}\right| \quad \text{..... (14)}$$

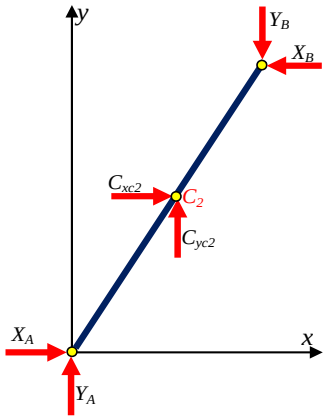

Fig. 9. *Linkage I–Equilibrium conditions for the point AB*

Linkage II

Also, for the linkage II are written the equilibrium conditions BC, which are X_B, Y_B , X_C, Y_C center C_3 body mass **BC** and moment of inertia for the point C_3.

$$\left|\begin{array}{l} X_C - X_B = m_3 \cdot a_{xc3}(\theta_2); Y_C - Y_B = m_3 \cdot a_{yc3}(\theta_2) \\ J_{C3} \cdot \varepsilon(\theta_2) = X_C \cdot \frac{r_3}{2} \cdot \sin(\theta_3(\theta_2)) - Y_C \cdot \frac{r_3}{2} \cdot \cos(\theta_3(\theta_2)) \\ - Y_B \cdot \frac{r_3}{2} \cdot \theta_3(\theta_2)) - X_B \cdot \frac{r_3}{2} \cdot \sin(\theta_3(\theta_2)) \end{array}\right| .(15)$$

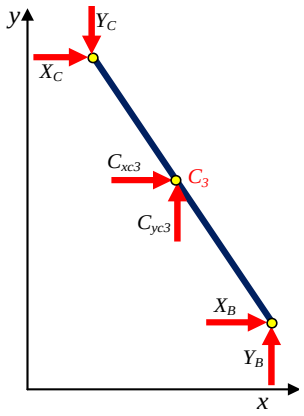

Fig.10. *Linkage II – Equilibrium conditions for the part* BC

Linkage III

$$\left|\begin{array}{l} X_C + X_D - X_E = m_4 \cdot a_{xC4}(\theta_2) \\ Y_C + Y_D - Y_E = m_4 \cdot a_{yC4}(\theta_2) \\ J_{C4} \cdot \varepsilon_4(\theta_2) = -Y \cdot r_{4a} + Y - r_{4b} - EH - \\ \qquad Y \cdot r_z(\theta_2) + X_D \cdot r_m(\theta_2) \end{array}\right| .....(16)$$

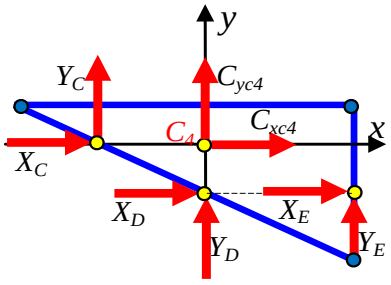

Fig.11. *Linkage III of the points C, D, E and center* C_4

$$\left|\begin{array}{l} X_E - X_F = m_5 \cdot a_{xC5}(\theta_2) \\ Y_C + Y_D - Y_E = m_4 \cdot a_{yC4}(\theta_2) \\ J_{C5} \cdot \varepsilon_5(\theta_2) = (X_E + X_F) \cdot \frac{r_5}{2} \cdot \sin(\theta_5(\theta_2)) - \\ \qquad (Y_E + Y_F) \cdot \frac{r_5}{2} \cdot \sin(\theta_5(\theta_2)) \end{array}\right| ..... (17)$$

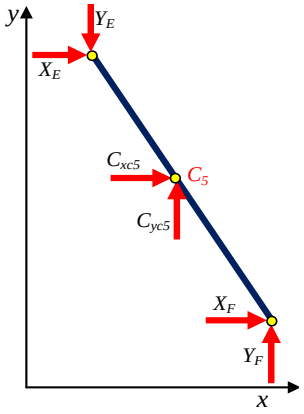

Fig. 12. *Linkage IV of the part EF in direction of x and y*

Linkage V

$$\left|Y = -(m_6 \cdot a_{yF}(\theta_2) + m_6 \cdot g)\right| ..... (18)$$

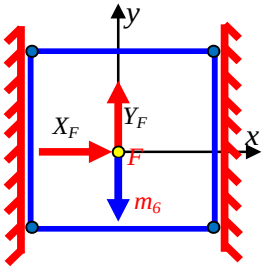

Fi.g.13. *Linkage V of the point F in direction of* x *and* y

All unknown parameters for the linkages in both directions ***x*** and ***y*** are calculated by Math Cad. From point A to the point Find the Transmission moment M_{tr}:

$$\left|\begin{array}{l} Solve(\theta 2) := Find(X_A \cdot Y_A \cdot X_B \cdot Y_B \cdot X_C \cdot \\ \qquad Y_C \cdot X_D \cdot Y_D \cdot X_E \cdot Y_E \cdot X_F \cdot Y_F \cdot M_{tr} \end{array}\right| ..... (18)$$

In the following diagrams are given the values of all unknown parameters for the positions (0; 0.5; 1) by Math Cad software. This it was really a tough work since the working process by Math Cad was very slow especially to follow the procedure which is given by kinetostatic analysis.

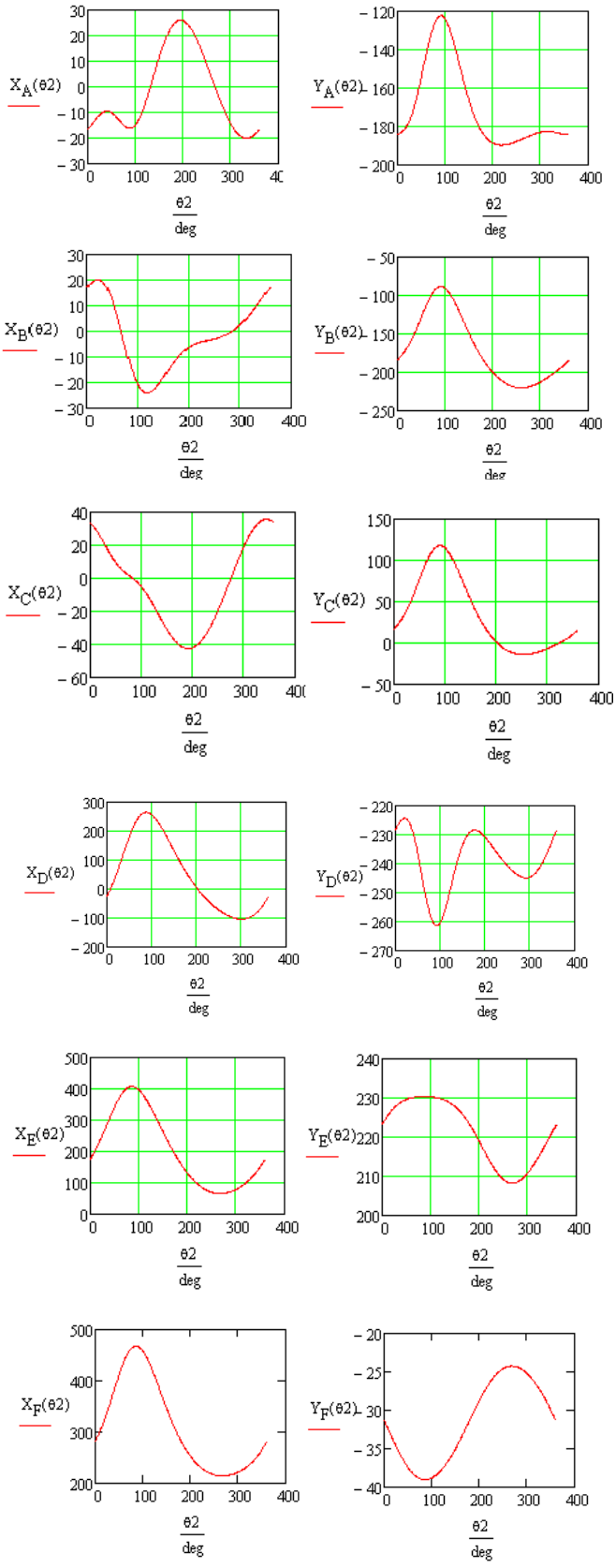

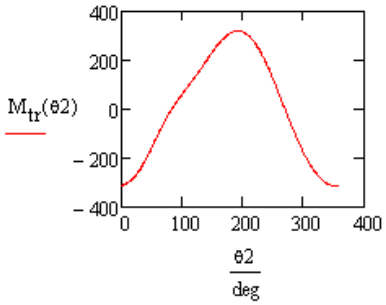

Fig.14*. Diagrams of kinetostatic analysis of the given mechanism for the points* ***A, B, C, D, E, F*** *and transmission moment* ***Mtr***

5. *Simulation for six-bar mechanism by Working Model software*

In the second part of this paper is performed the simulation for all points ***A,B,C,D,E,F*** and ***Mtr*** (time dependent) of the six bar linkage mechanism by Working Model, which is shown in the following.

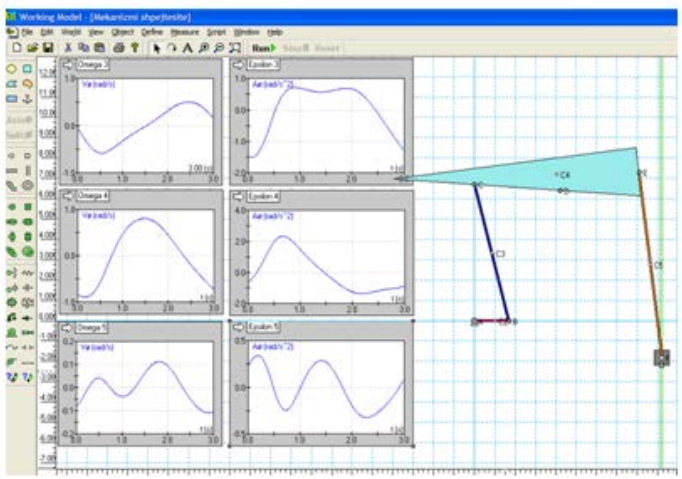

Fig.15*.Diagrams in Working Model for angular velocity and acceleration 3, 4 and 5*

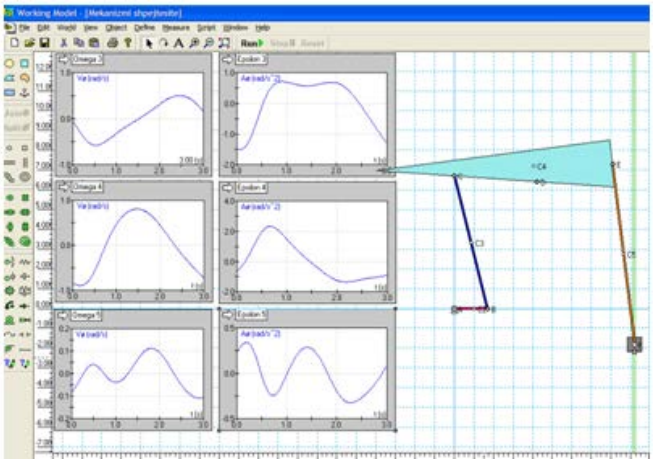

Fig.16:*. Diagrams in Working Model for equilibrium points* ***A, B, C, D, E, F*** *and transmission moment* $\boldsymbol{M_{tr}}$ *in direction* ***x***

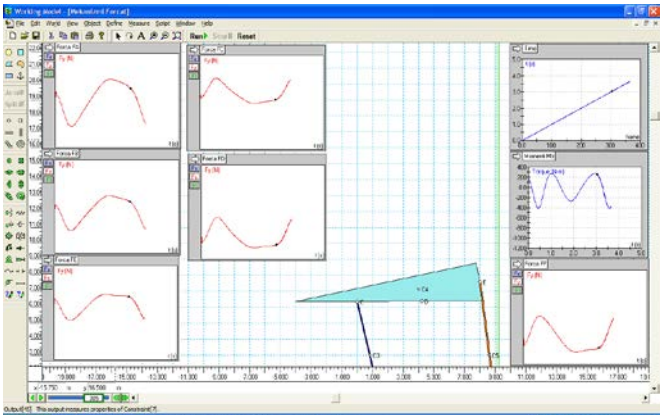

Fig.*17.Diagrams in Working Model for equilibrium points A,B,C,D,E,F and transmission moment (Mtr) in direction* ***y***

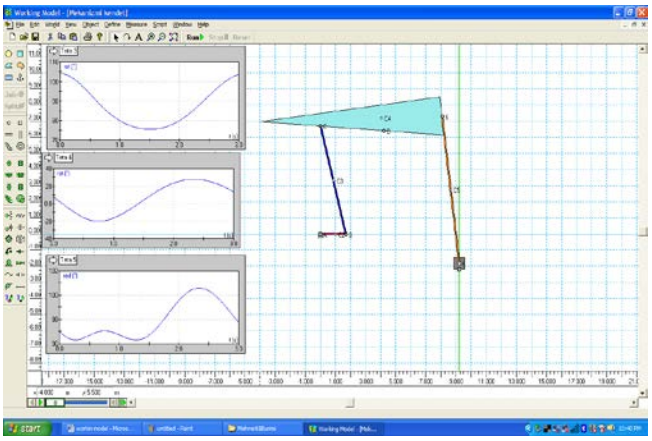

Fig.18. *Diagrams for* θ_3 , θ_4 *and* θ_5 *(time dependent), under command RUN*

6. Conclusions and recommendations

By application of the software's Math Cad or Matlab we have reached to carry out the full analysis of this paper. In this paper are made the calculations of all positions (displacement) for the whole mechanism, and also are determined the plans for velocities and accelerations for each point.

However, in this paper are shown the outline planes of the mechanism same as the diagrams for each linkage through Math Cad and Working Model software, Six-bar linkage mechanism diagrams which are derived by Working Model are almost similar to the diagrams derived by Math Cad, same as the derived results, Through Working Model software, are derived the results of reactions from the equilibrium conditions of six bar linkage mechanism, angular velocities and accelerations for the points 3, 4 and 5, for the angles θ_3 , θ_4 and θ_5 in time domain through the command Run,

As the general conclusion; the results derived by both software, same as for their diagrams, for all points of the six bar linkage mechanism are within the reasonable boundaries. Our expectations are that similar results will be derived by application of Matlab software.

2. References

Shala A: (2008), Disenjimi i Mekanizmave me Kompjuter, Ushtrime detyrash – Fakulteti i Inxhinierisë Mekanike, Prishtinë.

Rehwald, W., Luck, K.,(2007) Research of Coupler Curves of Geometrical Poles of first Order, Journal of Mechanisms and Manipulators, vol. 6, nr. 2, pp. 5-16.

Shala, Ahmet, Ramë Likaj, and Mirlind Bruqi. "Synthesis of Cam mechanism based on given program." IFAC Proceedings Volumes 46.8 (2013): 60-63.

Provatidis, Christopher G. "A novel mechanism to produce figure-eight-shaped closed curves in the three-dimensional space." Proceedings of Third International Conference on Experiments/Process/System Modeling/Simulation & Optimization, Athens. 2009.

Umesh Chavan., at all, (2010). Synthesis of coupler curves with combined planar cam follower mechanisms by genetic algorithm. Proveeding of 2nd International Conference on Computer Engineering and Technology, Chengdy, China.

U.S. Chavan, S.V. Joshi. (2010). Synthesis and analysis of coupler curves with combined planar cam follower mechanisms, International Journal of Engineering, Science and technology, Vol. 2, No. 6, pp. 231-243

VEHICULAR TRAFFIC FLOW MODELLING BY MEANS OF CAR-FOLLOWING APPROACH

Ph.D. student Kurtc V.[1], Ph. D. Anufriev I.[2]
Institute of Applied Mathematics and Mechanics – Peter the Great St. Petersburg State Polytechnic University, St. Petersburg, Russia

E-mail: [1]kurtsvv@gmail.com, [2]Igor.Anufriev@kronshtadt.ru

Abstract: *This paper concerns the problem of vehicular traffic flows simulation. We present a continuous car-following model with explicit reaction-time delay. This model is based on the Intelligent Driver Models and eliminates some drawbacks like unrealistic distance between vehicles in a homogeneous flow and instant reaction of a driver. The model is defined by a couple of delayed differential equations. Introducing reaction time explicitly one can simulate traffic flow instabilities such as kinematic waves with a greater degree of realism. We calculate conditions for that the linear stability occurs on a ring and in the finite platoon of cars. The parameters of the model are calibrated according to NGSIM trajectory data. Another method described in this paper allows to estimate parameters according to technical characteristics of the specific vehicle type. Simulating vehicular traffic for large cities with microscopic approach one needs to solve tremendous systems of differential equations. The speed of changes in the size of the components of such systems usually lies in a wide range, as the dynamics and behaviour of the vehicles can strongly differ. We introduce a multirate numerical scheme with a self-adjusting time stepping strategy. The step size for each component is determined by its own local temporal variation. The stability analysis for the developed scheme is performed and the stability conditions are obtained. The use of multiple time steps allows parallel computing.*

Keywords: VEHICULAR TRAFFIC, MICROSCOPIC MODELS, TRAFFIC FLOW INSTABILITIES, CALIBRATION, MULTIRATE SOLVERS

1. Introduction

Nowadays, the overall traffic demand has been increasing from day to day. The existing road network, as well as traffic management schemes, do not cope with the growing traffic flows. This fact leads to formation of traffic jams and, as a result, environmental pollution and increase of travel times. To tackle this problem, traffic flow modelling is used nowadays. Vehicular traffic simulation is one of the possible tool for studying phenomena of traffic flows oscillations [1-3] and testing schemes for optimal transportation planning.

Traffic flow models can be categorized with the respect to the way how reality is presented [4]. Macroscopic (hydrodynamical) models [5-8] describe traffic flow as liquids or gases in motion in terms of traffic density $\rho(x,t)$, flow $Q(x,t)$ and mean speed $V(x,t)$. Microscopic models include cellular automata [9,10] and car-following models [11-16] and describe "driver-vehicle particles" individually with such dynamical variables as vehicle acceleration, speed and position. Traffic flow models mostly microscopic ones are an integral part of commercial software products (Aimsun, MITSIM, VISSIM) used for investigating of vehicular dynamics, testing control algorithms of traffic management and for upgrading the existing or designing a new road network. Another application of vehicular flows simulation is driving simulators which admit only car-following approach. In spite of diversity of traffic flow models, development of realistic and elaborated models is required.

Driving styles, types of vehicles and traffic regulation rules vary from country to country. Consequently, parameters of the model should be adapted to the specific conditions, that is, calibrated [17,18]. Moreover, one needs to check if the calibration procedure was performed successfully by means of validation [17].

Nowadays**,** microscopic traffic data have become more available and provides information about thousands of vehicle trajectories [19,20]. As a result, the problem of analysing and comparing microscopic traffic flow models with real microscopic data has become more actual. In this paper, we consider the NGSIM I80 data set [19] for calibration. In addition, for realistic simulation of system containing diverse of "driver-vehicle particles" (inter-driver variation) model parameters should be properly calibrated according to technical characteristics of the specific vehicle model [21].

When simulating trajectories by integrating time-continuous car-following models, standard integration schemes such as the simple Euler method, ballistic update, Heun's method and the the fourth-order Runge–Kutta are used [31]. In case of simulation of vehicular traffic on large scales in large cities, the number of vehicles could reach tens of thousands, which, for the microscopic approach, corresponds to the solution of tremendous systems of differential equations. Such systems have such a feature as slow and fast components. This fact suggests the use of multirate approach for numerical integration [32, 33]. The multirate solver for numerical integration is described in this paper. The solver is based on automatic identification of an integration step (microstep) for each component separately. The microstep is determined on the basis of the required accuracy and the estimate of the numerical integration error. Due to the multiplicity conditions several consecutive microsteps for each equation of the system are carried out within one macrostep. This scheme is used to solve large systems which describes the dynamics of the traffic flows.

The paper is organized as follows. In section 2 we specify the car-following model with explicit reaction time delay. Section 3 contains some results on stability analysis of the underlying model. Calibration methodology with respect to trajectory data is described in Section 4. In Section 5 we introduce the approach for quantitative assessment of car-following models by means of comparison of fundamental diagrams. Finally, Sections 6 finishes with discussions and conclusion.

2. Car-following Model

Oscillations of traffic flow are well-known phenomenon in congested car traffic [1-3, 22], which is usually described in terms of linear and nonlinear string instabilities [4, 23]. One of the reason of emergence of traffic flow oscillations is finite driver perception [4, 24]. This fact speaks in favor of considering the driver reaction time explicitly.

The specified car-following model is the modification of the well-know "Intelligent Driver Model" (IDM) [13]. The acceleration function is defined as continuous function of the vehicle's speed v and distance to its leader h [25]

$$\dot{v}(t) = w(v,h)\cdot a\left(1-\left(\frac{v(t)}{V^0}\right)^{\delta}\right) + \left(1-w(v,h)\right)\cdot a\left(1-\left(\frac{s^*(v(t))}{h(t-\tau)}\right)^2\right), \quad (1)$$

where $s^*(v) = s_0 + Tv + cv^2$ is the "desired" distance, τ is driver's reaction time and a, b, V^0, s_0, T are the model parameters. The continuously differentiable function $w(v,h)$ is defined as follows

$$w(v,h) = \begin{cases} 0, h \in (-\infty, s^*) \\ -2t^3 - 3t^2 + 1, , h \in [s^*, s^* + D], \\ 1, h \in (s^* + D, +\infty) \end{cases} \quad (2)$$

where $t = \frac{h - s^*}{D} - 1$.

The distance between vehicles in a steady-state flow according to the IDM demonstrates unrealistic increase as the velocity approaches the desired speed V^0 [21] (Fig. 1). One of the feature of the model (1) is that the distance in a steady flow moving with speed v is equal to "desired" distance $s^*(v)$ which is defined as a quadratic velocity function. Taking into account reaction time explicitly allows sufficiently increase the realism of simulation results.

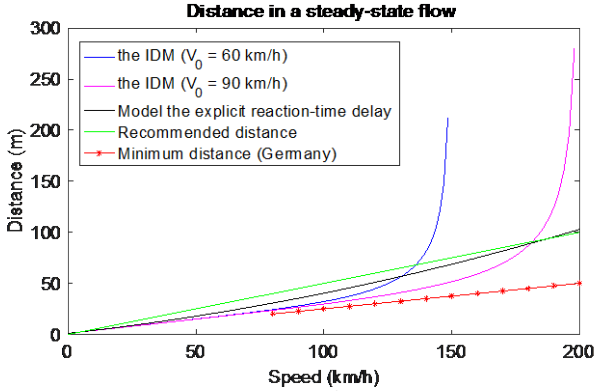

Fig. 1. *Distance in a steady state flow: the IDM, the model (1), recommended and minimum distance (Germany)*

3. Stability Analysis

In case of microscopic approach, the dynamics of many-body system is defined with system of differential equations (ordinary or delayed). Such systems admit uniform states, that is, all speeds and gaps are constant and equal. One of the method for benchmarking of the models is the stability analysis of the uniform solutions [4, 26]. Real observations of traffic flows proof the existence of non homogeneous configurations which are the formation and propagation of stop-and-go waves in case of high density values [22]. To sum up, elaborated models should admit unstable uniform solutions as well. It is worth to add, that oscillating solutions of corresponding systems of differential equations can have amplitudes which lead to backward motion and even crashes. Obviously, it is in contradiction with reality and should be controlled by means of stability conditions.

This section contains the results of stability analysis performed for car-following model (1) [25]. The local and string stability analysis of uniform solution is performed.

To study local stability we consider one vehicle following its leader. The acceleration of the follower is defined with (1) whereas the leader moves with constant speed v_L. The stability of the following stationary solution is investigated

$$\left(v = v_L, h = s^*(v)\right). \quad (3)$$

The following statement determines conditions on the parameters of the model for that the uniform solution is linearly stable.

Statement 1. The uniform solution (3) is linearly stable if and only if $\tau < \tau_{cr}, \tau_{cr} = \min_n\{\tau_{1,2}(n): \tau_{1,2}(n) > 0\}$. Here $\tau_{1,2}(n) = \frac{\pm arccos\left(-B^2/2C + \sqrt{B^4/4C^2 + 1}\right) + 2\pi n}{\beta}, n = 0, \pm 1, \pm 2, ..., \quad \beta^2 = \frac{-B^2 + \sqrt{B^4 + 4C^2}}{2}, B = -\frac{2a(T + 2cv)}{s_0 + Tv + cv^2}, C = \frac{2a}{s_0 + Tv + cv^2}$.

The local stability analysis (for a finite vehicle platoon with a leader travelling at a fixed speed) is different to the string stability, for vehicles on an infinite line or on a ring. The conditions for string stability are more restrictive because they include convective perturbations as well, which can locally vanish.

String stability analysis performed for N vehicles on a ring of length L. Dynamics of this system is described as follows

$$\ddot{x}_i(t) = w\left(\Delta x_i(t), \dot{x}_i(t)\right) \cdot a\left(1 - \left(\frac{\dot{x}_i(t)}{V^0}\right)^{\delta}\right) + \\ + \left(1 - w\left(\Delta x_i(t), \dot{x}_i(t)\right)\right) \cdot a\left(1 - \left(\frac{s^*\left(\dot{x}_i(t)\right)}{\Delta x_i(t - \tau)}\right)^2\right), \quad (4)$$

$$i = 1, \dots, N,$$

$$\Delta x_i(t) = x_{i+1}(t) - x_i(t), \quad i = 1, \dots, N - 1,$$

$$\Delta x_N(t) = x_1(t) - x_N(t) + L.$$

The uniform configuration

$$x_{i+1}^H(t) - x_i^H(t) = x_1^H(t) - x_N^H(t) + L = {}^1\!/\!_{\rho}, \\ x_i^H(t) = x_i^H(0) + v_\rho t \quad (5)$$

is a stationary solution of the system (4).

Statement 2. The uniform solution (5) of the system (4) is string stable if and only if $\frac{a(T + 2cv)}{s_0 + Tv + cv^2} > 1$ and $\tau < \tau_{cr}, \tau_{cr} = \min_n\{\tau_{1,2}(n): \tau_{1,2}(n) > 0\}$, where $\tau_{1,2}(n) = \frac{\frac{\theta}{2} \pm arccos\left(-\frac{\beta C}{2B sin\left(\theta/2\right)}\right) + 2\pi n}{\beta}, n = 0, \pm 1, ..., \quad \beta = \pm\sqrt{\frac{-C^2 + \sqrt{C^4 + 16B^2 sin^2(\theta/2)}}{2}}, B = -\frac{2a(t + 2cv)}{s_0 + Tv + cv^2}, C = \frac{2a}{s_0 + Tv + cv^2}$.

4. Calibration to Microscopic Observations

First calibration method allows to calibrate model parameters according to technical characteristics of the specific type of vehicle [21]. It could be applied to any car-following model with or without delay. Let the vehicle dynamics is defined by the following system with initial conditions for speed v and gap h

$$\begin{cases} \dot{v} = A(v, v_L, h, \theta) \\ \dot{h} = v - v_L \\ h(0) = h_0, v(0) = v_0 \end{cases}, \quad (6)$$

where θ is the vector of the model parameters, $h = s_L - s$. By means of numerical integration we can formulate the optimization problem with constraints

$$\begin{cases} \min_{\theta, \bar{s}, \bar{v}}\{w_1\|\tilde{s} - \bar{s}\|^2 + w_2\|\tilde{v} - \bar{v}\|^2\} \\ s_{i+1} - s_i = \Delta t \cdot \left(v_i - v_{L,i}\right) \\ v_{i+1} - v_i = \Delta t \cdot A\left(v_i, v_{L,i}, h_i, \theta\right), \\ i = 1, \dots, N - 1 \\ s_1 = \tilde{s}_1, v_1 = \tilde{v}_1 \\ \theta \in [\theta_l, \theta_u] \\ stability\ conditions \end{cases}, \quad (7)$$

where $\|\cdot\|$ is the Euclidean norm, w_1 and w_2 are weight factors, $\{\tilde{s}_i\}_{i=1}^N$ и $\{\tilde{v}_i\}_{i=1}^N$ are real trajectory data, $\bar{s} = \{s_i\}_{i=1}^N, \bar{v} = \{v_i\}_{i=1}^N$ mean simulated positions and speeds according to the model, θ_l, θ_u designate low and upper bound for parameter values. Stability conditions are incorporated in optimization problem in order to get parameters which guarantee stable solution.

We consider two subsequent problems which are free acceleration and the emergency deceleration to avoid crash. Solution of the free acceleration problem provides values of two parameters a and δ while the desired speed V^0 is fixed to the maximum vehicle speed. Emergency deceleration problem provides values of two other parameters T and c, whereas reaction time τ and minimum distance to the leader are not related to the dynamic properties of the underlying car.

Seconds approach exploits NGSIM I-80 data set which provides information about 5648 vehicle trajectories on a road section of approximately 500 m [19]. To find the optimal parameter values of a car-following model with a non-linear acceleration function (1), one needs to solve a non-linear optimization problem numerically. Initializing the microscopic model with the empirically given speed

and gap, one computes the trajectory of the following car with a real trajectory of its leader [17, 18, 27]. Afterwards it is directly compared to the speeds $v^{data}(t)$ or gaps $s^{data}(t)$ provided by the trajectory data. Here we use global and platoon methods in order to estimate the ratio between inter-driver and intra-driver variations [27].

The calibration procedure aims at minimizing the difference between the measured and simulated dynamic variables. Any quantity which represents aspects of the driving behaviour can serve as an objective function, such as the gap s, speed v, speed difference Δv, or acceleration a [28,29]. To assess quantitatively the error between measured and simulated data, different objective functions can be used. The absolute error measure reads

$$S_s^{abs} = \frac{\sum_{i=1}^{n}\left(s_i^{sim} - s_i^{data}\right)^2}{\sum_{i=1}^{n}\left(s_i^{data}\right)^2}. \quad (8)$$

In case of platoon calibration the error measure must have a double sum, one over the trajectory pairs j, and one over time i.

5. Multirate numerical integration scheme for time-continuous car-following models

Let the dynamics of N vehicles moving one by one is described with the following system of ordinary differential equations

$$\begin{cases} \dot{v}_1 = a^{(1)}(v_1, h_1) \\ \dot{h}_1 = v_L - v_1 \\ \langle \dots \rangle \\ \dot{v}_N = a^{(N)}(v_N, h_N) \\ \dot{h}_N = v_{N-1} - v_N, \end{cases} \quad (9)$$

with initial conditions $v_I(0) = v_{I0}, h_I(0) = h_{I0}, I = 1, \dots, N$. For brevity, we rewrite the system (9) in the following way

$$\dot{x}(t) = F\big(x(t)\big), \qquad x(0) = x^{(0)} \quad (10)$$

where $x = (v_1, h_1, \dots, v_N, h_N)^T$, $F_{2I-1} = a^{(I)}(v_I, h_I)$, $F_{2I} = v_{I-1} - v_I$.

Let us consider one macrostep of the underlying multirate scheme, which connects the solutions at the neighboring macrolevels t_{n-1} and $t_n = t_{n-1} + \Delta T$. Within one macrostep ΔT for each component x_i of the solution vector x one carries out k_i consecutive microsteps $\Delta t_i = \Delta T / k_i$ according to the basic numerical scheme, which is the explicit Euler method [30]. The multiplicity factors $\{k_i\}_{i=1}^{2N}$ are identified so as to satisfy the condition

$$\|x_n - \tilde{x}(t_n)\|_\infty < \varepsilon. \quad (11)$$

Here $\tilde{x}$ is the exact solution of the problem

$$\dot{x}(t) = F\big(x(t)\big), \qquad x(t_{n-1}) = x^{(n-1)} \quad (12)$$

One macrostep for the ith component is

$$\begin{cases} x_i^{(m+1)} = x_i^{(m)} + \Delta t_i \cdot F_i\left(x_1^{(m)}, \dots, x_i^{(m)}, \dots, x_{2N}^{(m)}\right) \\ x_i^{(m+2)} = x_i^{(m+1)} + \Delta t_i \cdot F_i\left(x_1^{(m)}, \dots, x_i^{(m+1)}, \dots, x_{2N}^{(m)}\right) \\ \dots \\ x_i^{(m+k_i)} = x_i^{(m+k_i-1)} + \Delta t_i \cdot F_i\left(x_1^{(m)}, \dots, x_i^{(m+k_i-1)}, \dots, x_{2N}^{(m)}\right) \end{cases}$$

Performing some analytical transformations one obtains the estimation of local integration error for the speed of Ith vehicle after k_{2I-1} consecutive microsteps

$$est_{2I-1,k_{2I-1}} = \frac{\Delta T^2}{2}\left|\frac{1}{k_{2I-1}} a_v^{(I)} a^{(I)} + a_h^{(I)}(v_{I-1} - v_I)\right| \quad (13)$$

and for the gap of Ith vehicle after k_{2I} consecutive microsteps

$$est_{2I,k_{2I}} = \left|\frac{\Delta T^2}{2}\left(a^{(I-1)} - a^{(I)}\right) + \frac{\Delta T^3}{6}\left(jrk^{(I-1)} - jrk^{(I)}\right)\right|, \quad (14)$$

where $jrk^{(I)} = a_v^{(I)} a^{(I)} + a_h^{(I)}(v_{I-1} - v_I)$, $a_v^{(I)}$ and $a_h^{(I)}$ are partial velocity and gap derivatives of acceleration function $a^{(I)}$. Let ε_h and ε_v are relative accuracy for gap and speed respectively. The time stepping strategy for ΔT and Δt_{2I-1} is

$$\begin{cases} \left|\frac{\Delta T^2}{2}\left(a^{(I-1)} - a^{(I)}\right) + \frac{\Delta T^3}{6}\left(jrk^{(I-1)} - jrk^{(I)}\right)\right| < h_I \varepsilon \\ \frac{\Delta T^2}{2}\left|\frac{1}{k_{2I-1}} a_v^{(I)} a^{(I)} + a_h^{(I)}(v_{I-1} - v_I)\right| < v_I \varepsilon_v, \\ I = 1, \dots, N \end{cases} \quad (15)$$

The value of Δt_{2I} is directly identified from (14). Values of $\Delta t_{2I-1}, \Delta t_{2I}$ and ΔT are calculated analytically.

Stability investigation is an integral part of the analysis of any numerical scheme [33]. The numerical scheme is stable if and only if all eigenvalues of the transition matrix are less than unity in modulus. Due to specific structure of the system (9) it is possible to identify all eigenvalues analytically. Consequently, stability conditions for the scheme with multiple steps are

$$\left|1 + {r_{2I-1}}^{k_{2I-1}} \pm \sqrt{(1 + {r_{2I-1}}^{k_{2I-1}})^2 - 4\frac{r_{2I-1}^{k_{2I-1}} - 1}{r_{2I-1} - 1} a_h^{(I)} \frac{\Delta T^2}{k_{2I-1}}}\right| < 2$$

where $r_{2I-1} = \left(1 + a_v^{(I)} \frac{\Delta T}{k_{2I-1}}\right), I = 1, \dots, N.$

6. Discussion and Conclusions

The model with explicit reaction-time delay represents plausible free-acceleration and following dynamics of car traffic. Regarding traffic flow instabilities, observed in reality, one can simulate propagation of stop-and-go waves using this model [25]. The speed of the backward propagation of the wave in a computer experiment is consistent with real observations.

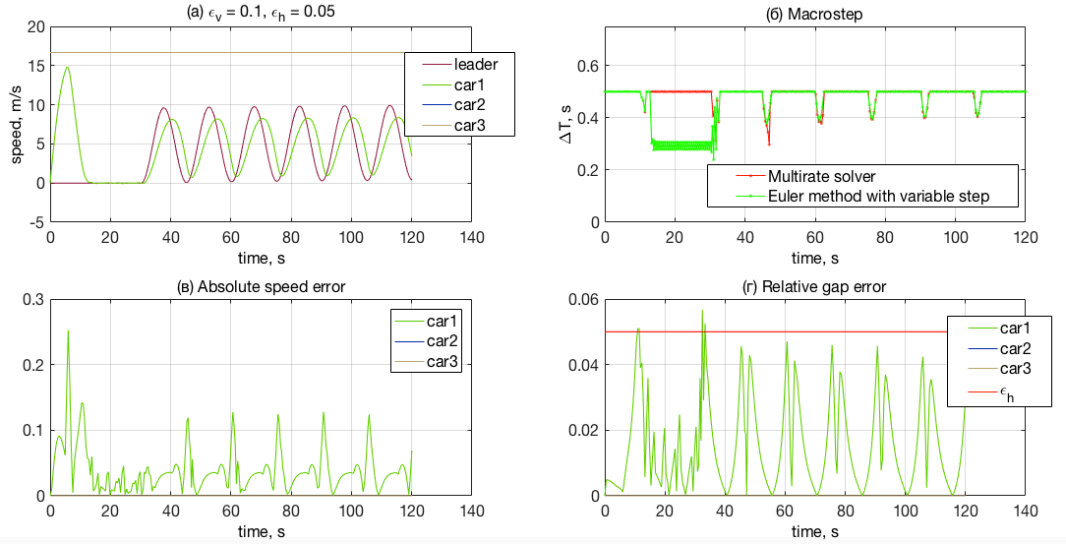

Fig. 2. *Speed time-series of 4 vehicles (upper-left). Macrosteps (upper-right). Absolute speed error (lower-left) and relative gap error (lower-right)*

We calculated stability conditions for the finite vehicles platoon (local stability) and for vehicles on a ring (string stability). Conditions on model parameters are obtained analytically. Numerical experiments confirm the correctness of these conditions [25]. Moreover, it is possible to find feasible values of reaction time τ, which simultaneously guarantee stability of the solutions.

Calibration of the underlying car-following model with explicit reaction-time delay according to NGSIM data set indicates its good fitting power. In other words, absolute minimums of the objective function are in the typical error range obtained in previous studies [17, 18]. Calibration approach exploiting technical characteristics of a car allows to obtain parameter values for specific vehicle models. In application to driving simulators, the quality of vehicular traffic simulation plays a major role, that is, each car should move according to its real dynamics, drivers behave in predictable manner and in accordance with traffic rules.

The numerical experiments show that the local error of the multirate integration method at the end of each macrostep does not exceed the required accuracy (Fig. 2). The results confirm that the speed of the method can be increased while preserving the requirements for the accuracy of the numerical solution if, at the same time, the speed of each component value is considered. Moreover, this multirate solver admits parallel implementation which will further accelerate calculations.

References

[1] M. Mauch, M.J. Cassidy, Freeway traffic oscillations: observations and predictions. Transportation and traffic theory in the 21st century: Proceedings of the Symposium of Traffic and Transportation Theory, p. 653-672, 2002.

[2] M. Schonhof, D. Helbing, Empirical features of congested traffic states and their implications for traffic modeling. Transportation Science, Vol. 41, Issue 2 (2007), p. 135-166.

[3] B. Zielke, R. Bertini, M. Treiber, Empirical Measurement of Freeway Oscillation Characteristics: An International Comparison. Transportation Research Record, No 2088 (2008), p. 57–67.

[4] M. Treiber, A. Kesting, Traffic Flow Dynamics: Data, Models and Simulation, Springer-Verlag Berlin Heidelberg, 2013.

[5] M.J. Lighthill, G.B. Whitham, On kinematic waves: II. Theory of traffic flow on long crowded roads. Proc. R. Soc. London, Ser. A. Vol. 229 (1955), p. 281-345.

[6] H.J. Payne, Models of freeway traffic and control. Simulation Council Proc. 28, Mathematical Models of Public Systems ed. by G.A. Bekey, Vol. 1 (1971), p. 51–61.

[7] B.S. Kerner, P. Konhäuser, Cluster effect in initially homogeneous traffic flow. Phys. Rev. E., Vol. 48 (1993), p. 2335-2338.

[8] A.A. Chechina, N.G. Churbanova, M.A. Trapeznikova, Two-dimensional hydrodynamic model for traffic flow simulation using parallel computer systems. Proceedings of the international conference of the numerical analysis and applied mathematics 2014. AIP Conference Proceedings, 1648 (2015), p. 530007.

[9] K. Nagel, M. Schreckenberg, A cellular automaton model for freeway traffic. J. Physique I France, Vol. 2 (1992), p. 2221–2229.

[10] J. Tian, G. Li, M. Treiber, R. Jiang, N. Jia, Sh. Ma, Cellular automaton model simulating spatiotemporal patterns, phase transitions and concave growth pattern of oscillations in traffic flow. Transportation Research Part B: Methodological, Vol. 93 (2016), p. 560-575.

[11] M. Bando, K. Hasebe, Dynamical model of traffic congestion and numerical simulation. Physical Review E, Vol. 51(2) (1995), p. 1035-1042.

[12] M. Bando, K. Nakanishi, A. Nakayama, Analysis of Optimal Velocity Model with explicit delay. Physical Review E Vol. 58(5) (1998), p. 5429-5435.

[13] M. Treiber, A. Hennecke, D. Helbing, Congested traffic states in empirical observations and microscopic simulations. Physical Review E, Vol. 62(2) (2000), p. 1805-1824.

[14] I. Lubashevsky, P. Wagner and R. Manhke, A bounded rational driver model. European Physical Journal B. Vol. 32 (2003), p. 243-247.

[15] A. Tordeux, S. Lassarre, M. Roussignol. An adaptive time gap car-following model. Transportation Research Part B, Vol. 44 (2010), p. 1115-1131.

[16] R. Jiang, Q. Wu, Z. Zhu, Full velocity difference model for a car-following theory. Physical Review E, Vol. 64(1) (2001), p. 017101.1-017101.4.

[17] E. Brockfeld, D. Kuhne, P. Wagner, Calibration and Validation of Microscopic Traffic Flow Models. In Transportation Research Record, 1876 (2004), p. 62-70.

[18] A. Kesting, M. Treiber, Calibrating Car-Following Models by Using Trajectory Data. In Transportation Research Record, Vol. 2088 (2008), p.148-156

[19] NGSIM: Next Generation Simulation. FHWA, U.S. Department of Transportation. www.ngsim.fhwa.dot.gov. Accessed May 5, 2007.

[20] Deutsches Zentrum für Luft- und Raumfahrt. www.dlr.de/cs/. Accessed May 5, 2007.

[21] V. Kurtc, I. Anufriev, Local stability conditions and calibrating procedure for new car-following models used in driving simulators. Traffic and Granular Flow'13, p. 453-461, 2015.

[22] Y. Sugiyama, M. Fukui, M. Kikushi, K. Hasebe, A. Nakayama, K. Nishinari, and S. Tadaki. Traffic jams witho bottlenecks. Experimental evidence for the physical mechanism of the formation of a jam. New J. Phys., Vol. 10(3) (2008), p. 033001.

[23] G. Orosz, R. Wilson, R. Szalai, G. Stepan, Exciting traffic jams: Nonlinear phenomena behind traffic jam formation onhighways. Physical Review E, Vol. 80 (2009), p. 046205.

[24] P. Wagner, I. Lubashevsky, Empirical basis for car-following theory development. preprint cond-mat/0311192 (2003).

[25] V. Kurtc, I. Anufriev, Car-following model with explicit reaction-time delay – linear stability analysis of the uniform solution on a ring. Mathematical Models and Computer Simulations, Vol. 29, No 4 (2017).

[26] G. Orosz, R.E. Wilson, and G. Stepan, Traffic jams: dynamics and control. Proc. R. Soc. A, Vol. 368 (2010), p. 4455-4479.

[27] V. Kurtc, M. Treiber, Calibrating the Local and Platoon Dynamics of Car-following Models on the Reconstructed NGSIM Data. Traffic and Granular Flow'15, p. 515-522, 2016.

[28] V. Punzo, B. Ciuffo, M. Montanino, May we trust results of car-following models calibration based on trajectory data? TRB 2012 Annual Meeting (2012).

[29] V. Punzo, M. Montanino, B. Ciuffo, Do we really need to calibrate all the parameters? Variance-based sensitivity analysis to simplify microscopic traffic flow models. IEEE Transaction on Intelligent Transportation Systems, 2014.

[30] V. Kurtc, I. Anufriev, Multirate numerical scheme for large-scale vehicle traffic simulation. Mathematical Models and Computer Simulations, Vol. 8, No. 6 (2016), p. 744–751.

[31] M. Treiber, V. Kanagaraj, Comparing numerical integration schemes for time-continuous car-following models. Physica A: Statistical Mechanics and its Applications, Vol. 419 (2015), p. 183-195.

[32] M. Gunther, A. Kvœnø, P. Rentrop, Multirate partitioned Runge-Kutta methods. *BIT*, Vol. 41 (2001), p. 504-514.

[33] V. Savcenco, W. Hundsdorfer, J.G.Verwer, A multirate time stepping strategy for stiff ordinary differential equations, BIT, Vol. 47 (2007), p. 137-155.

PERSPECTIVES AND CHALLENGES FOR RUSSIAN SYSTEM OF ENGINEERING EDUCATION

Ph.D., Aleksankov.A

International Institute of Economics and Politics - St. Petersburg State University of Economics, Russia

E-mail: alexankov@unecon.ru

Abstract: *Over the last decades Russian higher education institutions have been actively working in global education world and facing problems of adapting its education system to it. Specifically it concerns system of engineering education which has to overcome problems of the past and face modern reality of Industry 4.0. One of the major problems is low flexibility and adaption ability to rapidly changing external circumstances as well as liner and strict curricula structure. To overcome problems successfully, Russian engineering education has got substantial support of Russian government; system is going to be modified in leading Russian universities. General approach that needs to be implemented is focusing on re-adjusting curricula as the set of alternating study courses and work on engineering tasks. University networking supported by interactive platforms in close cooperation with industry should be also the basic for modernization.*

Keywords: TQM IN UNIVERSITY, EDUCATION REFORM, EDUCATIONAL CYCLE, UNIVERSITY NETWORKING

Introduction

The problem of returning global and national economies to sustainable economic growth is universal. In accordance to different expert analysis, economic growth can be ensured by design and introduction of new disruptive technologies and newly developed goods and services. Though in comparison to previous technological mode, the modern one differs in terms of lifecycle period, time for entering market and commercial usage, mutual integration of technologies. This situation poses considerable challenge to the universities' training system as the lifecycle of technologies and products has become comparable with the educational cycle. The increasing amount of distributed knowledge and simplified remote access to this knowledge forced to change traditional paradigm of universities and its training system.

Background

Modern Russian system of engineering education is traditionally based on features and achievements of soviet system of higher education. One of the peculiarities of traditional system was its linear character when expected result of education and relatively narrow specialization had been defined at the beginning of educational cycle. Educational cycle as a rule lasting for 5,5 years contained a lot of basic and specialized knowledge with gradual convergence with practical activities on upper level of education. Practical involvement into the solving of engineering problems had been rather limited and it led to situation when graduates had possessed a lot of theoretical knowledge but had not been able to use it practically. Finally, it took another 2-3 years to combine theory and practice to be really certified as an engineer.

Epic collapse of manufacturing industry in Russia in the early 90-s led to destruction of previously established links between universities and industrial sector. Losing part of public funding forced universities to look for other financial non-public resources along with considerable weakening of centralized university government [12]. Partly independent in terms of financing and acting new units started to born in universities being fully responsible for future survival and having rather low propensity to cooperation with other units. Generally speaking the whole university structure sometimes much more reminded holdings of independent entrepreneurs rather than educational corporations with centralized management system [3].

Since the beginning of 90-s number of state and non-state universities was doubled [18] mainly for the account of non-state universities, who were specializing primarily in Humanities, Business and Economics. The number of institutions as well as number of students reached the maximum in the year 2010.

Table 2.1 Number of students and institutions of higher education in Russia, 1990-2015 г.

Years	Number of institutions	Number of students, thousands	i.e. by form of education			Per 10000 pax
			Full-time	Partly full-time	Part-time	
1990/91	514	2824,5	1647,7	284,5	892,3	190
2000/01	965	4741,4	2625,2	302,2	1761,8	324

2005/06	1068	7064,6	3508,0	371,2	3032,0	493
2010/11	1115	7049,8	3073,7	304,7	3557,2	493
2011/12	1080	6490,0	2847,7	263,4	3289,7	454
2012/13	1046	6075,4	2724,3	229,7	3051,4	424
2013/14	969	5646,7	2618,8	189,2	2838,6	393
2014/15	950	5209,0	2575,0	158,5	2475,5	356

Analysis of structure of graduates' specialties shows sustainable growth of graduates in such areas as Humanities, Business and Economics from the year 2000. It ultimately led to the oversaturation of such specialists on labor market, increased number of over skilled employees, necessity to hire them at mid-professional level. Thus, in 2010 the number of graduates in Humanities achieved 178,0 thousands, Business and Management – 386,0 thousands, Energy Engineering – 24,0 thousands, Transport Systems – 34,7 thousands, Electronics – 14,7 thousands, Information Science and Computing – 22,3 thousands.

Due to unsatisfactory situation the Ministry of Education and Science of Russia initiated structural reform of higher education system after the year 2010. The reform was aimed at decreasing number of higher education institutions by indicating inefficient institutions as well as merging relatively small regional institutions with identical areas of training [7]. As a result, the number of students over the period from 2010 to 2015 was reduced by 26%, the number of educational institutions by 15%. While the number of teaching staff declined significantly faster in public than in private educational institutions, partly as a result of employees transition from public to private institutions.

Table 2.1. Teaching staff in institutions of higher education

1990/91	2000/01	2005/06	2010/11	2011/12	2012/13	2013/14	2014/15
Public Higher education institutions							
219,7	265,2	322,1	324,8	319,0	312,8	288,2	271,5
Private Higher education institutions							
-	14,4	36,7	32,0	29,2	29,2	31,1	28,2

The period of relatively low state regulation and participation in higher education had both positive and negative results [14]. The acquisition commercial and market skills by university staff, entering international market, maintaining teaching staff can be considered as a positive. Permanent weakness in integrating new educational techniques, low flexibility in designing curricula and low ability to diverse different resources should be noted as negative. Unfortunately quality of education also had lost its priority.

In the framework of traditional system the issue of quality had been interpreted more as a necessity to fulfil curricula rather than follow students' needs and requirements of potential employers. One of the major priorities in implementation university policies was given either by university management or Ministry of education to maintaining teaching staff and retaining it in universities. Due to implementation of those policies in the past nowadays universities encounter problems while trying to implement European approaches in quality management, in particular student-centered conception in study process. In fact it means advancing interests of students and employers over the interests of institution and its staff.

Since 2011 the major trend in reform of higher education system can be described as strengthening the role of government organizations but re-focusing its regulative efforts more on final results rather than current processes, yet Ministry of education and science retains sufficient control over the educational procedure.

Development of Total Quality Management System (TQM)

Over the long period professional qualifications had been described in Russian educational standards while representatives of business and industry did not strongly participate in creating new competences. In fact it meant professional qualifications had been issued by university without serious expertise of professional society (except for medical specialties). Nowadays situation is changing, at least new educational standards (to be issued at the end of 2016) will not contain professional requirements, which will be transferred to professional standards of the National Qualification Framework.

Training and re-training system is much related to development of quality management system and matching difference between European and Russian approaches. Being carefully considered Russian Federal educational standards and the Framework standards for engineering programs EUR-ACE show its equality in general with some obvious differences [13]. Learning outcomes in Russia and Europe are assessed in different "coordinate systems", i.e. in the Russian Federation learning outcomes are classi-

fied by types of activities (research, design, management etc.) but in European standards they are divided into phases (knowledge and understanding, engineering analysis, engineering design, research, engineering practice).

Russian standards do not specify procedure of monitoring customers' and employers' demands even do not identify any requirements to quality of resources and internal management systems, which are obligatory for EUR-ACE (ESG 2015). In addition, it seems reasonable to have aggregated criteria to describe ability of educational institution to modify its curricula within limited time and adapt it to updated market requirements with ensuring the same quality level.

Both Russian industry and education system face qualitatively new challenge that requires new mentality and approaches on different levels. Russian higher education system encounters the situation when it needs to overcome systematic problems of the past and change the whole paradigm of engineering education taking into consideration realities of Industry 4.0.

Development of engineering education

In the year 2013 Russian Ministry of Education and Science launched ambitious project entitled "Program 5-100-2020" aimed to having at least 5 Russian universities in the ranking list of TOP-100 world universities. Group of 15 candidates (in 2015 was extended to 21) was carefully selected among dozens applicants. Within the framework of this project series of education and creative seminars in cooperation with Skolkovo Business School were organized to work out various development projects in different areas. Priority was given to university education and innovation policy, student and staff recruitment activities, engineering education development and international branding and marketing.

One of the expert groups with representatives from Peter the Great St. Petersburg Polytechnic University, "MISIS" National University of Science and Technology, National Research University of Information Technologies, Mechanics and Optics, Kazan Federal University, Ural Federal University, Novosibirsk State University and Tomsk State University was focused on elaboration modern principles of engineering education in Russian universities.

Modification of engineering education was initially based on alteration of engineering cycle and its composition parts. In conditions of previous technological modes prototype model had been designed, produced and tested. The process of improving (see Fig. 1) was then implemented as the process of disassembling to integral parts with further modification. Within the framework of Industry 4.0 conception [17], [11] the number of decomposition cycles (disassembling – improvement – assembling - testing) and period of each particular stage have to be minimized. Computer modeling combined with technologies of prototyping could make characteristics of prototype model almost ideal and further decomposition redundant. New paradigm of engineering work might require qualitatively different engineering skills and knowledge, interdisciplinary and foresight mentality.

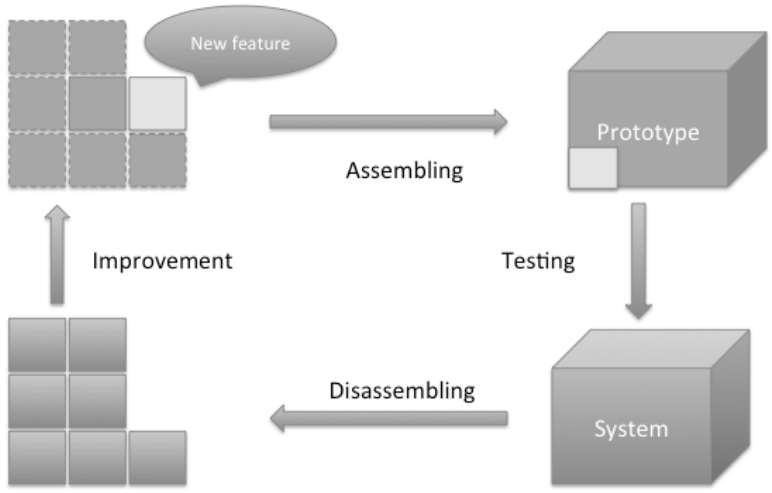

Fig. 1. Engineering cycle

Achieving appropriate level of qualification in previous technological modes was similar to engineering cycle in traditional Russian system. Thus initially student had been filled with massive set of different knowledge from different areas with comparatively low practical skills. Then required attainments and skills were enhanced, those not required became passive or even lost. This process can be identified as the process of knowledge and skills decomposition similar to decomposition of modules of prototype model.

Theoretical assumption for elaboration new concept of engineering education was that university system can efficiently communicate with external objects if universities' production cycles, organizational and management system, corporate culture and other characteristics would not seriously contradict similar characteristics of external objects. Though full coincidence is not required or even can be disadvantage because teachers' and scientists' mentality and labor substance would differ from those in business and industry. In terms of staff training it means training should be more effective in environments generally coinciding with those where graduates would be employed.

Making summary of all mentioned above, engineering education in new technological mode should be optimized in terms of having exactly those skills and attainments which required for engineering problems solving. Having enabling environment for fu-

ture success is a must. Though the issue of having knowledge deposit is still discussible. From the one side to store knowledge has become very expensive due to its obsolescence, from another – without fundamental ontological and axiological basis solving future engineering problems seems to be unproductive.

Practical recommendations

Major assumptions for further elaboration practical measures were the following:

- modern manufacturing process requires joint activities and cooperation of different types of engineers – researchers, innovators, designers and engineers of full lifecycle,
- acquisition new competences must be based on engineering tasks initiated by industrial sector, new competences should correspond to lifecycle stages,
- process of engineering task solving is cycled and divided to navigation course – engineering task solving – final course and testing (Fig. 2),

-forming new engineering competences requires transformation of linear model of study on early stage to linear-matrix model with extended variety of study courses on higher level. Networking, using on-line open courses in combination with study modules as knowledge cluster can substantially widen access to new knowledge.

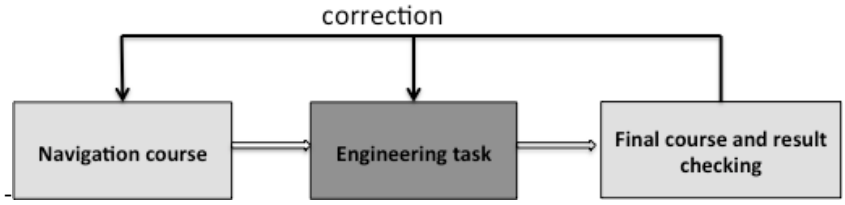

Fig. 2. Education based on engineering tasks

Expert group planned piloting it for Computer Science &Software Engineering in cooperation with Kazan Federal University, Peter the Great St. Petersburg Polytechnic University, Ural Federal University and Tomsk State University. For launching the pilot project the interactive platform providing full access to constantly updated study courses and engineering tasks was designed. Full access is available for all universities participating in the project. Engineering tasks are initiated and supplied by industrial companies but before being placed on the platform they have to be examined by university and probably adapted to current study purposes (see Fig. 3). The platform is used as an integrator providing optimal ways of problem solving, collecting various decisions, disseminating new knowledge for self-organized sub-consortia.

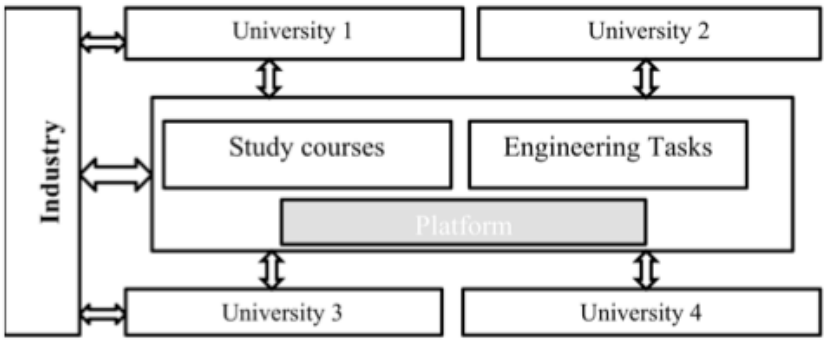

Fig. 3. Education platform

Approaches described allow enhancing quality of education and acquired competences but they formally focus on modifying forms of education and organizational model. Not mentioned aspect of engineering psychology should be noted here. Role and place of psychological aspects in engineering tasks was unfortunately underestimated in traditional system. For example, Theory of Inventive Tasks Solving (TRIZ) elaborated in the middle of XX century by outstanding Russian engineer and scientists Genrich S. Altshuller draws much more attention in foreign universities than in Russian ones, being an essential part of engineering study. In this context the work of Institute of Wideband Study located in St. Petersburg can be the case of interest. Institute has an official status of non-state organization but actively cooperate with state universities.

In addition to traditional aspects of educational activities the Institute of Wideband Study develops new approaches in so-called thinking management and resource state of future engineer. In traditional educational system the priority had been given to formulation of natural-science, systematic and logical types of student's thinking whereas such kinds of thinking as heuristic, divergent, strategic foresight were hardly used. The value of the IWS's techniques is much better self-tuning for a particular type of thinking (thinking as a project) and then comparing the "projects" results with further selection the best one. Self-management skills to manage resource state of an engineer are also unique. Management of resource state means management of the physical, cognitive and emotional states based on the perception of space as infinite, wave flow, a plurality of discrete objects or objects of chaos.

Final solution of engineering problems is improved by means of the best combination of traditional methods of engineering and thinking management and resource state. The integration tool is an interactive platform that allows improving and combining the range of academic disciplines, optimizing the educational route, learning outcomes and resource state.

One more aspect of manpower training should be considered here. It is the use of supercomputer technologies in training modern engineering competences. It is primarily connected to the growing role of the different modeling approaches that are basic for producing engineering products within the concept of Industry 4.0. The usage of the methods of mathematical modeling can reduce the product manufacturing cycle through rapid prototyping and testing engineering properties without making real model. At the same time, the complexity of the models, which can be calculated using supercomputer technologies can significantly improve their degree of detail and take into account the various aspects of their operations, which in turn enables interdisciplinary interaction. For example, Computer center of the Polytechnic University ranks third in Russia for the efficiency and within its activities up-to-date task performance is carried out. It uses mathematical modeling methods in the calculation of the strength characteristics of different constructions, hydro-aerodynamics, the analysis of large data, complex 3D model building.

Conclusions

The efficiency of Russian universities' training systems is determined by their ability to overcome the systemic problems of the past, to identify and develop the most valuable achievements of the traditional system of higher education, to adapt and implement the best international developments in university engineering education.

University management systems need to be modified in terms of strengthening centralized government, universities themselves need to be considered as corporation for knowledge and human capital production. The quality management system should be the basis for developing corporate culture. QMS must be primarily based on interests of employers and students.

Practical application in the process of engineering education should be implemented through solving engineering tasks. At any level educational cycle is starting with basic course – then work on engineering problems - then final course, testing and assessment. Switching to the modularity can shorten each of particular stages, for example from 1 term to 1 month.

Development of engineering education is impossible without development of engineering thinking based on psychological models (e.g. Theory of Inventive Tasks Solving), interdisciplinary collaboration with other educational establishments. The basis for overcoming traditional isolation of universities is in networking for the effective exchange of knowledge, engineering problems and their solutions, and the experimental results of high-speed computations and calculations. A possible solution is the foundation of real or virtual intercollegiate engineering centers, coordinating inter-university collaboration and cooperation.

References

[1] Akaev AA, and Rudskoi AI (2013) Analys I prognoz vliyania shestogo technologocheskogo uklada na dinamiku mirivogo economicheskogo razvitia [Analysis and forecast of the impact of the sixth technological mode on the global economic development dynamics]. In the book: «*Mirovaya dinamica: zakonomernosti, tendensii, perspectivi*» ["World dynamics; patterns, trtends and prospects"]. Moscow: LIBROCOM, pp. 142-166.

[2] Akaev AA (2014) *Novaya strategia V. Putina po dostizheniu visokih ustoichvih tempov rosta rossiiskoi economiki* [New strategy of V. Putin to achieve sustainable economic growth rate]. – St. Petersburg.: "Severnaya Zvezda". 268 p.

[3] Aleksankov AM, Mager VE., and Chernen'kaya LV (2016) Upravleniye kachestvom kak osnova reformirovaniya rossiyskikh universitetov [Quality management as a basis for the reform of Russian universities]. St. Petersburg.: "*Standarty i kachestvo*", 2016. Vol. 4, pp. 91-94.

[4] Bespamyatnyh EV, Kortov SV, Pilichev VV, and Terlyga NG (2010) Realizaciya kompetentnostnogo podhoda v podgotovke specialistov innovacionnoi sfery [The implementation of the competency approach in training the innovation sphere]. Vestnik UGTU-UPI. Ser. "*Ekonomika i upravlenie*" ["Economics and Management"]. 2010, Vol. 1, pp. 113-121.

[5] Deloitte. Industry 4.0 Challenges and solutions for the digital transformation and use of exponential technologies. http://www2.deloitte.com/content/dam/Deloitte/tw/Documents/manufacturing/tw-research-industry4-0-en.pdf

[6] Glaziev SY (1993) *Teoriya dolgosrochnogo tekhniko-ekonomicheskogo razvitiya* [The theory of long-term technical and economic development]. Moscow, Vladar.

[7] Grudzinskiy AO, Chuprunov YV, and Malinin VA (2010) Innovatsionnyy universitet i novaya shkola: napravleniya vzaimodeystviya [Innovation and New School University: directions of cooperation]. «*Vyssheye obrazovaniye v Rossii*» ["Higher education in Russia"].Vol. 4 pp 3-7.

[9] Hirooka M (2006). *Innovation Dynamism and Economic Growth. A Nonlinear Perspective*.-Cheltenham, UK – Northampton, MA, US: Edward Elgar.

[10] Institute of Wideband Education, http://humanworld.info/ru-RU/Users/119

[11] Jeschke S, 2015, Engineering Education for Industry 4.0. Challenges, Chances, Opportunities. World Engineering Education Forum 2015. http://www.ima-zlw-ifu.rwth-aachen.de/fileadmin/user_upload/INSTITUTSCLUSTER/Publikation_Medien/Vortraege/download//EngEducationInd4.0_22Sept2015.pdf

[12] Klyachko TL (2005), Funktsional'naya transformatsiya rossiyskoy sistemy vysshego obrazovaniya [Functional transformation of the Russian system of higher education] *Sotsial'naya differentsiatsiya vysshego obrazovaniya* [Social differentiation of higher education] Otv. Red. Shishkin SV, Nezavisimyy institut sotsial'noy politiki [Independent Institute for Social Policy]. Moscow, pp. 19-38.

[13] Kozlov VN, Rudskoy AI, and Chernenkaya LV (2009) Analiticheskiye obzory po osnovnym napravleniyam razvitiya vysshego obrazovaniya [Analytical review of the main directions of development of higher education]. *Zarubezhnyye sistemy upravleniya kachestvom vysshego professional'nogo obrazovaniya* [Foreign quality management system of higher education]. Moscow.

[14] Larionova MV (2004) Formirovaniye yevropeyskogo obrazovatel'nogo prostranstva: zadachi dlya rossiyskoy vysshey shkoly [Formation of a European educational space: the problem for the Russian higher schools] *Voprosy obrazovaniya* [Education issues]. 2004. Vol. 4 – pp 142-149.

[15] McKinsey Global Institute, (2012). The social economy: Unlocking value and productivity through social technologies. www.mckinsey.com/mgl

[16] McKinsey Global Institute, (2013). Disruptive technologies: Advances that will transform life, business, and the global economy. www.mckinsey.com/mgl

[17] McKinsey&Company, (2016). Industry 4.0 after the initial hype where manufacturers are finding value and how they can best capture it. www.mckinsey.com

[18] Rosstat, Educational institutions of higher education. http://www.gks.ru/bgd/regl/b15_13/IssWWW.exe/Stg/d01/07-44.doc

[19] Rosstat, Number of teaching staff in higher education institutions. http://www.gks.ru/bgd/regl/b15_13/IssWWW.exe/Stg/d01/07-46.doc

[20] Rosstat, Number of graduates with Bachelors Masters and Specialists degrees in 2005-2014. http://www.gks.ru/bgd/regl/b15_13/IssWWW.exe/Stg/d01/07-49.doc

[21] Russian education statistics. www.stat.edu.ru

[22] OECD. (2015), *Education at a Glance 2015*, OECD Indicators, OECD Publishing, Paris.

[23] OECD. (2016), *Getting Skills Right: Assessing and Anticipating Changing Skill Needs*, OECD Publishing, Paris.

OECD. (2015), *OECD Science, Technology and Industry Scoreboard 2015: Innovation for growth and society*, OECD Publishing, Paris.

[8] Recommendations for implementing the strategic initiative INDUSTRIE 4.0 Final report of the Industrie 4.0 Working Group. (2013). http://www.acatech.de/fileadmin/user_upload/Baumstruktur_nach_Website/Acatech/root/de/Projekte/Laufende_Projekte/Industrie_4.0/Final_Report_Industrie_4.0_engl_web.pdf

[24] The Standards and guidelines for quality assurance in the European Higher Education Area. ESG (2015) http://www.enqa.eu/index.php/home/esg/

[25] Vestnik UGTU-UPI. Ser. "*Ekonomika i upravlenie*" ["Economics and Management"]. 2010.- Vol. 1- pp. 113-121.

RISK-ORIENTED APPROACH IN QUALITY MANAGEMENT

PhD. Mager V.[1], PhD. Stepanova M.[2], Dr.Tech.Sc. Chernenkaya L.[1], M.Sc. Chernenkii A.[3]

Peter the Great St. Petersburg Polytechnic University, St. Petersburg, Russia
Institute of Computer Sciences and Technologies [1],
Institute of Humanities [2],
Institute for complementary education [3]

mv@qmd.spbstu.ru

Abstract: *In free market conditions the successful operation of enterprises is impossible, if requirements to the product quality are not improved. The article describes the necessity in creation of Quality management system, and specifics of risk-oriented approach in quality management are considered. The selection of methods for assessment of risks is justified, and recommendations on application of these methods during organizational activities' monitoring are formulated. It is shown that the implementation of risk management is aimed on the achievement of qualitative results and the enhancement of enterprise' competitiveness.*

Keywords: QUALITY MANAGEMENT, RISK-ORIENTED APPROACH, MONITORING OF ACTIVITIES, METHODS FOR ASSESSMENT OF RISKS

1. Introduction

Risk-based thinking was announced in the 2015 edition of ISO 9000 series of international standards. According to ISO 9001 (6.1), this kind of thinking has to be represented in the requirements for development, implementation, maintenance and continual improvement of a Quality Management System (QMS). The standards users, especially those who are going to recertify their organization's QMS in accordance with the new edition of the standards, see it as an innovation and are puzzled. They have to develop the ways of risk addressing in line with the recommendations listed in the annex to 6.1.1 of ISO 9001:2015.

In QMS models, including a Business Excellence model applied in the organization of competitions for the Awards of the Government of Russian Federation in the field of quality, companies have to provide evidence of risk management in their activities when forming their self-assessment reports. Risks are not just financial ones. This notion includes practically all the aspects of the organization's activity under assessment. However, when documenting QMS, it is not required to present any calculation results, there is no a calculation method, and in most cases risk assessment and accounting are described verbally.

2. Rational

What is risk? In accordance with the international standard ISO 9000:2015 [1] (3.7.9), "risk is an effect of uncertainty", which is "a state or condition that involves a deficiency of information and leads to inadequate or incomplete knowledge or understanding of an event, its consequences and likelihood", and an effect is a deviation from the expected result, both positive and negative. In this definition, the risk can be regarded as a deviation from the planned trajectory (scenario), and risk accounting reduces to an assessment of the possible outcomes of scenarios depending on variations in SWOT analysis components, a tool well known from strategic management. In this context, the following types of risks are usually analyzed: management risks, security risks, financial and commercial risks, industrial, environmental, social, political, etc., and risk refers to the discrepancy between the various possible outcomes of certain strategies. The main question that arises in this analysis is: how is this measure of discrepancy determined (measured, calculated)?

The definitions of the term "risk" in the standards directly related to this issue differ. So, ISO Guide 73:2009 Risk management - Vocabulary - Guidelines for use in standards [2] defines risk as a "combination of the probability of an event and its consequences", and the Large Economic Dictionary narrows the above definition by removing positive deviations: "Risk is the possibility of an event with negative consequences as a result of certain actions or decisions" [3]. Nevertheless, these definitions move the solution of the risk assessment problem into the field of the probabilistic approach, which is also widely used in practice.

The methodology of risk assessment is widely used in solving complex safety issues, while the risk is usually understood as a probabilistic measure of the occurrence of dangerous man-made or natural phenomena, as well as a description of the amount of damage and harm caused. The basis of this methodology is the definition of the consequences and likelihood of undesirable events, and analytically the risk is calculated as the ratio of the frequency of implementation of hazards to the possible number of them:

$$Risk = \frac{N(f)}{Q(f)},$$

where N is the quantitative measure of the frequency of undesired events in time *t; Q* is the number of risk objects subject to a certain risk factor *f*.

To solve such problems, it becomes necessary to determine the value of the acceptable level of risk under conditions of partial uncertainty associated with the inadequacy or inability to verify the information, then calculating the probability value of the risk and comparing it with the permissible value (it should be borne in mind that under conditions of total uncertainty, when the situation is not statistical, it is impossible to determine objective probabilities and to present the characteristics of a finite probabilistic scheme of variants of possible outcomes of the scenario, it is meaningless to calculate the risk value). In addition, risk analysis is a multicriterion problem, for which multidimensional statistics methods are applied.

Despite the thoroughness of this scheme, it is obvious that it is not reasonable to assess the risks in the organizations activities from the position of damage or harm. If benchmarking is involved, then the best practice, for sure, will be the methodology for assessing risks in the design and operation of complex technical facilities. Its conceptual focus is based on the scientific approaches of the theory of reliability, in which the main concept is a rejection. Failure is an event that causes the object in question to completely or partially stop performing the specified functions, and the total loss of the ability to perform functions is treated as a complete failure, partial loss is treated as a partial failure. The quantification of reliability for total and partial failures is different.

With reference to the activity of the organization, a variety of so-called initiated failures is identified, which include erroneous control actions and decisions. The human factor is at the forefront, since people who are prone to make mistakes are possible sources of secondary failures, if their actions lead to a malfunctioning system.

Reliability of a person's work is defined as the probability of successful fulfillment of a solution to the task at a given time interval under certain conditions of work performance, and a person's error is interpreted as a failure to perform the task (or

performing an activity forbidden in the performance of the task), which can lead to equipment breakdowns, damage or disruption of the process. According to data available in different sources, from 20% to 30% of failures of complex technical systems are associated with initiated failures caused by human errors. When considering the processes of the organization's activities with a full production cycle, the following list of personnel-related errors can be identified:

- design errors, including the development of operational documentation;
- planning errors and mistakes made in the organization of production;
- marketing and logistics errors that lead to the wrong choice of suppliers;
- production errors, including deviation from the requirements of design and technological documentation;
- violation by the personnel of the requirements of operational documentation for the equipment used;
- improper organization of workplaces;
- technical maintenance errors of the technical system, resulting in improper adjustment or calibration of process equipment;
- errors at the stage of technical control caused by the use of inappropriate measuring instruments or violation of the prescribed procedure for monitoring and documenting the results;
- violation of the conditions for storage or transportation of finished products;
- management errors that lead to psychological incompatibility or lack of motivation for employees, etc.

In general, failures of any kind of systems are divided into two types: gradual and sudden, the risk, on the one hand, is a surprise, however, on the other hand, it becomes possible to predict the risk, analyze it and assess its impact over time, which may subsequently be used for scientifically substantiated choice of management decisions to prevent the risk factors or weaken the risk's effect.

To develop a methodology for assessing risks in organizations, the foundations of reliability theory can be applied. When calculating the reliability of complex systems represented as the connection of elements with an established linear structure, it is assumed that the failure flow of the system is the simplest, satisfying the stationarity conditions, the absence of consequences and the ordinary, so the failures of the elements of a complex system are random and independent events. Then the probability of failure-free operation $P_c(t)$ of a complex system during the time t will be equal to the product of the probabilities of failure-free operation of its elements in time:

$$P_c(t) = p_1(t) \cdot p_2(t) \cdot \ldots \cdot p_N(t) = \prod_{i=1}^{N} p_i(t),$$

where p_i is probability of failure-free operation of the i-th element, N is a number of elements of the system.

Accepting the condition of stationarity of the failure flow, then $p_i(t) = e^{-\lambda t}$, and

$$P_c(t) = \prod_{i=1}^{N} e^{-\lambda t} = e^{-t} \sum_{i=1}^{N} \lambda_i$$

where λ_i is an intensity of the failure of the i-th element.

Hence, in order to calculate the reliability of such a complex system, it is necessary to be able to determine the failure rate of each of its elements (the number of failures for the selected time interval is a statistical indicator calculated on the assumption that failure is a random event). The average statistical data on the failure rates can be obtained from the data on the operation of systems similar to the analyzed.

However, the most important characteristic of the reliability of the system is the time of its trouble-free operation. It is also the calculated probability characteristic, which shows that the failure of the system does not arise within the given operating time. For example, if one uses the hypothesis of the equidistance of the elements of the analyzed system, that means that all elements have the same average failure rate, the intensity of the system failures can be expressed as the sum of the failure rates of the elements: $\lambda_c = \sum_{i=1}^{N} \lambda_i$ In this case, the estimated time of the no-failure operation of the system is defined as:

$$T_c = \frac{1}{\sum_{i=1}^{N} \lambda_i}.$$

The problem becomes more complicated if the structure of the system is not linear, i.e. the interaction between the elements of the system takes place in pairs, crosswise, backward. In this case, the simplest formula for the probability of failure-free operation of the system $P_c(t)$, expressed in terms of the product of the partial probabilities of failure-free operation of its elements, turns out to be incorrect, and it is required to evaluate the probabilities in accordance with the structure of the system.

An important condition for calculating the probability and time of failure-free operation is the assumption that at the initial time (the beginning of the run-time calculation) the system was in an operable state. This makes it possible to involve in the calculation of reliability the theory of Markov processes, which is also called the probability dynamics. Of course, the scope of application of this theory is limited (in particular, with the above-mentioned condition for partial uncertainty), but it is necessary in such areas as queuing theory, reliability theory, optimal decision making theory, etc., which operate with the concepts of random processes reflecting random change of system states in time (or depending on another chosen argument), described by random functions.

The use of Markov processes in reliability analysis is recommended by IEC 60300-3-1 "Dependability management: Part 3-1 - Application guide - Analysis techniques for dependability - Guide on methodology", NEQ [4]. In particular, the standard suggests that "the presentation of the behavior of the system through the Markov model requires the determination of all possible states of the system, preferably depicted schematically in the state diagram and transitions. In addition, the intensity of transitions from one state to another (the intensity of failure and recovery of components, the intensity of events, etc.) should be determined. A typical result of applying the Markov model is the probability of finding a product in a given set of states ...". It also points to the main advantage of this method: "the ability to obtain a flexible probability model for analyzing the behavior of the system ..." (A.1.5.3).

The above assumption about the operable state of the system at the beginning of the calculation of the operating time in the theory of Markov processes will be interpreted as a random process without aftereffects, characterized by the so-called transition probability - when the probability of a system transition to each subsequent state depends only on the previous state and does not depend on how the system has come (or has been reduced) to the previous state: $P_{i/i+1} = f(S)$. The selection of reference points in the form of system states, which are determined, for example, by the frequency of monitoring by management or by corrective measures, leads to the partitioning of the random process into its discrete states, and such a random process is regarded as a random sequence. If a random sequence has a Markov property, then it is called a Markov chain, and in the case of discretization of system states with respect to time, a discrete Markov chain in which the system can jump from one state to another after a certain impact.

3. Conclusion

In a free market, the successful operation of enterprises is impossible without increasing the requirements for quality products. This justifies the relevance of the implementation of a quality management system [5-7] and the need to use a risk-based approach in its formation.

The effectiveness of the quality management system can be enhanced through risk management activities aimed at achieving better results and preventing adverse consequences. For this, the organization needs to identify the risks and opportunities to be considered, plan and implement actions to reduce them and assess the effectiveness of these actions. At the same time, it is necessary to use a systematic approach that includes organizational issues of risk management associated with identifying and assessing risks, taking measures to reduce the negative impact of risks, as well as the monitoring and analysis order [8]. In [9] developed risk management methodology is presented, which is a tool for improving the process of making and executing management decisions aimed at reducing the likelihood of an adverse result and minimizing possible losses. The methodology was tested, brought to practical use and applied in the documented procedure "Risk Management" in the documentation for the quality management system of the ITMO University (St. Petersburg, Russia).

References

[1] ISO 9000:2015. Quality management systems – Fundamentals and vocabulary.

[2] ISO Guide 73:2009 Risk management – Vocabulary – Guidelines for use in standards.

[3] Large Economic Dictionary.

[4] IEC 60300-3-1 "Dependability management: Part 3-1 – Application guide – Analysis techniques for dependability – Guide on methodology", NEQ.

[5] A. Chernenkii, Management of organizations'' competitiveness, based on improved monitoring of Quality management system, *Proceedings of St. Petersburg State Economic University*, 2016, No. 2 (98), p. 142-146.

[6] A. Aleksankov, V. Mager, L. Chernenkaia, Quality management as a basement for reformation of Russian Universities, *Standards and Quality*, No. 4 (946), 2016, p. 91-94.

[7] A. Aleksankov, V. Mager, L. Chernenkaia, A. Chernenkii, Quality Assurance of High Education, *Open Education*, 2016, Vol. 20, No. 4, p. 10-16.

[8] A. Chernenkii, System analysis in Quality management of organizations' activities, *Collected papers of the Intern. Conference "System analysis in design and control"*, St. Petersburg Polytechnic University, 2016, p. 428-436.

[9] A. Chernenkii, Application of risk-oriented approach for creation of quality management system, *International Research Journal*, 2016, No. 8 (50), Vol. 1, p. 92-96.

MODEL OF QUICK RESPONSE PRODUCTION PLANNING SYSTEM

postgraduate student Skornyakova E.A.
Baltic State Technical University «VOENMEH» named after D.F. Ustinov, Saint Petersburg, Russia.

E-mail: elizavetasesina@mail.ru

Abstract: *Model of quick response system for production planning is described, main problems occurred during assessment of production options by responsible departments are overviewed and solution for optimization and speed-up of options assessment is suggested.*

Keywords: MODEL OF QUICK RESPONSE SYSTEM, PRODUCTION PLANNING, PRODUCTION PLANNING SYSTEM, PRODUCTION STRATEGY, REAL TIME.

1. Introduction

The most important problem of each company is quick reaction and proper management decision making. Main difficulties are related to high number of different internal and external factors.

External factors include fluctuation of market conditions (demand change, sales support and etc.), and also risks during parts and materials supply.

In internal factors can be included equipment capacity and it malfunctions, preparation for significant production modernizations and introduction of global projects, risks of human resource management.

To solve determined problems it is important to create balanced prompt response system for production planning.

Many different program products are existing for production and sales management, in most of the cases these products are based on MRP II (Manufacturing Resource Planning) standard.

Described below model of production strategy creation process is covered by most of the MRP II functions but present it special case. Accent in considered model is made on prompt response of all involved parties and “just-in-time” input of required data. In most of the cases such systems are created by companies from scratch because of its uniqueness and secret data content.

Prompt response systems are most important for high-productivity productions where any minute of unplanned stoppage bring significant financial losses. Such plants are very sensible to external and internal factors, risk assessment in these plants present the most complicated task comparing to other type of productions.

2. Model description

Interaction process of involved plant departments during creation and confirmation of production strategy can be described by block- scheme (Fig. 1).

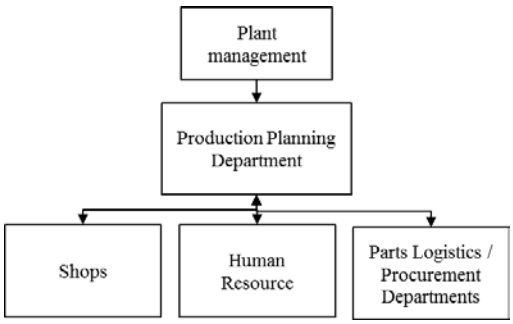

Fig. 1. *Scheme of production strategy creation and confirmation*

Creation of plant production strategies is managed by production planning department (production dispatcher division or production scheduling and control department). After receiving of the task for production option creation, Production Planning Department (PPD) is creating several options of the strategy and starting process of risk assessment with other responsible departments. Required hiring or excess of man power, members relocation between shops and morale conditions should be assessed with Human Resource, equipment capacity and modernization schedule should be assessed with shops, parts and materials stock level should be evaluated with Parts Logistics and Procurement Departments.

Oriented graph theory can be used as a mathematic model. Data connections between elements presented as a set E:

$$E=\{V_1,V_2,\ldots, V_5\} \quad (1)$$

where: $V_1,V_2,\ldots,V_5$ – graph nodes, presents participants of production planning system.

Interaction process as a graph:

$$G= (E, \Gamma), \quad (2)$$

where: E- set of elements, Γ – mapping of E set into itself.

Described scheme (Fig. 1) can be modified into oriented graph (Fig. 2).

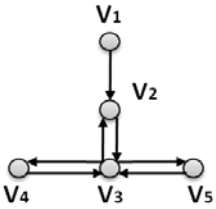

Fig. 2. *Interaction process as an oriented graph*

During such an interaction different problems can occur, production strategies cannot be assessed and choose without solving of these problems. Only after creation of all production options, PPD can start one by one assessment with involved departments. Such type of confirmation and risk assessment process is taking a lot of time and resources.

For the purpose of assessment acceleration during interaction between participants (V_1, V_2,…V_5), described graph can be modified by Malgrange's method [1].

Graph G is strongly connected if:

$$(\forall V_i \in E)\hat{\Gamma}V_i = E, \quad (3)$$

where: $\hat{\Gamma}$- transitive closure.

Transitive closure $\hat{\Gamma}V_i$ is multivalued mapping described by formula:

$$\hat{\Gamma}V_i = \{V_i\} \cup \Gamma V_i \cup \Gamma^2 V_i \cup \Gamma^3 V_i \ldots \quad (4)$$

Modified graph (Fig. 2) can be described as a Boolean matrix (Fig. 3).

	V_1	V_2	V_3	V_4	V_5	$\hat{\Gamma}V_3$
V_1		1				X
V_2			1			1
V_3		1		1	1	0
V_4			1			1
V_5			1			1
$\hat{\Gamma}^{-}V_3$	2	1	0	1	1	

Fig. 3. *Boolean matrix*

$$\hat{\Gamma}V_3 \cap \hat{\Gamma}^{-}V_3 = \{V_3, V_2, V_4, V_5\} \quad (5)$$

After elimination of vertex V_3, V_2, V_4 and V_5 from graph, modified graph will be created (Fig. 4).

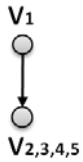

Fig. 4. *Graph modified by Malgrange's method*

Such a transformation allows to conduct independent real-time documents workflow inside of any subset ($V_{2,3,4,5}$).

3. Conclusion

After creation of program product based on proposed model and it introduction to the electronic documents flow several production strategies can be assessed at the same time.

Therefore, specialists workload will be equally spread and time of options creation and check will be significantly reduced.

Ideal case of internally stable set usage is advanced data entry from all responsible department and it real- time usage. Herewith each specialist can input or correct data based on necessity.

In reviewed system corrective actions (correction of created strategies) are replaced by preventive actions (real-time data input). As a result, PPD will always operate with latest data, this will allow to make correct management decisions.

Proposed model is very useful for supervisors and top managers due to full information receiving in real- time and reduction of company losses for optimal selection.

References

[1] Kofman, A.: Introduction into Applied Combinatorial Analysis. Nauka, Moscow (1975)